Doctoral Thesis

RUNOFF REGIMES ALONG ALTITUDINAL TRANSECTS AND THEIR POTENTIAL FOR MODEL BUILDING – A COMPARISON BETWEEN PERU AND AUSTRIA

submitted in satisfaction of the requirements for the degree of
Doctor of Science in Civil Engineering
of the Vienna University of Technology, Faculty of Civil Engineering

---

Dissertation

ABFLUSSREGIME ENTLANG SEEHÖHENTRANSEKTEN UND IHR POTENZIAL FÜR DIE MODELLBILDUNG - EIN VERGLEICH ZWISCHEN PERU UND ÖSTERREICH

ausgeführt zum Zwecke der Erlangung des akademischen Grades eines
Doktors der technischen Wissenschaft
eingereicht an der Technischen Universität Wien Fakultät für Bauingenieurwesen
von

Dipl.-Ing. María Magdalena Cárdenas Gaudry, Ing. MSc.

Supervisor: Univ. Prof. Dipl.-Ing. Dr. techn. Günter Blöschl
Institute for Hydraulic and Water Resources Engineering, TU Vienna
1040 Vienna - Karlsplatz 13

Supervisor: Em.O.Univ.Prof. Dipl.-Ing. Dr.techn. Dr.h.c. Dieter Gutknecht
Institute for Hydraulic and Water Resources Engineering, TU Vienna
1040 Vienna - Karlsplatz 13

Vienna, November 2015

Acknowledgements

Vienna, November 2015

Agradecimientos

Quiero agradecer a mi querido mentor, profesor, colega y buen amigo Prof. Dieter Gutknecht por su guia; por creer en mi idea; por su entusiamo y pasión en profundizar aspectos claves, bajo su convicción de que la hidrologia es una ciencia con matices forenses; por compartir conmigo cafés con croissants y tortas, almuerzos, caminatas, arte y cultura; y por su apoyo personal en momentos donde la duda intentaba reinar en mi.

Asimismo quiero agradecer al Prof. Günter Blöschl por su apoyo incondicional en las ideas del proyecto, en su guia de linea clara, directa y ordenada para el desenvolvimiento en mi desarrollo profesional y personal.

Es un lujo haber tenido la experiencia única de trabajar con dos celebridades de la hidrologia como Prof. Gutknecht y Prof. Blöschl, con amplios conocimientos y personalidades muy ricas y complementarias, en términos hidrológicos como mis cuencas peruanas y austriacas.

Muchas gracias a todos mis compañeros y amigos que he conocido en el Instituto, por su apoyo. Especialmente aprecio las valiosas discusiones y aportaciones de Juraj "Duro" Parajka y Rui A.P. Perdigão.

Quiero agradecer a mi Dios ausente por estar siempre conmigo; a mis padres, abuelita y hermanos por su infinito amor y apoyo a lo largo de mi vida; a mi querida familia en Austria: Oskar Berger y los Kozubek-Delgado por quererme sin condiciones y cobijarme siempre.

Finalmente agradezco al amor de mi vida - mis dos pedacitos de Dios por ser mis grandes maestros por lo que me queda de vida.

Viena, Noviembre 2015

Runoff regimes along altitudinal transects and their potential for model building – a comparison between Peru and Austria

Abstract

Runoff predictions are needed for many purposes including hydrological design, flood warning and water resources management. Predictions are invariably based on hydrological models that are tailored to the local conditions of the catchments of interest. In order to increase the efficiency of model building, this thesis analyses the hydrological patterns in the landscape. Specifically, the thesis aims at identifying dominant hydrological processes and their controls. The analysis is framed as a comparative study between Peru and Austria. Both countries exhibit enormous spatial gradients in precipitation and runoff which facilitate the identification of dominant hydrological processes.

Chapter 2 of this thesis examines the seasonality of precipitation and runoff along transects in Peru and Austria. The results suggest that, in the dry Peruvian lowlands of the North, the strength of the runoff seasonality is smaller than that of precipitation due to a relatively short rainy period from January to March, catchment storage and the effect of upstream runoff contributions that are more uniform within the year. In the Austrian transect, the strength of the runoff seasonality is greater than that of precipitation due to the influence of snowmelt in April to June. The effects of El Niño Southern Oscillations are also examined for the Peruvian catchments.

Chapter 3 analyses the dominant runoff variability for six hydro-climatic regimes in Peru. Specifically, the interest resides in understanding the within-year (short term or intra-annual) runoff variability vis a vis the between-year (long term or inter-annual) runoff variability in order to infer the runoff generation processes most relevant for a particular hydro-climatic regime. The results suggest that there are indeed clearly discernable patterns of runoff generation that are reflected in the variance components of runoff at different time scales as well as in the temporal correlation lengths of runoff. During the filling phase within the year (austral summer), inter-annual runoff variability tends to dominate, while during the depletion phase (austral winter) intra-annual runoff variability tends to dominate. The findings are compiled into a catalogue of runoff generation mechanisms with respect to the six hydro-climatic regimes in Peru.

Chapter 4 applies the finding of the seasonality (regime) and time scale analyses of the previous chapters in order to explore their potential for hydrological model building. The chapter proposes a strategy for bridging the gap between available concepts of landscape classification and hydrological approaches. Three existing concepts are linked: the life zone concept of Holdridge that classifies landscapes by climate and vegetation; the Budyko concept that splits precipitation into runoff and evapotranspiration; and the Kirkby concept that accounts for runoff generation mechanisms as a function of climate. The final model framework is constructed around a group of modules, each of which representing specific conditions with respect to the geomorphologic and ecohydrologic characteristics of the particular landscape type. The framework is applied to Ramon lagoon and its tributaries in northern Peru.

Overall, the results of this thesis suggest that altitudinal transects are indeed a valuable perspective for studying contrasting hydrological processes. The proposed framework results in a perceptual model of the catchment under study which can be very valuable for providing guidance in hydrological model building.

Abflussregime entlang Seehöhentransekten und ihr Potenzial für die Modellbildung - ein Vergleich zwischen Peru und Österreich

Kurzfassung

Abflussvorhersagen werden für viele Zwecke benötigt, wie Bemessungsfragen im Wasserbau, Hochwasserwarnung und die Bewirtschaftung von Wasserressourcen. Vorhersagen basieren immer auf hydrologischen Modellen, die auf die örtlichen Gegebenheiten der Einzugsgebiete abgestimmt sind. Um die Effizienz bei der Modellbildung zu erhöhen, untersucht diese Dissertation die hydrologischen Muster in der Landschaft. Insbesondere soll diese Arbeit dominante hydrologische Prozesse und ihre Einflussgrößen bestimmen. Die Untersuchung wird als Vergleichsstudie zwischen Peru und Österreich angelegt. Beide Länder weisen enorme räumliche Gradienten in Niederschlag und Abfluss auf, die die Identifizierung der dominanten hydrologischen Prozesse zu erleichtern.

Kapitel 2 dieser Arbeit untersucht die Saisonalität des Niederschlages und des Abflusses entlang von Transekten in Peru und Österreich. Die Ergebnisse zeigen, dass im trockenen peruanischen Tiefland im Norden der Abfluss weniger saisonal ist als der Niederschlag wegen der relativ kurzen Regenzeit von Januar bis März, der Wasserspeicherung im Einzugsgebiet sowie des jahreszeitlich eher gleichförmigen Zuflusses von oberhalb liegenden Gebieten. Im österreichischen Transekt zeigt der Abfluss eine stärkere Saisonalität als der Niederschlag wegen des Einflusses der Schneeschmelze von April bis Juni. Für die peruanischen Einzugsgebiete werden auch die Auswirkungen von El-Niño Perioden untersucht.

Kapitel 3 analysiert die dominierende Abflussvariabilität für sechs hydroklimatische Regime in Peru. Insbesondere wird die Variabilität des Abflusses innerhalb des Jahres (kurzfristige oder intra-annuelle Variabilität) und zwischen den Jahren (langfristige oder inter-annuelle Variabilität) untersucht, um die Abflussbildungsprozesse für die einzelnen hydroklimatischen Regime zu erschließen. Die Ergebnisse zeigen, dass tatsächlich charakteristische Muster der Abflussbildung existieren, die sich in den Varianzkomponenten über unterschiedliche Zeitskalen sowie in den zeitlichen Korrelationslängen des Abflusses widerspiegeln. Während der Füllungsphase innerhalb des Jahres (südlicher Sommer) dominiert meist die inter-annuelle Variabilität des Abflusses, in der Entleerungsphase (südlicher Winter) hingegen die intra-annuelle Variabilität. Die Ergebnisse werden zu einem Katalog von Abflussentstehungsmechanismen für die sechs hydro-klimatischen Regime in Peru zusammengestellt.

Kapitel 4 wendet die Ergebnisse betreffend Saisonalität (Regime) und Zeitskalen aus den vorangegangenen Kapiteln an, um deren Potenzial für die hydrologische Modellbildung auszuloten. Das Kapitel schlägt eine Strategie vor, um die Kluft zwischen vorhandenen Konzepten der Landschaftsklassifikation und hydrologischen Ansätzen zu überbrücken. Drei existierende Konzepte werden verknüpft: Das Konzept nach Holdridge, das die Landschaft nach Klima und Vegetation klassifiziert; das Konzept nach Budyko, das den Niederschlag auf Abfluss und Verdunstung aufteilt; und das Konzept nach Kirkby, das die Abflussentstehungsmechanismen als Funktion des Klimas klassifiziert. Die sich daraus ergebende Modellierungsstrategie besteht aus einzelnen Modulen, die jeweils die spezifischen Bedingungen in Hinblick auf die geomorphologischen und öko-hydrologischen Eigenschaften des Landschaftstyps berücksichtigen. Die Strategie wird auf die Ramon Lagune und deren Zubringer im nördlichen Peru angewandt.

Insgesamt zeigen die Ergebnisse dieser Dissertation, dass Seehöhentransekte einen zweckmäßigen Ansatz für die Untersuchung unterschiedlicher hydrologischer Prozesse darstellen. Die vorgeschlagene Modellierungsstrategie führt zu einem konzeptuellen Modell des Untersuchungsgebietes, das eine wertvolle Hilfestellung bei der hydrologischen Modellierung solcher Gebiete leistet.

Regímenes de escorrentía a lo largo de transectos altitudinales y su potencial para la construcción de modelos - una comparación entre Perú y Austria

Resumen

Las predicciones de la escorrentía son necesarias para muchos propósitos, incluyendo el diseño hidrológico, sistemas de alerta temprana por inundaciones y la gestión de recursos hídricos. Las predicciones se basan siempre en los modelos hidrológicos que se adaptan a las condiciones locales de las cuencas de interés. Con el fin de aumentar la eficiencia de la construcción de modelos, esta tesis analiza los patrones hidrológicos en el paisaje. En concreto, la tesis tiene como objetivo identificar los procesos hidrológicos dominantes y sus controles. El análisis se enmarca como un estudio comparativo entre Perú y Austria. Ambos países presentan enormes gradientes espaciales en precipitación y escorrentía que posibilitan la identificación de los procesos hidrológicos dominantes.

El capítulo 2 de esta tesis analiza la estacionalidad de la precipitación y la escorrentía a lo largo de transectos en Perú y Austria. Los resultados sugieren que, en las tierras bajas peruanas secas del Norte, la intensidad de la estacionalidad de la escorrentía es menor que el de la precipitación, debido a un período relativamente corto de lluvias de enero a marzo, el almacenamiento de la cuenca y el efecto de las contribuciones de escorrentía de aguas arriba que son más uniforme en el año. En el transecto de Austria, la intensidad de la estacionalidad de escorrentía es mayor que el de la precipitación debido a la influencia de la fusión de la nieve de abril a junio. Los efectos de El Niño-Oscilación del Sur también son examinados para las cuencas peruanas.

El capítulo 3 analiza la variabilidad de la escorrentía dominante para seis regímenes hidro-climáticas de Perú. En concreto, el interés reside en la comprensión de la variabilidad de la escorrentía dentro de un año (corto plazo o intra-anual) vis a vis la variabilidad de la escorrentía entre-años (a largo plazo o interanual), con el fin de inferir los procesos de generación de escorrentía más relevantes para un particular régimen hidro-climático. Los resultados sugieren que efectivamente existen patrones claramente discernibles de la generación de escorrentía que se reflejan en los componentes de varianza de la escorrentía en diferentes escalas de tiempo, así como en las longitudes de correlación temporal de la escorrentía. Durante la fase de llenado dentro del año (verano austral), la variabilidad interanual de la escorrentía tiende a dominar, mientras que durante la fase de agotamiento (invierno austral) tiende a dominar la variabilidad intra-anual de la escorrentía. Los resultados se compilan en un catálogo de mecanismos de generación de escorrentía con respecto a los seis regímenes hidro-climáticas de Perú.

Capítulo 4 emplea los resultados de los análisis de los capítulos anteriores respecto a la estacionalidad (régimen) y la escala de tiempo, con el fin de explorar su potencial para la construcción de modelos hidrológicos. El capítulo propone una estrategia para la reducción de la brecha entre los conceptos disponibles de clasificación paisaje y enfoques hidrológicos. Tres conceptos existentes están vinculados: el concepto de zonas de vida de Holdridge que clasifica paisajes de clima y la vegetación; el concepto Budyko que divide precipitación en escorrentía y evapotranspiración; y el concepto Kirkby que da cuenta de los mecanismos de generación de escorrentía en función del clima. El marco final del modelo se construye en

torno a un grupo de módulos, cada uno de los cuales representa a condiciones específicas del tipo de paisaje, con respecto a las características geomorfológicas y ecohidrologicas. El marco final del modelo es aplicado a la Laguna Ramón y sus afluentes situado en el norte de Perú.

En general, los resultados de esta tesis sugieren que los transectos altitudinales son de hecho un valioso enfoque para el estudio constratado de procesos hidrológicos. El marco propuesto tiene como resultado un modelo peceptual de la cuenca de estudio, el cual puede ser una guia valiosa en la construccion de los modelos hidrológicos de cuenca.

Table of Contents

Figures

Tables

1 Introduction

1.1 Motivation and significance

Hydrological models are needed for many purposes. Investigative models are needed for better understanding the components of the hydrological cycle at a range of space-time scales as well as the fluxes of matter in the hydrosphere. Predictive models are needed for managing water resources in a sustainable way, assessing the effects of land use and climate change, forecasting floods and droughts as well as for engineering design purposes. There are also a range of interdisciplinary issues such as ecological modelling and assessment where hydrological models are needed.

Hydrological processes vary widely around the world depending on climate, soils, geology, vegetation and landscapes. Even for the same catchment, processes vary between events depending on storm characteristics and time of the year. At the local scale, runoff generation processes may include infiltration excess, saturation excess and macro pore flow. At larger scales there may or may not exist interactions of groundwater flow and surface flow. The processes are driven and modulated by climate through precipitation and evapotranspiration in a range of regimes with soil moisture playing a critical role. Evapotranspiration and snow processes imprint a strong seasonal pattern on these processes that varies widely between climates.

Because of this immense diversity, models need to be adjusted to the particular situation to accurately portray the hydrological fluxes. The standard procedure in hydrology has been to adjust the model parameters to the local situation but to choose the model structure based on software availability, convenience or other logistic considerations (Holländer et al., 2009). However, because of the wide variety of processes, choosing a suitable model structure for a particularly setting may be just as important, if not more important, than choosing suitable model parameters. In a conceptual hydrological model the model structure consists of a system of storage and transfer functions for particular space-time scales.

Ideally, a suitable model structure should reflect the most important hydrological processes in a catchment. For example, one particular model structure may give emphasis to macropore flow in the soil for conditions where vegetation allows the soil to drain quickly. Another model structure may involve a ground water store (or no ground water store) depending on the role groundwater plays. However, it is difficult to quantify the processes at the catchment scale because of the enormous spatial variability. One possibility is to use landscape characteristics to infer the spatial variability of water flow in the catchment. The topography directly drives surface water flows through topographic gradients but, unfortunately, subsurface processes are often more important for the hydrological response than are those at the land surface. Landscape processes, however, are also related to vegetation, soils and geomorphology through their co-evolution subject to the forcing of climate and geology (Blöschl and Merz, 2010). There is interplay across time scales. Slow processes such as landscape evolution and soil formation interact with fast processes such as floods, sediment production and evaporation. There is also an interplay across space scales. Large scale forcings such as climate cascade to finer scales with an effect on biomes. Conversely, water flow aggregates from local to river basin scales. It would be appealing to exploit these patterns of landscape processes that indirectly reflect the structure of hydrological processes. The idea of this doctoral research is to use the landscape characteristics as an indicator for a much wider suite of long term processes that affect the water flow today, including subsurface

flows. By identifying dominant processes the idea is a "mapping" between landscape structure and model structure. As the dominant hydrological controls may differ between landscapes, the model structures should also differ to reflect the specific hydrological processes in each landscape type.

1.2   Thesis aims

The aim of this doctoral thesis is to understand hydrological patterns at the landscape scale as a basis for hydrological model building. The more specific aims of the thesis are:

- To identify the dominant hydrological processes and their controls at various space and time scales and across spatial gradients of these controls;
- To analyse how the controls differ between landscape types, such as plateaus, hillslopes and wetlands, and the hydrological setting with respect to climate, geology, soils and vegetation; and
- To establish the foundations that would assist in linking processes, controls and a suitable model structure at various space and time scales.

1.3   Data preparation and field trips

The test bed regions used in this research are in Peru and in Austria. The main advantages of using these regions are the enormous spatial gradients in the process controls (climate, geology, air temperature through altitude, soils, vegetation, meso-topography). In fact, the regions in Peru have some of the strongest precipitation gradients in the world which makes them an ideal test bed for the framework to complement the analyses in Austria. The precipitation gradients in Peruvian regions are from the West to the East. In the coastal plain mean annual precipitation is a few millimetres while in the Andes mountains it is more than 4000 mm/yr. These spatial precipitation gradients translate into even larger runoff gradients. The Austrian catchments also feature significant gradients with mean annual precipitation ranging from 400 to 3000 mm, and the climate ranging from continental to Alpine. One would expect that the large spatial gradients in these regions will allow to more clearly identify the strengths and weaknesses of the method than would be possible in regions with spatially more uniform controls.

- An overview of the Peruvian data sets that have been used is given below. The data have been provided by the Servicio Nacional de Meteorologia é Hidrología del Perú (SENAMHI) and Autoridad Nacional del Agua del Perú (ANA).
- Stream flow data from the standard hydrographic network: Daily stream flow (different series from 1976-2008).
- Precipitation data from the standard hydrographic network: Daily precipitation (different series from 1976-2008).
- Other climatic data (daily air temperature, potential evapotranspiration).
- Digital maps of geology, land use and river network density, and physiographic attributes for each catchment.

The Austrian data have been provided by the Austrian Hydrographic Central Office (HZB) and the Central Institute for Meteorology and Geodynamics (ZAMG) through existing cooperations with the Institute for Hydraulic and Water Resources Engineering of the Vienna University of Technology. From the comprehensive Austrian data listed below a number of

representative catchments have been selected based on regional cross sections (see Parajka et al., 2009).

- Stream flow data from the standard hydrographic network: Daily stream flow (1045 catchments, 1971-2008).
- Precipitation data from the standard hydrographic network: Daily precipitation (1066 stations, 1971-2008).
- Other climatic data (daily air temperature, potential evapotranspiration, 1971-2008).
- Austrian stream network and catchment boundary data set of 7000 catchments including 900 gauged catchments.
- Digital maps of geology, land use and river network density, and physiographic attributes for each catchment.

The research is mainly based on existing data. However, a number of reconnaissance field trips in Peruvian and Austrian catchments were performed. The purpose of these field trips was to collect proxy or soft data by "reading the landscape" and collect any other information that is possible at the scale of the region. The interpretation of the landscape (or reading the landscape) is very important in guiding the analysis of research results as it could give information that complements the hard hydrological data.

1.4 Outline of thesis

This thesis is organised into five main chapters. The first chapter provides the introduction. The second chapter analysis the seasonality of the runoff regime along altitudinal transects in Peru and Austria and links it to the seasonality of the precipitation regime. For the same study regions, chapter three examines the runoff time scales separately for different hydro-climatic regimes in order to assist in the process interpretation. The fourth chapter brings the process understanding together with a view of exploring the potential of regime analysis along transects for informing hydrological modelling building. Finally, chapter six summarises the main findings of the thesis.

2 Seasonality of the runoff regime along altitudinal transects in Peru and Austria

2.1 Introduction

The runoff regime of catchments is a result of numerous interacting processes including the movement and phase change of water in the atmosphere and in the vegetation, on the land surface and in the soils. Investigating these processes is challenging because of their large spatial and temporal variability. One approach of exploiting this variability is comparative hydrology (Falkenmark & Chapman, 1989; Gaál et al., 2012) which aims at learning from the differences in different parts of the landscape to understand the process controls of runoff. This may help with building catchment classification schemes (Wagener et al., 2007), developing and selecting hydrologic model structures (Fenicia et al., 2013) and mapping of hydrological signatures for predictions in ungauged basins (Blöschl et al., 2013).

One of the signatures used for identifying process controls is the seasonality of the runoff regime. There are numerous studies on the seasonality of monthly runoff (e.g. Pardé, 1947; Gottschalk, 1985; Haines et al., 1988; Bower et al., 2004; Johnston & Shmagin, 2008), but many of them examine the hydrological regime only over a single region (e.g. Petrow et al., 2007; Molnar & Burlando, 2008; Sauquet et al., 2008). The advantage of using large datasets crossing the borders of administrative and climate units has been pointed out by Gupta et al. (2014). While such studies are less common (see e.g. Krasovskaia, 1995, 1996; Dettinger & Diaz, 2000; Krasovskaia & Gottschalk, 2002; Parajka et al., 2010) there is renewed interest in them in connection with improving hydrological predictions under changing conditions (Montanari et al., 2013).

This paper explores the seasonalities of runoff and precipitation regimes in Peru and Austria. Seasonality assessments in Peru in the past focused mainly on the precipitation regime, its temporal variability and the impact of the El Niño Southern Oscillation (ENSO) signal on monthly and extreme precipitation. For example, Lagos et al. (2008) examined statistical relationships between monthly precipitation and sea surface temperature anomalies in Peru and delineated three El Niño precipitation regimes (North, centre and South) in the Andean mountain region. Espinoza et al. (2009a) found low rainfall seasonality in Ecuador, and a bimodal rainfall regime with peaks in April and October in the intra-Andean basins in Peru and the Amazon plain (at the border of Peru, Brazil and Colombia). Rau and Condom (2010) observed a marked seasonality in precipitation above 3000 m in Peru with maxima in January to March and minima in June to August. Lavado et al. (2012) investigated rainfall-runoff variability and its trends in three Peruvian regions (Pacific, Amazonas and Titicaca basins). They found low correlations between monthly precipitation and runoff in some Pacific basins which they attributed to the effects of groundwater storage, glacier melt and anthropogenic activities such as water abstraction for irrigation, hydropower production and water supply. A global analysis of Dettinger & Diaz (2000) found that the lag times between the months of maximum precipitation and those of runoff vary smoothly from long delays in mountainous regions to relatively short delays in the lowlands.

In Austria, the seasonality of hydrological regimes was analyzed mainly in the context of flood producing processes (Merz et al., 1999; Piock-Ellena et al., 2000; Merz & Blöschl, 2003). For example, Merz & Blöschl (2003) identified and analyzed different types of causative mechanisms of floods by using the seasonality of maximum annual flood peaks as an indicator describing the timing of floods. Parajka et al. (2009) analyzed the differences in

the climatic conditions, long-term hydrological regime and flood processes along a transect between Austria and Slovakia. Their results suggest that the seasonality of precipitation and runoff regimes is an important indicator of flood processes. It varies considerably in space as a result of the relative role of soil moisture, evaporation and snow processes. The differences in the seasonality between precipitation and runoff were found to be more pronounced in the lowland and hilly regions than in the mountains. Parajka et al. (2010) extended the seasonality analysis to the Alpine Carpathian range and demonstrated the important role of regional soil moisture.

The aim of this paper is to examine the seasonalities of precipitation and runoff regimes across altitudinal transects in Peru and Austria in order to understand the factors that control the seasonalities in different climate and physiographic settings. The main advantage of altitudinal transects is that altitude is expected to have strong effects on snow and evaporation processes as well as on the precipitation magnitudes which will facilitate identifying the controls. The selected transects show similar topographical variability, but cross different climate zones in the two countries which facilitates a comparative analysis. We believe that the assessment and comparison of hydrologic regimes in regions with such large gradients allows inferring more robust interpretations than by using results from a single region only.

2.2 Study sites, data and methods

2.2.1 Study Sites

The seasonality of the precipitation and runoff regimes and their controls are analysed for three transects in Peru and Austria (Fig. 2.1). Transect 1 extends from North to South along the west slope of the Andes from 3°S to 18.5°S in Peru (Fig. 2.1, left). Transect 1 is the longest (1512 km) and represents large variations in the latitude, a large diversity of climate classes, and the influence of Pacific sea water currents or the Atlantic regime. Most of the catchments in Transect 1 drain to the Pacific Ocean with an exception in section km 250-320, 450-460 and 960-1330 that drain to the Atlantic (the Amazon basin).

Transect 2 cuts across the coastal plain and the Andes from Southwest to Northeast in Northern Peru (Fig. 2.1, centre). It extends from the coastal plain and depressions to the occidental mountain range and ends in the Andes Valleys. Transect 2 features differences in climate due to both altitudinal effects, and Pacific (km 0-130) and Atlantic (km 130-260) climatic regimes.

Transect 3 cuts across the Eastern Alps in Austria from North to South extending from 48.5°N to 46.5°N (Fig. 2.1, right). It features differences in climate due to both altitudinal effects, and Atlantic and Mediterranean Sea climatic regimes. Transects 2 and 3 have a similar length of about 260 km.
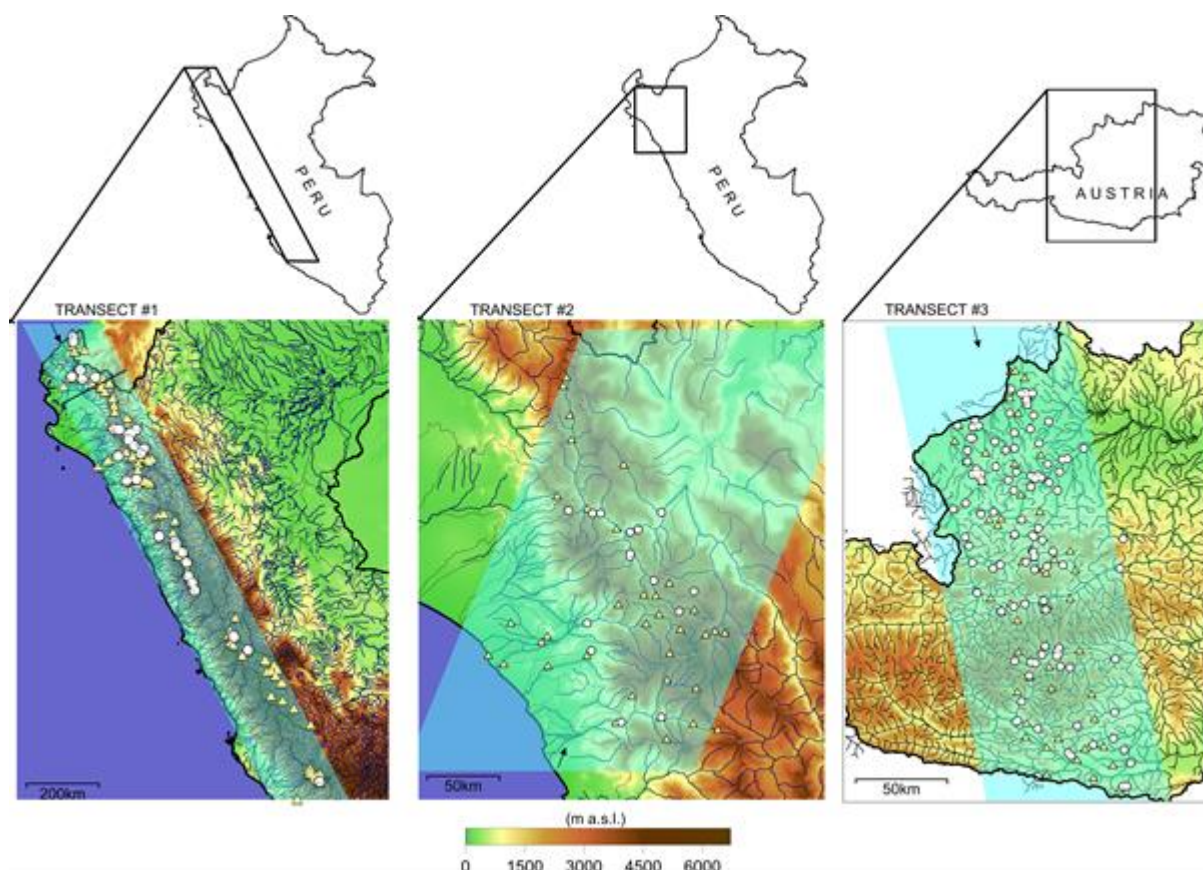
Figure 2.1: Topography and rivers of Peru (left: Transects 1 and 2) and Austria (right: Transect 3), with location of precipitation (triangles) and runoff stations (circles) along the transects.

2.2.2 Data

The hydrological data used in this study are monthly precipitation and discharge data from the period 1961–2010. Precipitation data from 111 and 61 climate stations in Peru and in Austria were used, respectively (Figure 2.1). The stations are situated at a wide range of elevations ranging from 1 to 4633 m a.s.l. in Peru, and from 308 to 1820 m a.s.l. in Austria. Mean monthly temperatures at the climate stations were used as a reference for discussing the runoff controls. Discharge data from 51 and 110 gauging stations in Peru and Austria were used, respectively. Catchment areas range from 6 to 14560 km². All input data were carefully screened for errors and, where possible, the data were corrected. Otherwise they were removed from the data set. The final data set contains at least 10 years of data in the period 1961–2010. The stations were assigned to the axes of the transects on a nearest neighbour basis of their locations.

2.2.3 Controls

The Köppen climate classification was used to identify the climate zones of the sites (Köppen 1884). The following Köppen climate groups can be found in the transects (Köppen indices in brackets):

- Tropical savanna climate (Aw)
- Semi arid climate (BS)
- Desert climate (BW)
- Temperate climate (CW)

- Hemiboreal climate with dry winter and warm summer (DWb)
- Snow dominated mountain climate (E)

Peru should have a predominantly tropical climate with abundant rainfall, high temperatures and busty vegetation due to its geographical location. However, climate is affected by the presence of the Andes mountain range, the Humboldt Current and the South Pacific anticyclone which result in a more diverse climate (UNESCO, 2006). Sites located in the Pacific catchments in the North of Peru have Tropical savanna, semiarid and desert climates. The other Pacific catchments have semiarid and desert climates up to 2000 m a.s.l. Temperate climates with dry winters are found in the steppe and low Andean valleys. Temperate humid climates are found in the Austrian transect. Snow dominated climates occur in the highest parts of Transect 1 and much of Transect 3.

Lowest annual precipitation occurs at the Peruvian coast (0-500 m a.s.l.) with a mean annual precipitation (MAP) of 3-870 mm/yr. In the highlands (500-4633 m a.s.l.) the range of MAP is from 62 to 1466 mm/yr. MAP decreases from North to South. In the Austrian lowlands (330-500 m a.s.l.) MAP ranges from 809-1520 mm/yr and in the highlands (500-1820 m a.s.l.) from 750-1943 mm/yr. Mean annual temperatures vary from 19°C in the coastal plains of Peru to 9°C in the highlands, and from about 10°C in the Austrian lowlands to around -8°C in the highest parts of the Alps.

The Peruvian transects are affected by a range of air fluxes. In the North, the greatest single control on the annual cycle is the meridional migration of the Inter-tropical Convergence Zone (ITCZ) (Poveda et al., 2006). The annual cycle of precipitation in the Peruvian Andes is related to the seasonal displacement of the South Pacific and South Atlantic anticyclones, the north-south seasonal displacement of the Intertropical Convergence Zone, humidity transport from the Amazon, and the formation of a center of high pressure in high levels of the atmosphere (Lagos et al, 2008). In this paper, we classified the catchments of Transects 1 and 2 according to the air mass fluxes as follows:

- Catchments with Pacific outlet and Pacific influence
- Catchments with Pacific outlet and Atlantic influence
- Catchments with Pacific outlet and ITCZ influence
- Catchments with Atlantic outlet and Atlantic influence

All catchments that drain into the Atlantic Ocean through the Amazon system are considered as Atlantic influence. The ITCZ is present between km 0-95 in Transect 1. The Pacific influence can be modulated by ENSO (warm sea water from North to South direction) and the Humboldt Current (cold sea water from South to North direction).

The Austrian Transect 3 shows Zonal West influence of air masses in the North and centre, and Meridional Southeast and South influence in the South of the transect (Parajka et al., 2010). In this paper, we classified the catchments of Transect 3 according to the air mass fluxes as follows:

- Catchments with Zonal West influence
- Catchments with Meridional Southeast and South influence

ENSO is a phenomenon manifested by an increase of the sea surface temperature in the Eastern and Central Equatorial Pacific, which generates an atmospheric instability and therefore affects the temperature and rainfall regime of the coast and the Western side of the

Andes. This phenomenon is cyclical with an average periodicity of 7 years (UNESCO, 2006). The Pacific sea water current is present under El Niño conditions (warm seawater) between km 0-227 in Transect 1 and km 0-125 in Transect 2. The Humboldt Current (cold seawater from South to North) is present between km 400-1500 in Transect 1. In order to understand the effect of ENSO events on the seasonalities of precipitation and runoff in Peru we selected two strong ENSO events: for La Niña the period 1973-1974 and for El Niño the period 1982-1983. Precipitation and discharge data were analysed for both events.

2.2.4 Seasonality analysis: Pardé coefficient and regime

The seasonality of the monthly precipitation and runoff regimes is evaluated by the index proposed by Pardé (1947). For each month of the year, an index Pk_i is estimated as:

$$Pk_i = \frac{12}{n} \sum_{j=1}^{n} \left(Q_{ij} \Big/ \sum_{i=1}^{12} Q_{ij} \right)$$

(1)

where Q_{ij} represents the mean monthly runoff (or precipitation) in month i and year j, and n is the record length. The Pk_i values range between 1 and 12, where $Pk_i=1$ represents a uniform (non-seasonal) distribution of mean monthly runoff (or precipitation) around the year, while $Pk_i=12$ indicates a very strong seasonality when all the runoff (or precipitation) occurs only in one month. The strength of runoff or precipitation seasonality Pk_{max} is defined here as the maximum value of Pk_i:

$$Pk_{max} = \max(Pk_i)$$

(2)

The month i_{max} in which the maximum occurs is also noted. In the following, Q-Pk_{max} and P-Pk_{max} refer to the maximum Pardé coefficients for runoff and precipitation, respectively.

2.3 Results and discussion

The results of the seasonality strengths along the three transects are presented in Figure 2.2, Figure 2.3 and Figure 2.4. In each of the figures, the top panels show the long term water balance for two basins on the transect, i.e. monthly precipitation (triangles) and monthly runoff depths (circles) as well as monthly average air temperatures (squares). The middle panels show the Pk_{max} values of precipitation (full triangles) and of runoff (full circles) along the distance of the transects with the month i_{max} of Pk_{max} colour coded. The bottom panels show the median and maximum elevations of the transects. Table A1 in the appendix gives a summary for selected climate stations and stream gauges used to illustrate the water balance in Figure 2.2-2.4.

2.3.1 Seasonality of precipitation and runoff along transects

Transect 1: Peru North-South

The Pk_{max} - values of precipitation of Transect 1 (triangles in Figure 2.2) are high (up to 5) in the North, decrease until km 800 and then increase again. The Pacific North of Transect 1 is influenced by the El Niño current with greater precipitation amounts than the Pacific-Central and southern part influenced by the Humboldt current, restricting the evaporation of the cold water and increasing the aridity of the region. The ITCZ influence for the austral autumn (Vera et al., 2000) is also evident in section km 0-95 (Tumbes basin) where precipitation

peaks occur in February-March and P- Pk_{max} are somewhat smaller than around km 145-230. The sites with Atlantic influence of Transect 1 are controlled by the trade winds where precipitation maxima occur in January-March.

Mean annual precipitation (MAP) decreases from North to South. Differences in elevation are the main reason for differences in MAP for the same location along the transect. Wet season precipitation in the lowlands is concentrated in three months, resulting in large seasonality strengths. In the highlands, precipitation is spread over more months, resulting in a smaller seasonality strength. Espinoza et al. (2009a) studied the length of the dry season in the tropical Andes (highlands) and noted that only 5% of the annual rainfall is registered from June to September. A similarly strong seasonality was found by Rau and Condom (2010) in the Peruvian Andes above 3000 m a.s.l. coinciding with km 603-803 and 960-1330 of Transect 1.

The timing of the runoff regime is similar in all basins, with runoff maxima mostly in March (Espinoza et al., 2009 a), coinciding with the time of Pk_{max} of precipitation. An exception are the Atlantic basins located in the Andes Valleys where maximum runoff occurs between March and May and maximum precipitation between December and April.

The trend of the maximum seasonality of runoff in Transect 1 (circles) follows basically the trend of the maximum seasonality of precipitation with Q- Pk_{max} around 3.5 in the North, km 38-69 (Tumbes basin), a decrease towards the South until km 750 with values around 2 and then an increase to values around 4, at km 1480 (Acari basin). However, there are important differences between the seasonality of runoff and precipitation. In the North, the Q- Pk_{max} are smaller than those of precipitation while the opposite is the case in Central and Southern Peru.

To explain the differences between the seasonalities of precipitation and runoff it is useful to examine the water balance of two typical basins. Fig. 2.2 top left shows the water balance components of the Chancay-Lambayeque basin (km 400-438 of Transect 1) that drains into the Pacific Ocean with two typical precipitation stations within the basin. Precipitation station P1a is located at the coast at 250 m a.s.l. and is under the influence of Pacific air fluxes. Precipitation station P1b is located in the Andes at 2750 m a.s.l. and is under the influence of Atlantic air fluxes. The maximum Pardé coefficient of precipitation decreases with increasing altitude. Discharge station Q1a is located at 250 m a.s.l.. The runoff regime of Q1 is a composite of the Atlantic and Pacific influences. The Chancay-Lambayeque basin is an example where the runoff seasonality is smaller than the precipitation seasonality at the coast. This is because of catchment storage effects as well as the runoff contributions from higher parts of the catchment where the rainfall regime is more uniform.

The Ica and Acari basins (Fig. 2.2 top right), again draining into the Pacific Ocean, illustrate examples in the South where runoff seasonality is greater than precipitation seasonality, or similar. Precipitation station P2a and discharge station Q2a are located at 3900 m a.s.l.. Precipitation station P2b is located at 2500 m a.s.l. and discharge station Q2b is located at 420 m a.s.l.. In these catchments annual precipitation is relatively low. Rather uniform evaporation throughout the year results in losses that reduce the average annual runoff while leaving the amplitude (mm/month) of runoff similar. This then translates into Q- Pk_{max} that are larger than the P- Pk_{max}.
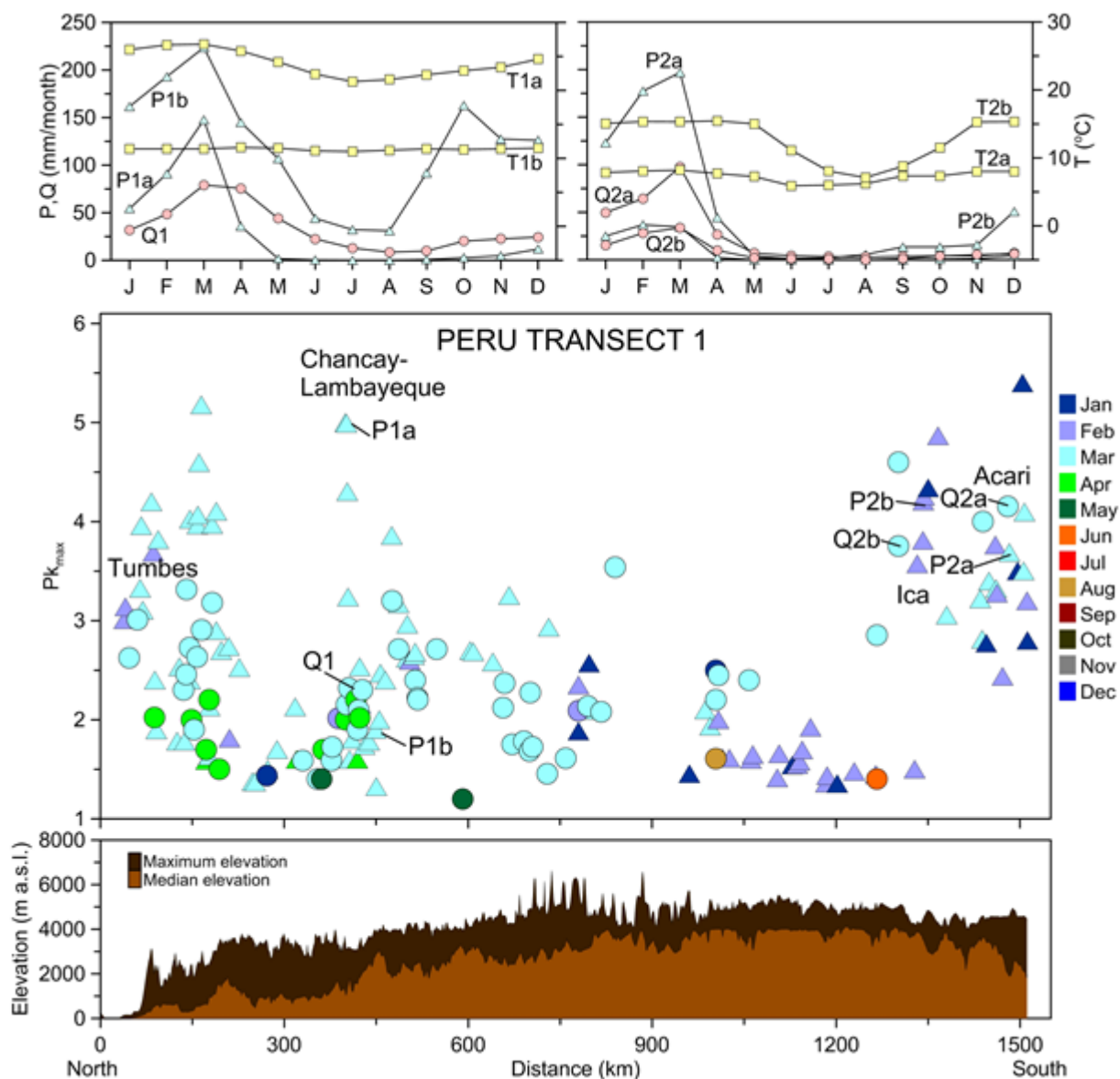
Figure 2.2: Top: Long term water balances for the Chancay-Lambayeque basin (2400 km2) (left), and the Ica (2600 km²) and Acari basins (250 km2) (right). Precipitation (triangles), runoff depths (circles) and air temperatures (squares). Middle: Maximum seasonality strength Pk_{max} and month of ocurrence along Transect 1 for precipitation (triangles) and for runoff (circles). Bottom: median and maximum elevations of the transect.

Transect 2: Peru Southwest-Northeast

The Pk_{max} - values of precipitation of Transect 2 (triangles in Figure 2.3) strongly decrease with the distance from the coast from P- Pk_{max} 5 to 1.3. Similar to precipitation, the maximum runoff seasonality decreases with the distance from the coast from Q- Pk_{max} 3.2 to 1.4. However, the maximum Pardé coefficient of runoff is smaller than that of precipitation in the Southwest (Pacific and Atlantic influence) up to km 130. Conversely, the Pardé coefficient of runoff is greater than that of precipitation in the East, for example at km 135-140, where Q4 is greater than P4 (Atlantic influence).

The water balance components of the Zaña basin in Fig. 2.3 top left, again, help explain the seasonality. P3a and Q3 are located at the coast at 200 m a.s.l., and P3b in the Andes at 2300 m a.s.l.. Q3 is affected by both storage and inflow from the headwaters with high precipitation seasonality, resulting in a runoff seasonality smaller than that of precipitation at the coast. In

Chotano in the Northeast of Transect 2 (Fig. 2.3 top right) the role of upstream headwaters is small, similar to Acari. A rather uniform evaporation throughout the year results in a reduction of average annual runoff, and therefore a Q- Pk_{max} larger than P- Pk_{max}.
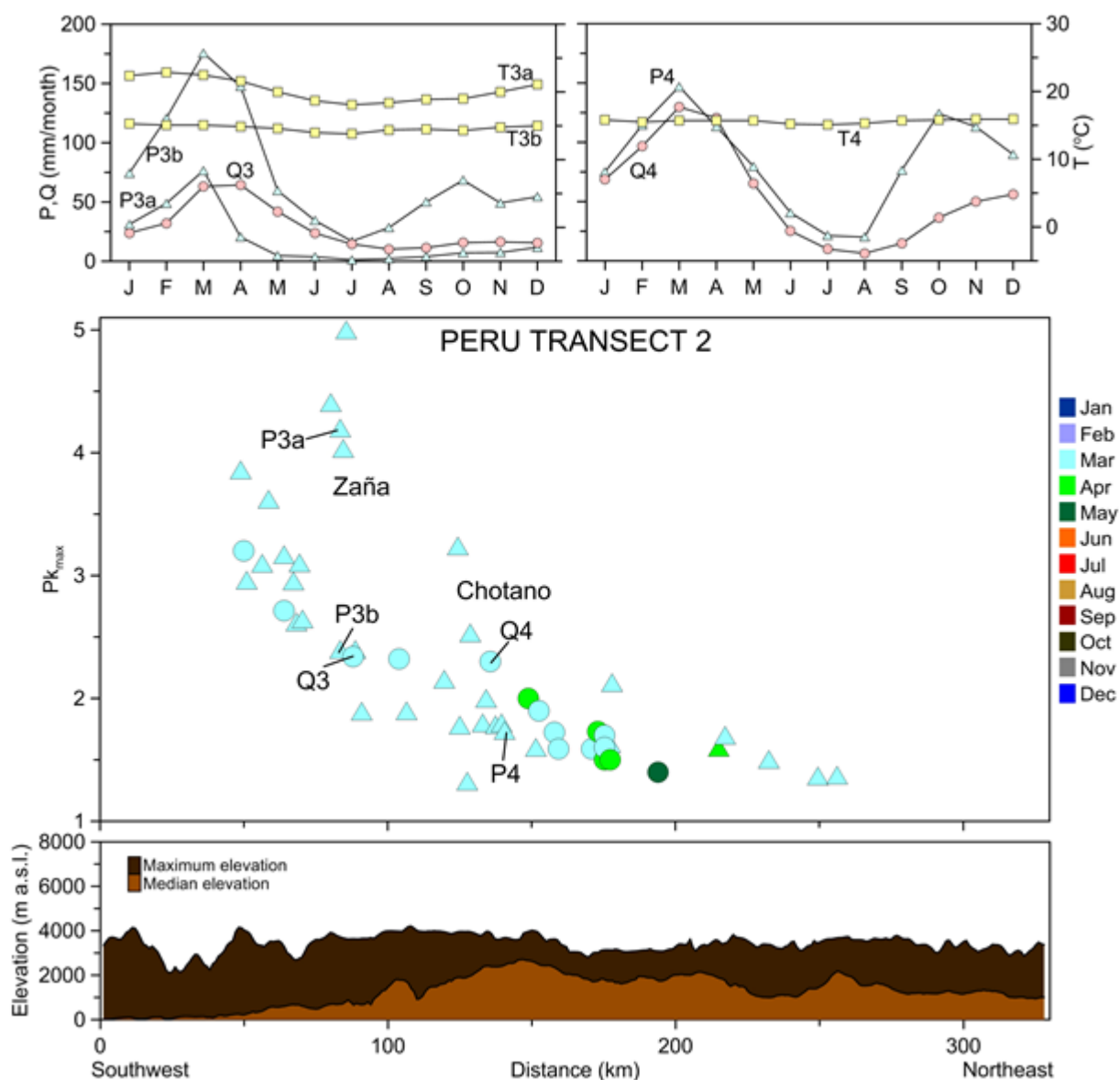
Figure 2.3: Top: Long term water balances for the Zaña basin (673 km2) (left) and the Chotano basin (356 km2) (right). Precipitation (triangles), runoff depths (circles) and air temperatures (squares). Middle: Maximum seasonality strength Pk_{max} and month of ocurrence along Transect 2 for precipitation (triangles) and for runoff (circles). Bottom: median and maximum elevations of the transect. Note that, inside a basin, the Maximum Pardé coefficients Pk_{max} of runoff (circles) are smaller than those of precipitation (triangles) in the Southwest (Pacific basins) and greater than those of precipitation in the Northeast (Atlantic basins).

Transect 3: Austria North-South

The Pk_{max} - values of precipitation of Transect 3 (triangles in Figure 2.4) slightly increase from the northern Alpine lowlands (P- Pk_{max} around 0.9) to the high Alps (P- Pk_{max} around 1.6) and in turn somewhat decrease as one moves to the Southern Pre-alps (P- Pk_{max} around 1.4). The stronger seasonality in the Alps is due to orographic effects (Parajka et al., 2010).

The maxima of mean monthly precipitation generally occur in summer from June to August. The exception is the very South of the transect where they tend to occur in November. The latter values are due to weather patterns from the Mediterranean which tend to bring moist air to the Alps when the Mediterranean Sea surface is still warm, so can transfer moisture and energy to the atmosphere. Their influence only extends to the southernmost part of the Alps.

The runoff seasonality shows a more heterogeneous pattern than that of precipitation. In the northern lowlands (km 0-100) Q- Pk_{max} are around 1.5 and the maxima occur in March. In the High Alps in the middle of the transect, the Q- Pk_{max} are significantly higher (around 1.9) and the maxima occur in April, May and June. Finally, in the South, Q- Pk_{max} are around 1.3 and the maxima occur in either April-May or November. The Maximum Pardé coefficients Pk_{max} of runoff (circles in Fig. 2.3) are almost always greater than those of precipitation (triangles), particularly in the high mountains.

The water balance for the Mattig Basin (Fig. 2.4 top left) in the Northern lowlands of Austria shows that, although precipitation occurs throughout the year, it is summer dominated from June to August. This is also the time when the maximum evaporation occurs as indicated by the strong seasonality of air temperature. The strong seasonality of evaporation that is in phase with that of precipitation (Sivapalan et al., 2005) results in a very uniform runoff regime throughout the year and therefore a slightly smaller Q- Pk_{max} (1.3) than P- Pk_{max} (1.4). This is typical of the lowlands in the region (Parajka et al., 2009). The runoff shows a small peak in March when the soils are still wet, so runoff coefficients are higher than in summer.

The Alpine areas show quite a contrasting behaviour as illustrated by the Enns basin (Fig. 2.5 top right). The precipitation regime is similar to Mattig, but evaporation contributes less to the water balance due to lower temperatures in the higher elevations. Even more importantly, snow storage and snow melt play a clear role. The runoff maxima occur in May as a result of snow melt. Runoff is relatively low in December and January due to snow storage. This explains the fact that Q- Pk_{max} (2.0) is greater than P- Pk_{max} (1.7) in this basin. There are catchments that are located at higher elevations than the Enns basin and these exhibit even bigger Q- Pk_{max} (up to 3) due to the stronger effect of snow melt and storage on the water balance. Runoff seasonalities larger than precipitation seasonalities are typical of many regions around the world where the runoff regime is dominated by snowmelt (Dettinger & Diaz, 2000).

In the very South of Transect 3, precipitation is bimodal (not shown in the figure) and similarly the runoff regime is bimodal with a main maximum in May and a secondary maximum in November. The May maximum is related to snow melt, the November maximum is related to the precipitation maximum. One basin on Transect 3 (at km 255) in fact shows the main runoff maximum in November.
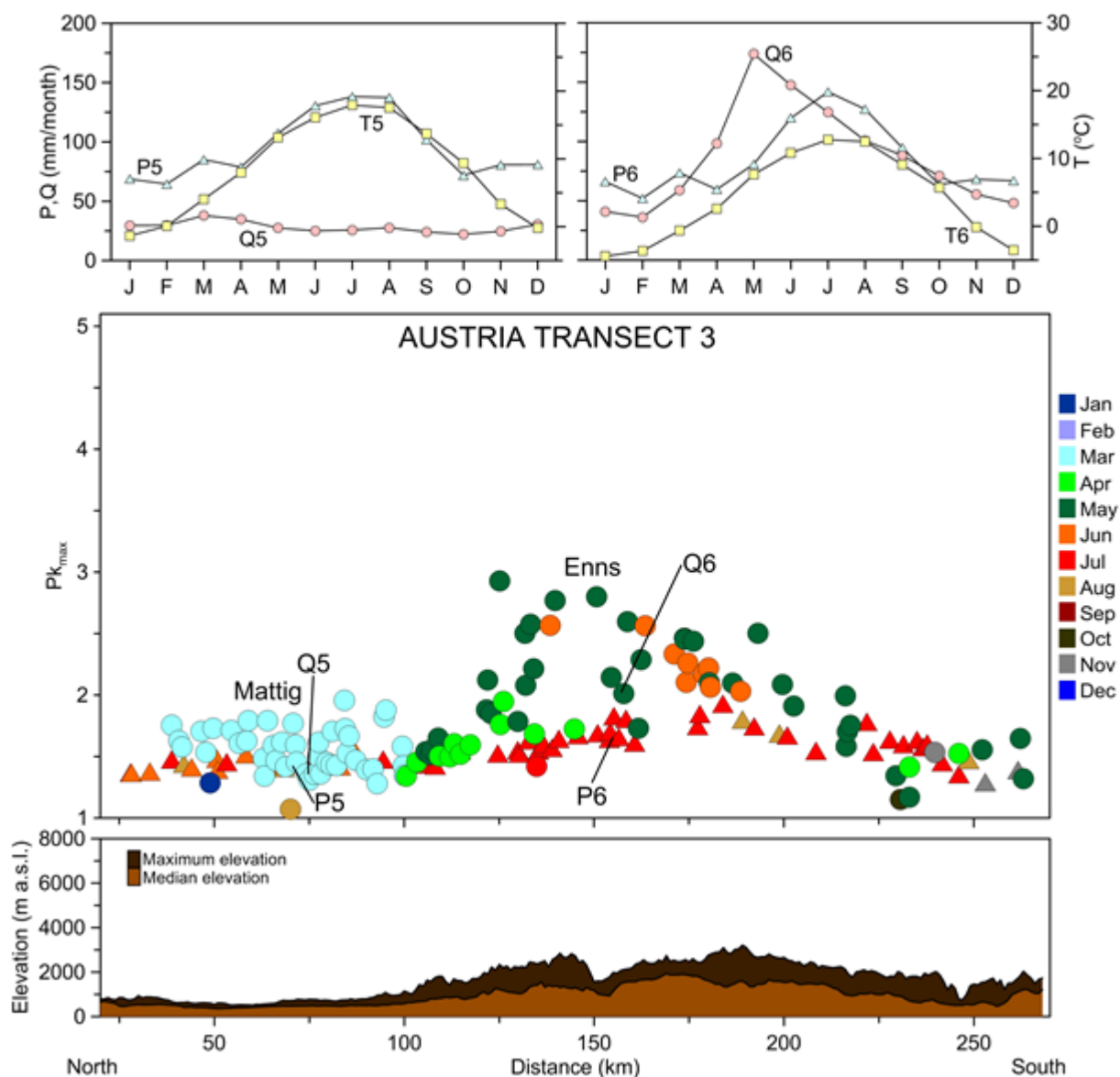
Figure 2.4: Top: Long term water balances for the Mattig basin (447 km2) (left) and the Enns basin (649 km2) (right). Precipitation (triangles), runoff depths (circles) and air temperatures (squares). Middle: Maximum seasonality strength Pk_{max} and month of ocurrence along Transect 3 for precipitation (triangles) and for runoff (circles). Bottom: median and maximum elevations of the transect. Note that the Maximum Pardé coefficients Pk_{max} of runoff (circles) are almost always greater than those of precipitation (triangles), particularly in the high mountains.

2.3.2 Controls on the seasonality of runoff and of precipitation in the Austrian and Peruvian transects

2.3.2.1 Climate regime effects on seasonality

While the transects in Figure 2.2-2.4 have highlighted the seasonality with respect to mountain ranges and atmospheric moisture fluxes, it is also useful to explicitly analyse the seasonality with respect to climate. Five Köppen climate groups were identified for the Peruvian transects, and two groups for the Austrian transect.

The Peruvian Pacific lowlands are characterized by desert and arid climates (P1a and P3a) with precipitation from 0 to 300 mm/yr per year, where rainfall tends to occur as discrete and

intense events (Takahashi, 2004). Semiarid and temperate climates with dry winters are found in the Peruvian Pacific highlands with Atlantic influence (P3b and P1b), and semiarid and hemiboreal climates are found in the Peruvian Pacific highlands with Pacific influence (P2b, P2a). Transect 3 in Austria shows two main climates: temperate in the lowlands (P5) and snow dominated in the highlands or Alps (P6). The comparison between the Peruvian and Austrian transects indicates that the variability of the strength of seasonality in Austria is much more limited than that in Peru. This is due to the more limited range of climate zones in Austria. Table 7.2 in the appendix shows the ranges of the maximum strength of seasonality. Because of the different latitudes, the snow dominated regimes in Peru are found above around 4000 m a.s.l., while in Austria above around 600 m a.s.l..

Fig. 2.5 shows the relationship between P- Pk_{max} and Q- Pk_{max} stratified by the Köppen climate classes for the three transects. Overall, P- Pk_{max} decreases from tropical savanna climate (Fig. 2.5 top left) to snow dominated climate (Fig. 2.5 bottom right). For the desert climate and the semi arid climate, Q- Pk_{max} is smaller than P- Pk_{max} while for the snow dominated climate it is bigger. The other climate zones show a more mixed pattern.
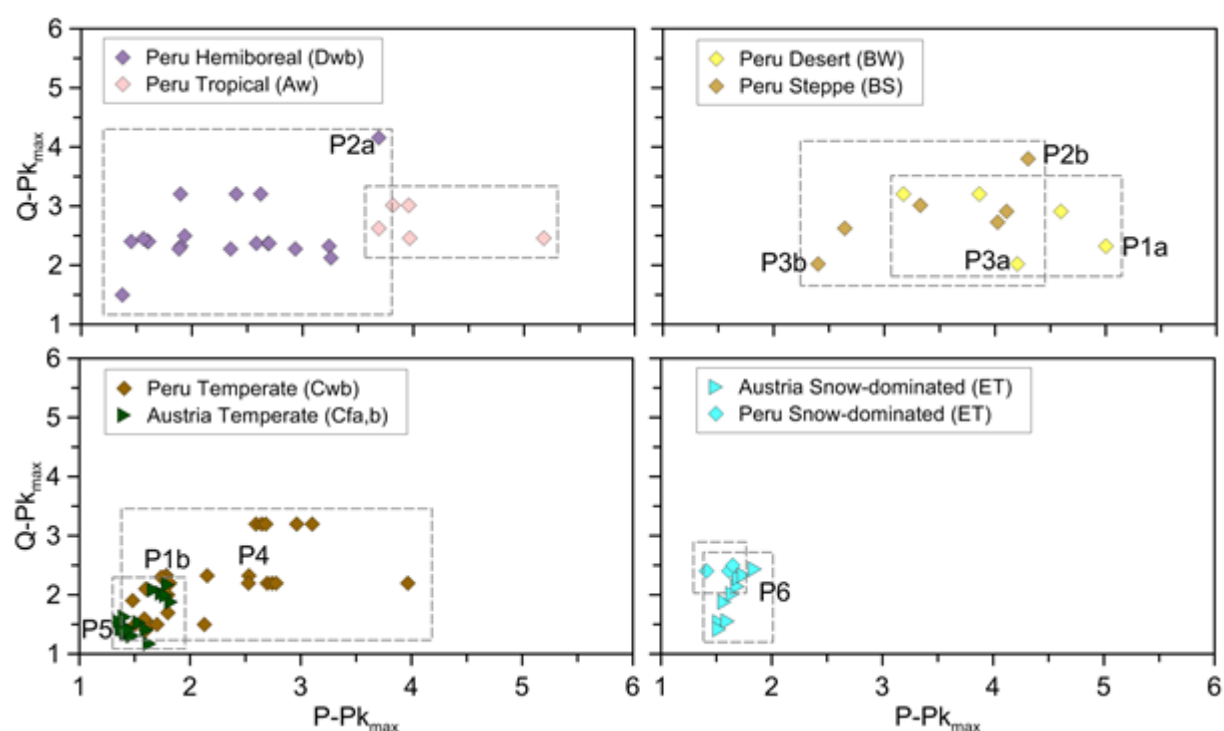
Figure 2.5: Relationship between maximum seasonality index of precipitation P- Pk_{max} and runoff Q- Pk_{max} stratified by Köppen climate classes for Peru and Austria: Labels refer to the example stations of Figure 2.2-2.4 top.

2.3.2.2 Altitude, latitude, mean annual precipitation and air flux influences

In order to put the seasonalities into context, Fig. 2.6 shows mean annual precipitation (MAP) plotted versus station altitude. In the Peruvian transects, MAP increases clearly with altitude. In the North of Transect 1 (Tumbes basin) the increase is large with stations at 1000 m a.s.l. exhibiting 900 mm/yr. The gradient becomes gradually flatter (smaller altitudinal dependence of MAP) as one moves to the South. Acari, located in the South of Transect 1, has the same MAP for stations at an elevation of 4500 m a.s.l. Although stations P3b and P2b have similar altitudes and semiarid climates, the stronger Atlantic influence is reflected in significantly larger MAP and lower strength of seasonality of precipitation in P3b.

Transect 3 (Fig. 2.6 right) shows that the altitudinal effect on MAP in Austria is much less pronounced than in Peru. It appears that MAP is more affected by the location relative to the Alpine range than altitude per se, as the largest MAP occurs at the northern (windward) fringe of the Alps rather than the highest mountain tops. The latter exhibit less MAP as much of the moisture has already precipitated at the time the air masses arrive at the main ridge of the Alps. Fig. 2.6 also clearly illustrates that the Austrian transect (Transect 3) overall is much wetter than the Peruvian transects.
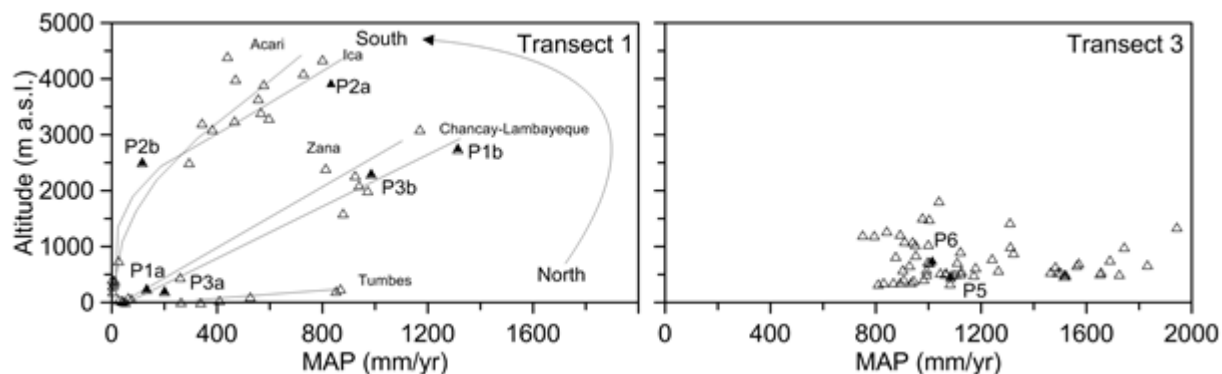
Figure 2.6: Relationship between mean annual precipitation (MAP) and altitudes of the precipitation stations in the Peruvian transects (left) and Austrian Transect 3 (right). Lines link the stations inside of five Peruvian basins (Tumbes, Chancay-Lambayeque, Zaña, Ica and Acari).

Table 2.1 groups the basins of Transects 1 (Peru) and 3 (Austria) according to their drainage outlet and their air mass influences with seasonality characteristics.

Basins with a Pacific outlet and Pacific air flux influence are characterized by P- Pk_{max} greater than 2.5 and MAP less than 940 mm/yr (Fig.2.7a), a highly seasonal rainfall regime with a long dry season. They are located at low elevations in the North and Centre of Transect 1 and at all elevations in the South of Transect 1. The northern coastal region of Peru is well known for its seasonal summer precipitation (Chira, 2003). The corresponding climate regions are desert, arid and semiarid climates (P2b) to hemiboreal climates (P2a) in the highlands of the South. Accordingly, the P- Pk_{max} are the highest for these basins and the MAP are the lowest (Fig. 2.7a). Q- Pk_{max} tend to be lower than P- Pk_{max} because of the headwater effects.

Basins with a Pacific outlet and Atlantic influence are characterized by P- Pk_{max} less than 2.9 and MAP of 360-1470 mm/yr, with a relatively uniform rainfall regime and short to no dry periods. They are mainly located in the high valleys of the Andes. The corresponding climates are temperate, hemiboreal and snow dominated. Accordingly, the P- Pk_{max} are lower and the MAP are higher (Fig. 2.7b).

Basins with a Pacific outlet and ITCZ influence are characterized by P- Pk_{max} near 3.7 and MAP around 850 mm/yr. The influence is observed in Transect 1 km 39-250 km (Tumbes and Piura) during the austral autumn, resulting in relatively large P- Pk_{max} and a MAP of around 850 mm/yr (Fig. 2.7c). The corresponding climate is Tropical savanna.

Basins with an Atlantic outlet are all influenced by Atlantic air fluxes and are characterized by P- Pk_{max} of 1.3 -3.0 as there is essentially no dry season. The corresponding climates are temperate, hemiboreal and snow dominated (Figure 2.7d).

Basins with Zonal West influence in Austria are characterized by P- Pk_{max} less than 2.0 and temperate climate (Figure 2.7e). Basins with Meridional Southeast and South influence are

characterized by P- Pk_{max} less than 1.9 and temperate and snow dominated climate (Fig. 2.7f). Q- Pk_{max} is similar or somewhat larger than P- Pk_{max}.

Table 2.1: Groups of basins of Transects 1 (Peru) and 3 (Austria) classified according to their drainage outlet and their air mass influences with seasonality characteristics shown.

Basins	Transect	Precipitation (P)				Runoff (Q)				
		Pk_{max}	MAP (mm/yr)	MAX P (mm/month)	Altitude (m a.s.l.)	Pk_{max}	MAQ (mm/yr)	MAX Q (mm/month)	Altitude (m a.s.l.)	Area (km²)
Pacific Outlet with Pacific influence	1	2.4-5.4	4-940	1-292	1 - 4400	2.2-4.2	163-1038	60-241	1-3900	250-14560
Pacific Outlet with Atlantic influence	1	1.8-2.9	366-1463	97-421	980-4200	2.2-3.2	167-906	60-202	250-1880	673-3421
Pacific Outlet with ITCZ influence	1	3.7-3.8	851-868	241-373	205-250	2.6-3.0	640-868	177-227	1-22	3700-5508
Atlantic Outlet with Atlantic influence	1	1.3-3.1	324-1466	62-267	910-4633	1.4-2.5	234-491	32-360	660-4230	44-6020
Zonal West influence	3	1.4-1.9	750-1943	103-261	330-1820	1.1-2.9	177-1793	21-308	308-1179	6-3387
Meridional Southeast and South influence	3	1.3-1.4	1503-1743	171-208	540-995	1.2-1.5	310-605	43-59	452-504	57-91

2.3.2.3   Effects of ENSO

Fig. 2.8 shows the seasonality of precipitation and runoff with respect to two ENSO events in Transect 1: the period 1973-1974 which was strongly affected by La Niña and the period 1982-1983 which was strongly affected by El Niño. Fig. 2.9 gives annual precipitation and runoff for Transect 1 and Fig. 2.10 shows two example catchments.

Fig. 2.8a suggests that, in the Pacific Outlet basins with Pacific influence (circles), P- Pk_{max} during the El Niño event (black full circles) is greater than during the La Niña event (grey full circles). Although the P- Pk_{max} are similar in the Northern and Southern basins, the reasons how the strength of the seasonality comes about differ by: (a) greater MAP in the North than in the South; (b) larger amplitude of monthly precipitation in the North than in the South; (c) annual precipitation increases in the North during an El Niño event relative to the long term mean, and it increases in the South during a La Niña event; and (d) the wet period of the La Niña event (about 5 months) is greater than that of the EL Niño event (less than 3 months) in the South, which results in a greater P- Pk_{max} during the El Niño event than during the La Niña event. Runoff follows the differences in precipitation between the ENSO events, and Q- Pk_{max} during the El Niño event is greater than during La Niña (Fig. 2.8b). El Niño events in the lowlands of northwestern Peru are discrete and intense. Takahashi (2004) noted that rainy days during El Niño are associated with an enhanced onshore westerly low-level flow, which helps trigger convection by orographic lifting over the western slope of the Andes, modulated by tropical synoptic scale disturbances. The Northern basins registered more runoff for the El Niño event than for La Niña, while the opposite is the case in the South (Fig. 2.9 and Ica basin in Fig. 2.10 right) as pointed out by Lavado et al. (2013).

Pacific basins with Atlantic influence show MAP decreasing from North to South of Transect 1 (Fig. 2.9a, squares). Both MAP and P- Pkmax increase for the El Niño event in Transect 1 until km 438. Further in the South, however, they increase for the La Niña event (Fig. 2.8a

and Fig. 2.9a). Similar patterns are found for runoff. The induced westerly (El Niño) or easterly (La Niña) wind anomalies above the Cordillera Blanca (km 705-795 of Transect 1) were suggested by Vuille et al. (2008) as being responsible for the reduced (El Niño - dry conditions) or enhanced (La Niña - wet conditions) moisture influx from the East. Dry periods are preserved in all events, accentuating the P- Pkmax as illustrated for the Chancay-Lambayeque basin (Fig. 2.10 left).

Pacific basins with ITCZ influence (diamonds) show MAP and MAQ for El Niño to be greater than for the La Niña events. El Niño episodes associated with deep convection by anomalously high coastal ocean temperatures increase rainfall by several orders of magnitude in regions a few degrees south from the Equator during February to April (Aceituno et al., 2009). The seasonality strength of precipitation of EL Niño is greater than for La Niña and the same is the case for runoff at the transition from the low to the highlands.
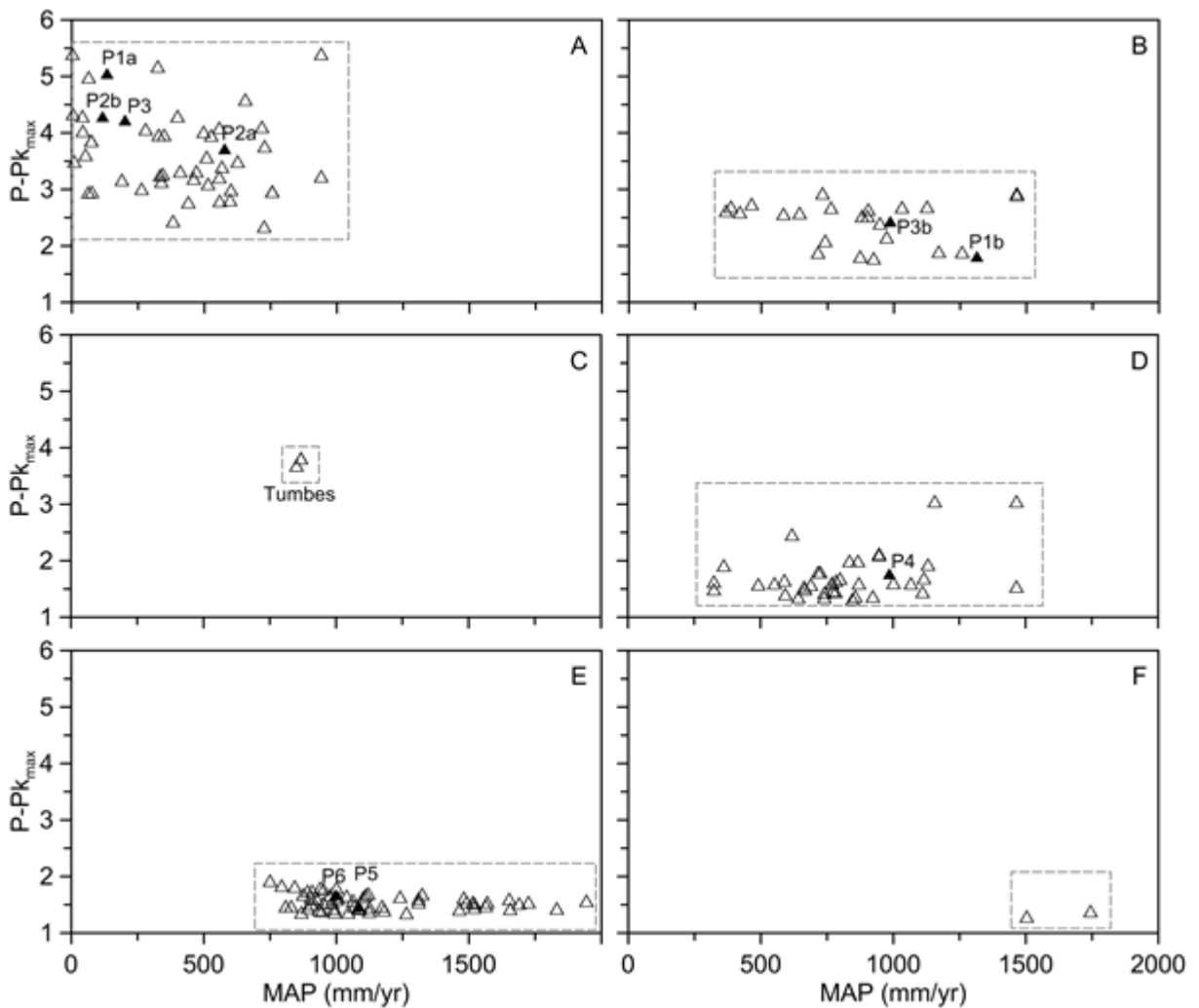
Figure 2.7: Relationships between mean annual precipitation (MAP) and the maximum Pardé coefficients of precipitation (P- Pk$_{max}$) in Transects 1 and 2 (a-d) and Transect 3 (e-f), grouped by air masses: a) Pacific Outlet with Pacific influence; b) Pacific Outlet with Atlantic influence; c) Pacific Outlet with ITCZ influence; d) Atlantic Outlet with Atlantic influence; e) Zonal west; and f) Meridional Southeast and South.

Atlantic basins with Atlantic influence (triangles) show MAP for El Niño to be smaller than that of La Niña. In the North, MAQ for El Niño is greater than that of La Niña, while in the South the opposite is the case. Indeed, Espinoza et al. (2009a) noted below-normal rainfall in

the North and Northeast of the Amazon Basin during El Nino events, but excess rainfall during La Niña. The strength of precipitation seasonality during the El Niño event is greater than for La Niña in the North; the opposite is the case for the Centre and South. The strength of runoff seasonality during the El Niño event is smaller than La Niña in the North and Centre; the opposite is the case for the South. Espinoza et al. (2009b) reported on strong opposite tendencies of regional runoff during ENSO events in the North and South. Milly et al. (2002) suggest that the influence of seasonality of the precipitation anomaly on the interannual variance in runoff is almost negligible under humid conditions as is shown in Fig. 2.8b (triangles at km 404), where the Q- Pk_{max} between ENSO events almost does not vary (Atlantic influence), but varies systematically under arid conditions (Pacific influence) as in Fig. 2.8b (circles at km 1341), where the Q- Pk_{max} between ENSO events does vary.
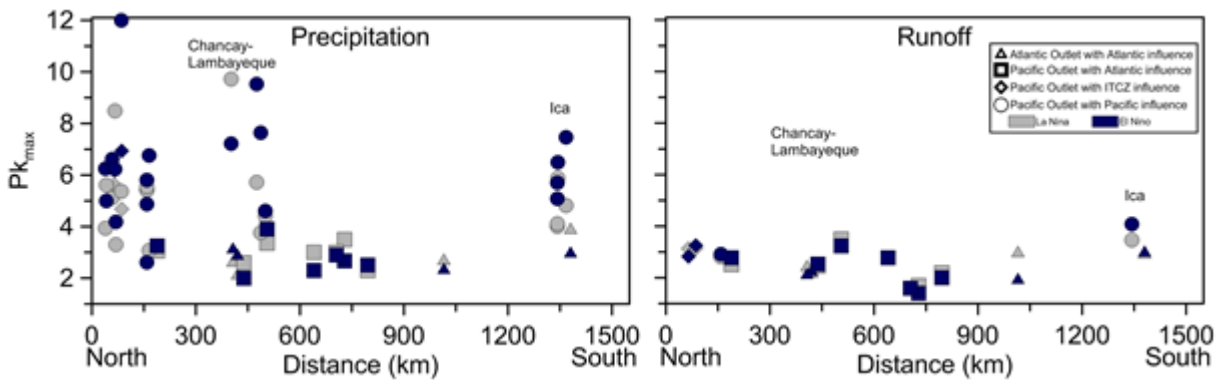
Figure 2.8: Maximum Pardé coefficients for precipitation (a) and for runoff (b) along Transect 1 according to air flux influence (see Table 2.1 and Figure 2.7). Pacific Outlet with Pacific influence (circles), Pacific Outlet with Atlantic influence (squares), Pacific Outlet with ITCZ influence (diamonds), and Atlantic Outlet with Atlantic influence (triangles). La Niña 1973-1974 event (grey symbols) and El Niño 1982-1983 event (black symbols).
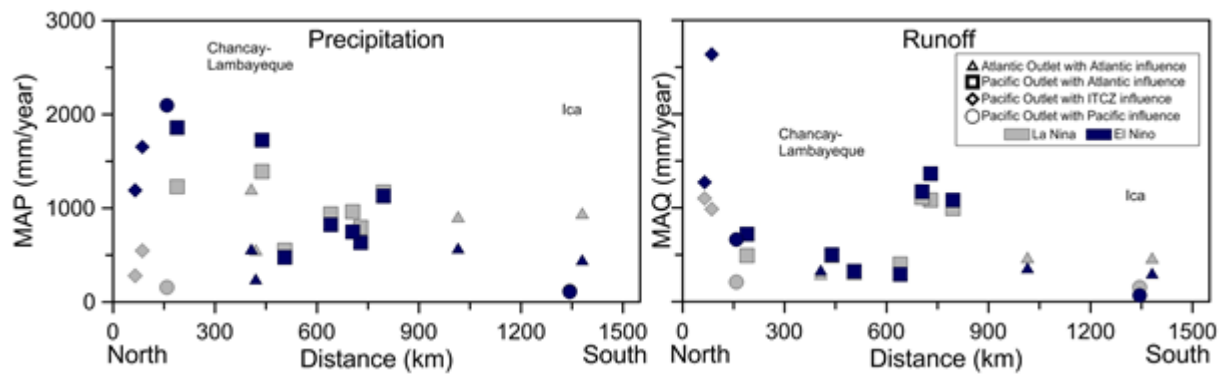
Figure 2.9: Mean annual precipitation (MAP) (a) and runoff (MAQ) (b) along Transect 1 for ENSO events according to air flux influence similar to Fig. 2.8.
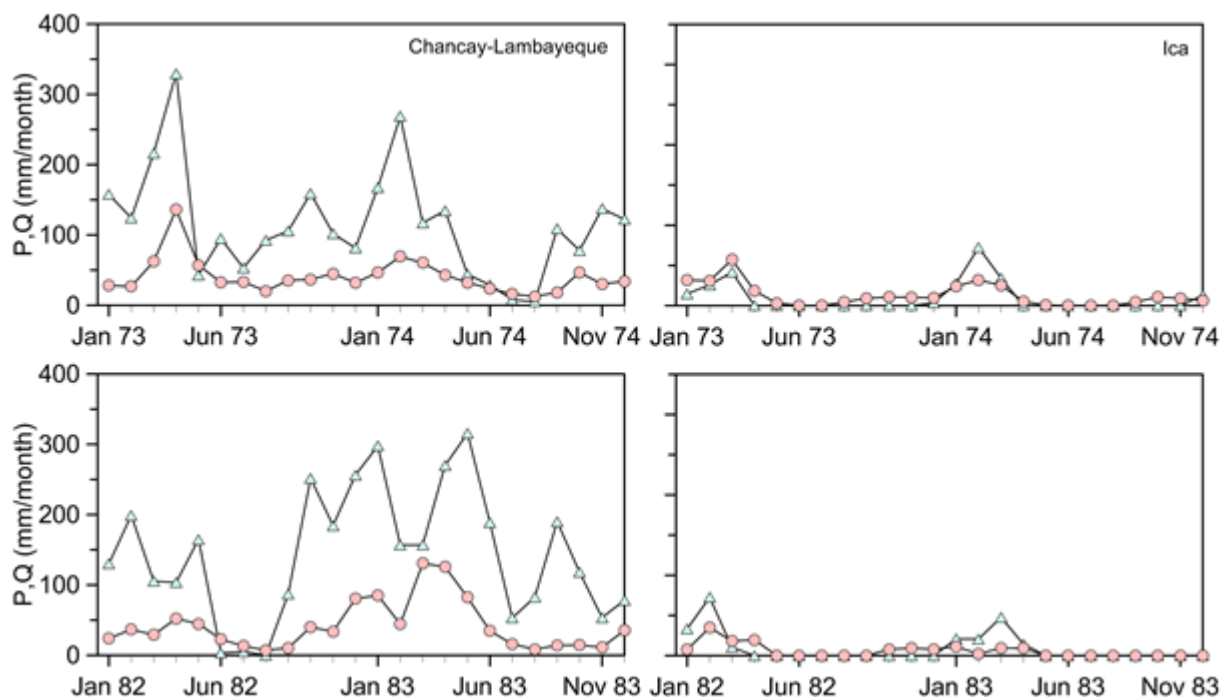
Figure 2.10: Monthly precipitation (triangles) and monthly runoff (circles) for La Niña 1973-1974 (top) and El Niño 1982-1983 (bottom) events. Chancay-Lambayeque basin which is a Pacific Outlet basin with Atlantic influence (left). Ica basin which is a Pacific Outlet basin with Pacific influence (right).

2.4 Conclusions

The analyses of precipitation and runoff data along topographic gradients in Peru and Austria showed that, overall, in Peru the spatial variation in seasonality is much larger than in Austria. This is because of the larger diversity in climate and topography.

In the Atlantic influenced Peruvian basins and most Austrian basins the strength of the seasonality of runoff is greater than that of precipitation. In Peru this is because evaporation is rather uniformly distributed throughout the year, which reduces the mean more than the amplitude. In most of the Austrian basins, snowmelt increases runoff seasonality relative to that of precipitation. In the Pacific influenced Peruvian basins, the strength of the seasonality of runoff is mostly smaller than that of precipitation at the coast which is due to the more uniform precipitation in the mountainous headwaters of these basins.

In the Peruvian basins with Pacific air flux influence, the strength of seasonality of precipitation during El Niño years is greater than during La Niña years, but the opposite is the case in basins with Atlantic influence, with an exception of Atlantic basins in the North of Peru. In Peruvian Pacific basins with Pacific influence and South Peruvian basins with Atlantic influence, the strength of seasonality of runoff during El Nino years is greater than during La Nina years, but the opposite is the case in the basins with Atlantic influence in the North of Peru.

The present analyses could be expanded by studying the dynamics of the water balance components in more detail, in particularly the role of catchment storage on the seasonality of runoff.

3 Runoff time scale disentangling and process interpretation by hydro-climatic regimes and landscape characteristics

3.1 Introduction

Hydrological runoff is the result of a diversity of processes at different scales and levels of contribution to the overall variability. Understanding the temporal characteristics of runoff is therefore useful for getting a better idea of runoff generation processes that would help with hydrological model building (Sivapalan and Blöschl, 2015).

The disentanglement of the runoff variability in terms of its process contributions can be performed by decomposition of the runoff time series components into different time scales and frequencies, and associated process analysis of each extracted contribution. The variance contributions of the runoff time series components (related to intra-annual, inter-annual and trend) reflect the role of storage and carry-over effects in the daily and monthly data series and contribute to a better assessment of storage related controls in distinct landscapes. Process controls are indexed by hydrological signatures such as hydro-climatic regimes and landscape characteristics (e.g. storage), contributing to the variability of the surface runoff. Even though these processes influence runoff at all scales, the intrinsic scales of their own dynamical variability are dominant in different scales: while the underlying atmospheric variability is dominant in the intra-annual dynamics within the seasonal cycle, the catchment process variability may dominates at longer, inter-annual, time scales. Longer time scale processes have relevance at both climate and landscape level (e.g. multidecadal oscillations, millennial landform), but those fall beyond the sampling time scale of the data used in the present chapter. Therefore, such very low frequency dynamics shall be treated as "trend variance".

Again due to limited data availability and the dominant cycles at play, in this chapter periodicity is related to cycles that can actually be observed as such, such as the seasonality character of runoff with short residence times in the storage reservoir. Longer cycles associated with such landscape-related inter-annual variability will be elusive as periodic controls since their wavelength may exceed the time interval covered by the data. The signature from storage in this sense is related to the portion of runoff from a reservoir source with a certain residence time in the catchment.

The time scales of runoff shed light on those of its underlying controls. A long groundwater process of several years may result in a water table emergence at a certain short time, affecting how runoff evolves from one day to the next. What a scale separation actually aims at is disentangling time scales of runoff controls from its spectral analysis.

The variability of each control can be detected via the explained variance in the resulting signal, i.e. the runoff series, for each time scale of interest, e.g. the one most relevant to hydro-climatic related periodicity, and the one most relevant to storage. The explained variance provides a measure of statistical predictability (or information content) associated with the corresponding underlying control. Therefore, the process contributing with the most explained variance to runoff is the one that has more statistical predictive power with respect to the runoff variability. The relative dominance of climatic vs. landscape characteristics in the runoff signature at different scales can thus be inferred.

With this, a hierarchy of process contributions, their dominant time scales and relative contributions to the runoff variability can be established. The hierarchy of classification

analyses will proceed from inter-annual variability (lower frequency events) to intra-annual variability (up to one year).

Once the dominant variability of runoff has been identified, it may help to simplify model building. Not all effects and influences of the complex overall process has to be formulated, it may suffice to consider only the effect of the identified dominant runoff mechanism. Thus, knowledge of the dominant variability is useful for the selection and hypothesis establishment of hydrological models, concentrating its formulation on meteorological or hydrological factors as well as storage effects (linear storage, cascade storage or nonlinear storage. The hydrological modelling of a catchment with dominant intra-annual variability may concentrate on the long-term water balance model, and dominant inter-annual variability may concentrate on the non periodical character of runoff process generation.

The main rationale behind the spectral decomposition stems from the importance of the time scales at play. Atmospheric processes may be dominant (albeit not exclusively) at shorter time scales, e.g. up to a year, with the astronomically driven annual or seasonal cycle. Hydrological processes taking place on such scales are thus mainly atmospherically driven, although catchment dynamics also has fast components (e.g. erosion due to intense rainfall and runoff). On the other hand, multiannual processes are mainly associated with the dynamics taking place at longer time scales, e.g. oceanic and landform processes (in that order of scale length). Therefore, their imprint on shorter time scale processes will consist of increasing their persistence or temporal coherence.

The residence time of water is the time of water retention in the subsurface before turning into surface runoff. The residence time may be inferred from the inter-annual signal (low frequency signal), which illustrates the shift from inter-annual components with short water residence times (such as snow and river storage with typically periodical dynamics) to those with longer residence times (especially groundwater) when long-term water storage variations are of concern (Güntner, et al., 2007). Thus, correlation lengths are closely related to the processes in the subsurface. Schädler (1990), Blöschl and Sivapalan (1995) and Schwarze (2007) have pointed out runoff generation processes and their prevailing discharge mechanisms from different storage compartments. The contribution of individual water storage compartments to total storage change varies with the climate region and the timescale under consideration (Güntner et al., 2007). Thus, we propose for the tested hydro-climatic regimes, a link between runoff processes and correlation lengths (Table 3.1).

Hydro-climatic regimes are related to runoff, which enables a catchment characterization in terms of the meteorological and hydrological conditions, which is then analysed in connection with the landscape components for the interpretation of the results. In hydrology, the characterisation of catchments in terms of hydro-climatic regimes does not imply that the landscape properties are ignored. Winter (2001) suggested that hydrological landscapes are multiples or variations of fundamental hydrological landscape units, and defined fundamental hydrological landscape units on the basis of land-surface form, geology and climate. By describing actual landscapes in terms of land-surface slope, hydraulic properties of soils and geology, and the difference between precipitation and evapotranspiration, the hydrological system of actual landscapes can then be conceptualised in a consistent way. Savenije (2010) argued that plateaus, hillslopes and wetlands are associated with different flow pathways, so the model structures for these units should also differ. This is particularly important in water-limited landscapes (Caylor et al., 2006). Wagener et al. (2007) and Gutknecht et al. (2008) summarised the storage and transport characteristics of a landscape by the notion of "catchment functions". In fact, hydro-climatic regimes and landscapes are intimately related

via coevolution processes. Both landscapes characteristics (e.g. elevation, slope, soil depth and storage capacity) and hydro-climatic conditions (e.g. precipitation, temperature, flow) result from landscape-climate coevolution and thus their spatiotemporal patterns express a legacy of such coevolution processes. Perdigão and Blöschl (2014) introduced a stylised model framework relating landscape and climate processes, in such a way that spatial properties in the landscape are indicative of dominant hydro-climatic regimes, and vice-versa. By having hydro-climatic information and knowledge on general coevolution mechanisms, the landscape including geological properties can be inferred, i.e. to each typical landscape (e.g. mountainous, wide plains, valleys) typical hydro-climatic regimes arise. Likewise, in the absence of geological information, the hydro-climatic feature (e.g. flow sensitivity to rainfall and temperature) is informative of such geological properties. For instance, a swift hydro-climatic response is associated to shallow soils and rather limited storage capacity. The geology is embedded in the hydro-climatic dynamics. The interaction of climate and landscape is very close, under the premise that there is a certain landscape under certain climate conditions and vice versa. Therefore, the characterisation of hydro-climatic regimes is thus a surrogate that indirectly provides information on the most likely landscape properties.

Table 3.1: Correlation lengths for different processes controlling runoff variability.

Correlation length	Up to hours	Days	Weeks	Months	Years
Weather and Climate processes	Abrupt frontal transitions; mesoscale, convective storms	Progressive Synoptic depressions	Synoptic depressions under blocking (a); persistent lack of rain from high-pressure blockings (b)	Seasonal (e.g. semi-annual, annual cycles)	Climate variability (e.g. ENSO dynamics)
Associated Precipitation features	High intensity, short duration	Variable intensity and duration	Large accumulated rainfall volumes in (a); persistent scarcity in (b)	Oscillatory driven by seasonal cycles	From interannual trends to multidecadal fluctuations
Associated Temperature features	Abrupt cooling/warming across cold/warm front	Oscillatory (diurnal cycle)	Intra-seasonal trends and inter-storm fluctuations	Oscillatory driven by seasonal cycles	From interannual trends to multidecadal fluctuations
Soil profile	Overland flow	Upper soils, shallow soils	Deeper soils	Groundwater	Groundwater
Runoff generation response	Horton / subsurface overland flow (HOF, SOF)	Subsurface flow (SSF)	Fast groundwater (FGW)	Slow groundwater (SGW)	Slow groundwater (SGW)
Water balance	See above	See above	Process interplay (e.g. precipitation, temperature, soil moisture dynamics)	Dynamics of soil moisture regimes	Dynamics of soil moisture regimes

The organisation of the results in hydro-climatic regimes allow to apply the "comparative hydrology" concept (Falkenmark and Chapman, 1989) where spatial differences in the processes are exploited to better understand the controls and their effects. For example, in an arid regime the main control on evaporation will be the water availability while in a more

humid regime (or wet parts of the landscape, e.g. a flood plain) the main control will be the energy.

The aim of this chapter is to determine the dominant runoff variability relative to hydro-climatic regimes; and the storage effect in the runoff process generation of the inter-annual component through the correlation length. The paper is set in Peru where very large hydrological gradients exist. These gradients assist in identifying dominant processes based on runoff time scales.

Section 3.2 of this chapter summarises the data used, the methodology as well as the hydro-climatic regimes and landscape features of the study catchments. Section 3.3 presents the results of the correlation lengths of precipitation and the runoff components. The section presents the analysis for a common series (1964-1968), and for longer, complete time series. These are organized by hydro-climatic regimes. In addition, the analysis stratifies the data by filling and depletion phases of runoff. Section 3.4 discusses the results of the previous section and proposes a catalogue based on the dominant runoff variability related to the correlation length of runoff. Finally, section 3.5 summarises the conclusions of the chapter.

3.2 Data and methodology

3.2.1 Data

The hydrological data used in this study consist of daily discharge records for different uninterrupted series in the period 1927–1996 of six catchments with diverse hydro-climatic conditions from Peru. The long-term data set contains at least 10 years of uninterrupted records. Discharge data were used from gauging stations in catchment areas ranging from 64 to 3496 km², with mean catchment elevations from 1857 m above sea level (m.a.s.l.), up to the high Andean catchments with mean catchment elevations of 4792 m.a.s.l. Mean annual precipitation ranges from 537 mm/year in the west to 1262 mm/year in the east, where orographic effects of the Amazon tend to enhance precipitation. Mean annual precipitation and temperatures at the climate stations (Table 3.2) were used as a reference for discussing the dominant variability of runoff. All input data were carefully screened for errors and, where possible, the data were corrected. Otherwise they were removed from the data set.

Catchment rainfall was taken from MEM (2011), which elaborated a precipitation map of Peru from satellite data of the Tropical Rainfall Measuring Mission (TRMM) and precipitation station data of the National Service of Meteorology and Hydrology SENAHMI. The results were interpolated by cokriging using a Digital Terrain Model to estimate precipitation for areas without precipitation records. Catchment rainfall was calculated from the generated grids in the catchment areas by using HEC-GEOHMS. Soil characteristics were taken from the Soil Map elaborated by MINAG (2009).

3.2.2 Statistical method: Time Series Analysis

Our aim is to disentangle contributions from atmospheric and catchment/hydrological processes, namely the annual cycle associated to atmospheric dynamics from fast event-scale processes and slow hydrological processes at the level of storage dependent flow. For this purpose, a linear scale separation of the flow time series is conducted whereby the following steps are taken:

1. Detrending: The trends are calculated and removed from the series, thus leading to detrended series.

2. Smoothing: The direct contributions from high frequencies are then extracted, with the remaining terms of the Fourier series producing a smoothed time series for each catchment. This procedure is essentially a low-pass filter, whereby only the frequencies lower than 1/d, d=cut-off day for smoothing (akin to smoothing window size) are retained. It was selected for d = 3 days, considering that the shorter the low-pass filter (up to data resolution) is, the more deseasonalised variability will be conserved.

3. A deseasonalisation is also conducted whereby the harmonics with periods of up to one year are removed from the detrended series. This is akin to a low-pass filter where only the inter-annual signals are left. A deseasonalised series is then obtained by Fourier expansion of the remaining frequency modes.

The purpose of the study is to disentangle runoff timescales and associated controls in order to study their relative contribution to the overall runoff variability and volume. The components contributing to the variability of surface runoff are calculated from their respective variance.

- Intra-annual part: it is the variance of the signal composed by integrating the Fourier harmonics within the intra-annual period (between 3 and 365 days).
- Inter-annual part: it is the variance of the signal comprising the harmonics with periods exceeding one year till the record length i.e. that of the deseasonalised signal produced in step 3 above.
- Trend part: the variance of the harmonics truncated out during detrending, i.e. of very low frequency signatures appearing as trends in the original series due to the practical limits in the time window resolved by the data (periods exceeding the record length).

The three parts are then expressed in percent of the total variance of runoff. A hierarchy of components in terms of contributed variance can then be established, beginning with the one having the highest variance down to the variance of the residuals.

4. Linear autocorrelations are then computed mainly for the deseasonalised cycle (contributions from inter-annual variability) in the results section. In hydrology inter-annual scales may be perceived as year-to-year carryover. It is thus important to clearly state that in the broader scientific sense inter-annual scales span everything from 1 year onwards, e.g. even 1 year and 1 day.

By associating a time series (signal) to an underlying physical process in the light of process understanding, its autocorrelation can thus be interpreted as informing on the linear memory of that process. That way, the autocorrelation of a deseasonalised time series will relate to the linear memory of the inter-annual processes, whereby the intra-annual cycle is no longer a direct factor.

The intra-annual and inter-annual contributions to the variability in runoff can be interpreted in terms of intervening processes and respective time scales by resorting to Table 3.1. Both climate and hydrological processes span all time scales under analysis, and so do their impacts on runoff generation. Still, in the intra-annual scales there is dominance in the atmospheric

variability, whereas non-atmospherically forced hydrological variability is dominant in the inter-annual scales.

Hydrological processes with variability at intermediate scales (e.g. the intra-annual component of groundwater dynamics) owe their dynamics to the interaction between the faster atmospheric scales (that would otherwise drive faster responses) and the buffering, storage effect from the low-pass filter exerted by the catchment depending on its storage capacity. In terms of variability of the intervening processes, it is the atmospheric variability that exerts dominant control in the monthly scales, as the landscape features are not changing significantly in those time scales. That is, although the runoff volume is strongly conditioned by both atmospheric dynamics and landscape features at the intra-annual scales, its variability is mainly atmospherically driven, as the landscape is more often a filter rather than an agent at those time scales.

Both the atmosphere and the landscape play a crucial role in runoff at all scales, but the contribution of landscape-related variability mainly takes place at slower, inter-annual scales whereas the variability in atmospheric processes is mainly within the intra-annual scales. This can be seen by a typical exponential decay of the autocorrelation of the deseasonalised signal of runoff, which is consistent with the response of a linear reservoir to white noise.

Autocorrelation can be seen as a surrogate, or proxy, of storage, informing about the evolution of that quantity. The correlation length is obtained from the autocorrelation function of the deseasonalised series (inter-annual series), and expressed in terms of correlation length (table 1). The correlation length refers to the e-folding distance (or time) at which the autocorrelation function is the inverse of the Eulerian constant ($1/e = 1/2.718$, as in Blöschl 1996, p. 57).

Our interpretation of the correlation length is related to the activation of the soil profile part, in which the water contribution of the soil storage compartment is dominantly represented in surface runoff. This assumption implies that, if the correlation length is shorter, the dominant active soil storage compartment and runoff processes will be closer to the surface, and if the correlation length is longer, the dominant active soil storage compartment and runoff processes will be deeper in the subsurface. In hydrological terms, the overland flow will be related to a correlation length up to hours and will come from the land surface. The interflow or subsurface flow will be related to a correlation length of days and will come from the upper or shallow soils. The fast groundwater will be related to a correlation length of weeks and will come from the deeper soils, and the slow groundwater will be related to a correlation length of years and will come from deep aquifers. All correlation lengths are associated with the storage-dependent flow with the exception of correlation lengths of up to hours, which are associated with "atmospheric-forcing" dependent flow.

3.3 Study catchments

In order to assist in the climate-based interpretation of the hydrological regimes, we identified six climate regimes in Peru, and for each regime with selected one typical catchment. We use the Peruvian climatological distribution/scale in terms of humidity and temperature. This is a relative classification for our study since, for global standards, most Peruvian regions are rather dry. The delineation of the regimes enables a catchment characterization in terms of the meteorological and hydrological conditions, which is then analysed in connection to the landscape components for the interpretation of the results.

Choice of hydro-climatic regions as proxies for regional hydrological processes is based on the rationale of the existence of typical climates for typical landscapes. The evaluation and characterisation of catchments in terms of hydro-climatic regimes does not mean that the landscape properties are ignored. As noted before, they are intimately related via coevolution processes. Therefore, the characterisation of hydro-climatic regimes is a surrogate that indirectly provides information on the most likely landscape properties. For example, the climate regime and the terrain slope impact on soil loss or soil accumulation with typical profiles from the headwaters to the river mouth into the ocean. Similarly, vegetation is conditioned on the precipitation and temperature regimes.

Figure 3.1 shows the location of the runoff stations in the selected catchments. Figure 3.2 shows an artist's view of the catchment types from the headwaters to the runoff station, in particular our perception of the runoff generation processes as controlled by the landscape characteristics. Each perceptual catchment and hydro-climatic type is represented by one Peruvian catchment which the corresponding dominant processes. Below, each hydro-climatic catchment type is described regarding climate and landscape features.
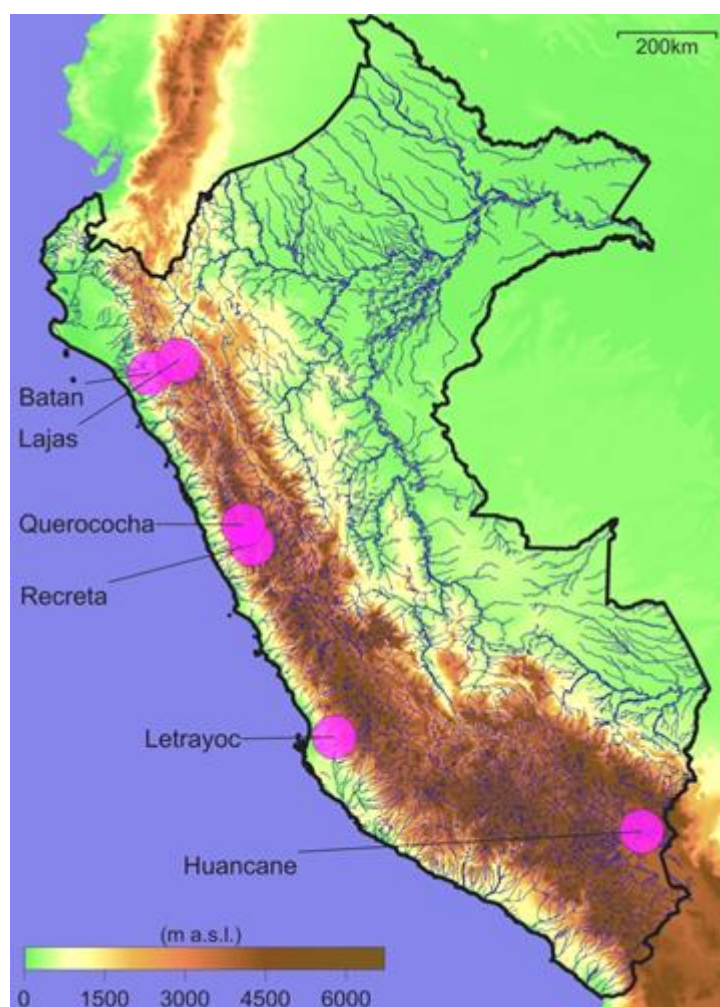
Figure 3.1: Location of the runoff stations in selected catchments.

The **''semi-arid warm regime''** is represented by the Zaña – Batan catchment located at the Pacific in the north of Peru (Fig. 3.1). Runoff generation is mainly produced by precipitation over the high mountains, which strongly affects the soil moisture variability (MINAG, 2010; ONERN, 1972). The overall climate is dry warm to semi dry warm. The soil texture is from

medium to coarse, including gravel. The soils in the lower catchment are deep and developed from recent fluvial sediments (Fluvisols). In the upper catchment they are shallower and developed from varying compositions (Leptosols and Regosols). The geology consists of sedimentary, igneous and metamorphic rocks as well as alluvial- and river deposits. The vegetation is composed of cloud forest (upper region), forests, shrublands, grasslands and crops.

The **"very humid and cold regime with lake influence"** is represented by the headwater of the Santa catchment (Recreta), where a prominent lake (Conococha Lake), located 13 km upstream of the stream gauge, takes up 13% of the catchment area. The hydrological situation is strongly influenced by the effect of the evaporation of the lake and its surrounding wetlands (Baraër et al., 2015; Kuroiwa, 2001). The climate is very humid and cold, marked by two precipitation seasons: a wet period during the austral summer (October to April) and a dry period during the austral winter (May to September). The catchment has both shallow and deep soils, usually developed from alluvial sediments, sedimentary rocks and volcanic rocks, generally with medium texture, including gravel (Leptosols, Cambisols). The geology is defined by moraine deposits and associated sand, clay and gravel fillings of varying depths, permeability and faults. The vegetation is mainly composed of grass and pasture. The valley is wide with humid plains and a high Andean plateau landscape.

The **"very humid and cold regime with glacial influence"** covers most of the catchments in the Cordillera Blanca along the Santa River, and is represented in this paper by the Querococha catchment. The stream gauge is located immediately below the Querococha Lake which is of glacial origin and takes up 2% of the catchment area. Runoff generation in the catchment is strongly affected by snow and glacier melt (Baraër et al., 2015; Kuroiwa, 2001). The mean annual temperature is less variable than the daily temperature. The daily temperature amplitude is higher in the dry season than in the wet season, due to higher direct ground access of solar radiation in the dry season than in the wet season, and due to the higher cloud coverage in the wet season, since clouds attenuate the solar input reaching the ground during the day and reduce thermal losses by ground-emitted radiation during the night both by reflecting long-wave radiation back into the ground and from emitting such radiation themselves. Therefore, snowmelt, which is strongly influenced by the daily temperature variations with sustained periods during the day having temperatures above freezing level, is more significant in the dry season. This effect has a direct consequence in the water balance through decreasing evaporation with altitude. The climate is very humid and cold. The precipitation regime has the same temporal variation as in the Santa River. The soils of the lower catchment are deep and have developed from colluvial-alluvial deposits with few coarse fragments up to 70 cm of depth (Regosols). Soils in the upper catchment developed from sedimentary and volcanic rocks with coarse fragments. Medium texture predominates in the whole catchment (Leptosols). The geology is defined by meta-sedimentary rocks (Baraër, 2012), moraine deposits with sand, clay and gravel of varying permeability. Sedimentary fill of the glacial valley is the main aquifer, assuming that water infiltration occurs through the fissure systems of the rock massifs, which are recharged by precipitation and melt water from thawing ice in the glacial foreland (Vilímek et al, 2005). The vegetation consists of grass and pasture.

The **"semi-humid temperate regime"** covers the South Pacific area of Peru, and is represented here by the Pisco – Letrayoc catchment (MINAG, 2003). Rainfall is lower than in the northern Pacific regime mainly due to the strong influence of the Humboldt storm systems and to a lesser extent due to the overall circulation in the Intertropical Convergence Zone (ITCZ). Runoff is produced by precipitation from the humid part of the catchment over 2400

m.a.s.l., which represents 62% of the total catchment area. The predominant climate types are semi humid micro thermal, humid tundra, and humid. Soils have medium texture, and vary from very shallow with presence of gravel in the lower part of the catchment (Leptosols), to deep soils with some gravel in the upper catchment, originated from different lithologies (Regosols). The geology is consists of sedimentary, igneous and metamorphic rocks, and faults exist. The vegetation is composed of natural grasses such as "stipa ichu", half desert forest and savanna forest vegetation.
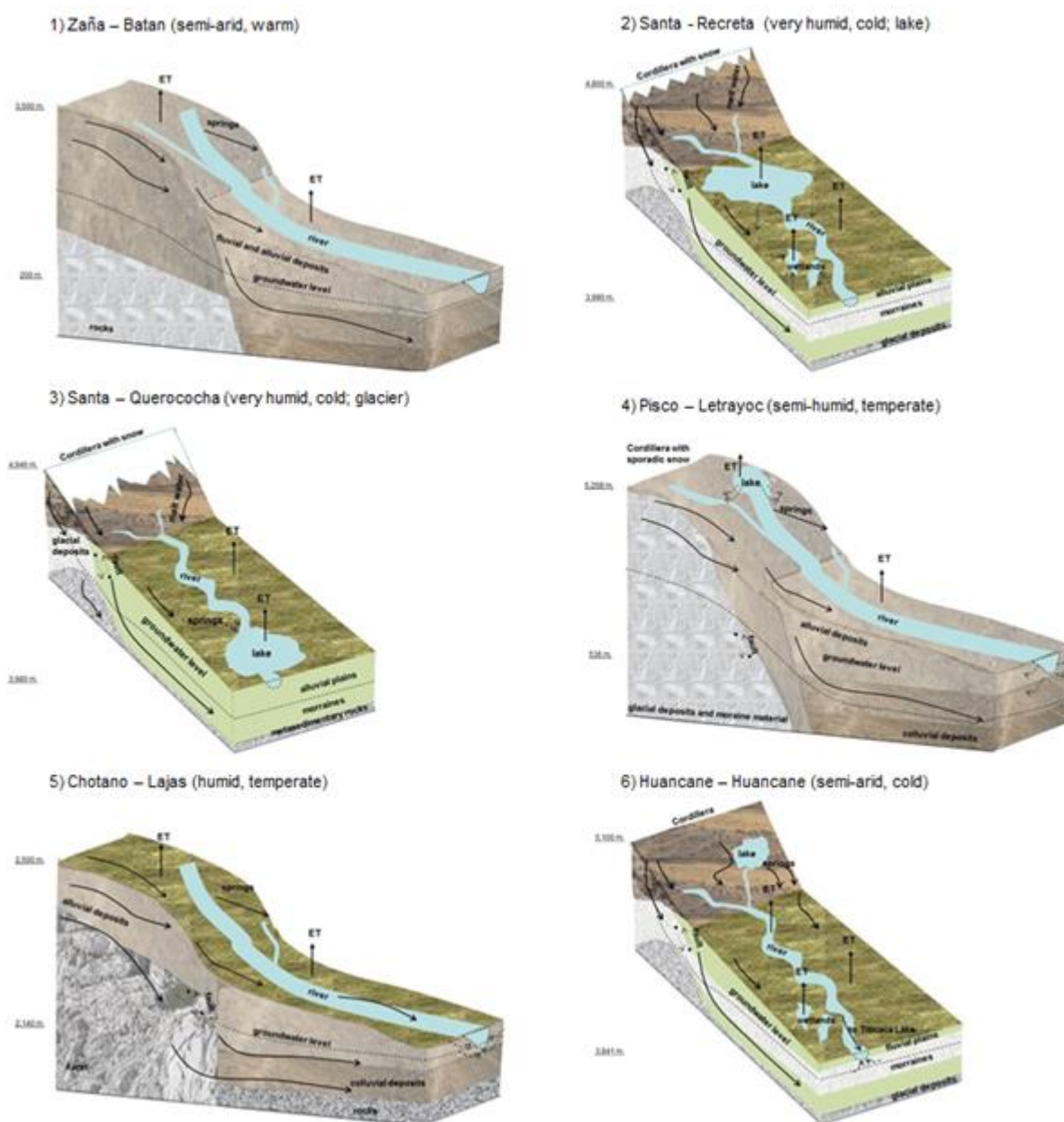
Figure 3.2: Artist's view of the six catchments that are considered representative of the six hydro-climatic regimes (see Table 3.2).

The **"humid temperate regime"** is represented by the Chotano – Lajas catchment (MINAM, 2010; ONERN, 1977). The Chotano is a tributary to the River Marañon which is, in turn, a tributary to the Amazon. The climate is humid and temperate, with precipitation occurring throughout the whole year. The soils are shallow with medium texture (Leptosols). They have developed from sedimentary and volcanic rocks with a high content of coarse fragments on

the surface, underlain by the rock or skeletal horizon. The catchment topography is rather flat and the geology is composed of alluvial and fluvial deposits, along with a strongly folded and faulted structure. The vegetation is mature, with predominating forests and crops.

The **''semi-arid cold regime''** is represented by the Huancane catchment, located North of the Titicaca basin (UNEP and OAS, 1996). The climate is predominantly dry and cold, with drier falls, winters and springs, and wetter summers. The soils of the lower catchment are shallow (Regosols and Cambisols), those of the upper catchment are deep (Regosols). They have developed from various lithologies. Their texture is medium to coarse. The geology is composed of glacial moraines with faults, river sediments on the foothills and plains, and lacustrine and evaporite formations in the central part of the plains. The vegetation is composed of natural grasslands.

Table 3.2 summarises the hydrological characteristics of the six catchments that are typical of the six hydro-climatic regimes. The characteristics include statistical signatures of runoff (mean annual runoff, Pardé coefficient, low and high flow statistics normalised by the mean annual runoff, and the correlation length) which were calculated from the runoff series. Figure 3.3 and Figure 7.1 provide additional hydrological characteristics.

Table 3.2: Six catchments representing hydro-climatic regimes according to precipitation and air temperature.

Hydro-climatic Regime/Characteristics	Semi-arid warm catchment	Very humid and cold with lake influence catchment	Very humid and cold with glacial influence catchment	Semi-humid temperate catchment	Humid temperate catchm.	Semi-arid cold catchm.
Station	Batan	Recreta	Querococha	Letrayoc	Lajas	Huancane
Catchment	Zaña	Santa (river origin)	Santa (tributary)	Pisco	Chotano	Huancane
Area (km^2)	673.0	289.0	64.3	3496.0	356.0	3400.0
Mean altitude (m.a.s.l.)	1857.0	4299.3	4792.0	3460.3	2858.0	4266.0
Mean catchment slope (%)	2.84	2.22	3.80	3.67	2.3	0.08-3.5
Mean annual temperature (°C)	18.0	7.9	7.3	8.4	16.6	7.0
Mean annual precipitation (mm yr^{-1})	795.0	916.0	1029.0	537.0	1262.0	691.0
Max. Pardé coefficient of precipitation and month of occurrence	2.3 March	2.6 March	1.9 February	2.0 March	2.0 March	2.5 January
Mean annual runoff (mm yr^{-1})	340.4	367.9	831.1	232.4	702.5	172.5
Max. Pardé coefficient of runoff and month of occurrence	2.3 April	3.8 March	2.2 March	2.3 March	2.3 March	3.2 February
Normalized low flow q95 (-)	0.17	0.13	0.20	0.04	0.05	0.08
Normalized high flow q05 (-)	2.50	3.54	2.61	4.15	3.51	3.88
Correlation length - Time lag (days) original series	32	11	19	9	13	13
Runoff coefficient	0.43	0.40	0.81	0.43	0.56	0.25
Aridity index	2.26	1.32	1.00	1.69	0.77	1.81
Runoff time series	1964-1993	1960-1973	1955-1973	1927-1971	1960-1996	1957-1974
Precipitation time series	1963-2004	1998-2007	1966-2001	1966-1987	1970-2010	1964-2009
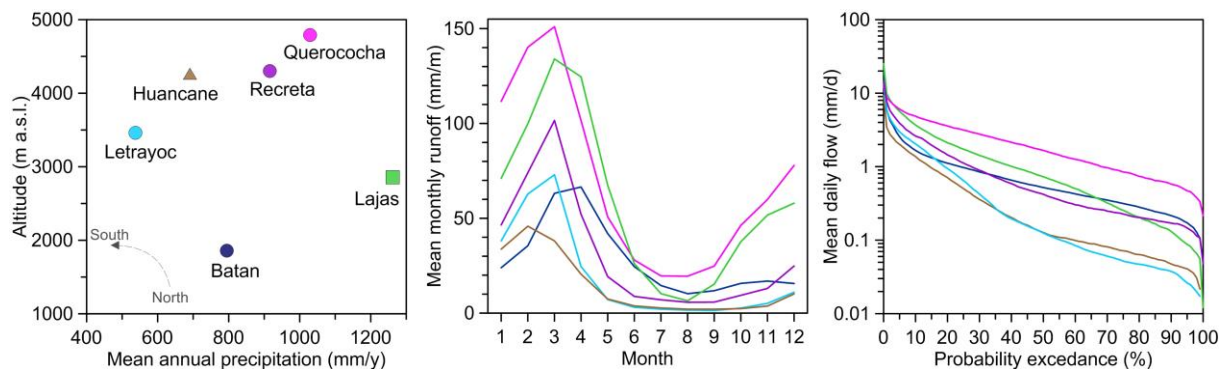
Figure 3.3: Characteristics of the six catchments representing six hydro-climatic regimes. Left: mean annual precipitation vs. mean catchment altitude. Centre: mean annual runoff regimes. Right: daily flow duration curves.

3.4 Results

3.4.1 Correlation lengths of precipitation and runoff components

Figure 3.4 shows the autocorrelation plots of the original precipitation time series (P) and runoff time series (Q) of the six catchments. As would be expected, the runoff series show a much more persistent behaviour (higher autocorrelation) than the precipitation time series. This is because of the storage effects of the catchments. Clearly visible too is the effect of the annual periodicity imposed by catchment processes (evaporation and snow), as a more pronounced minimum at a lag time (delay time) of 180 days. The figure also shows the curvature of the autocorrelation plot with the influence of the intra-annual signal (up to one year). The inter-annual signal and the between intra-annual and inter-annual signal are not clearly identified at first sight.
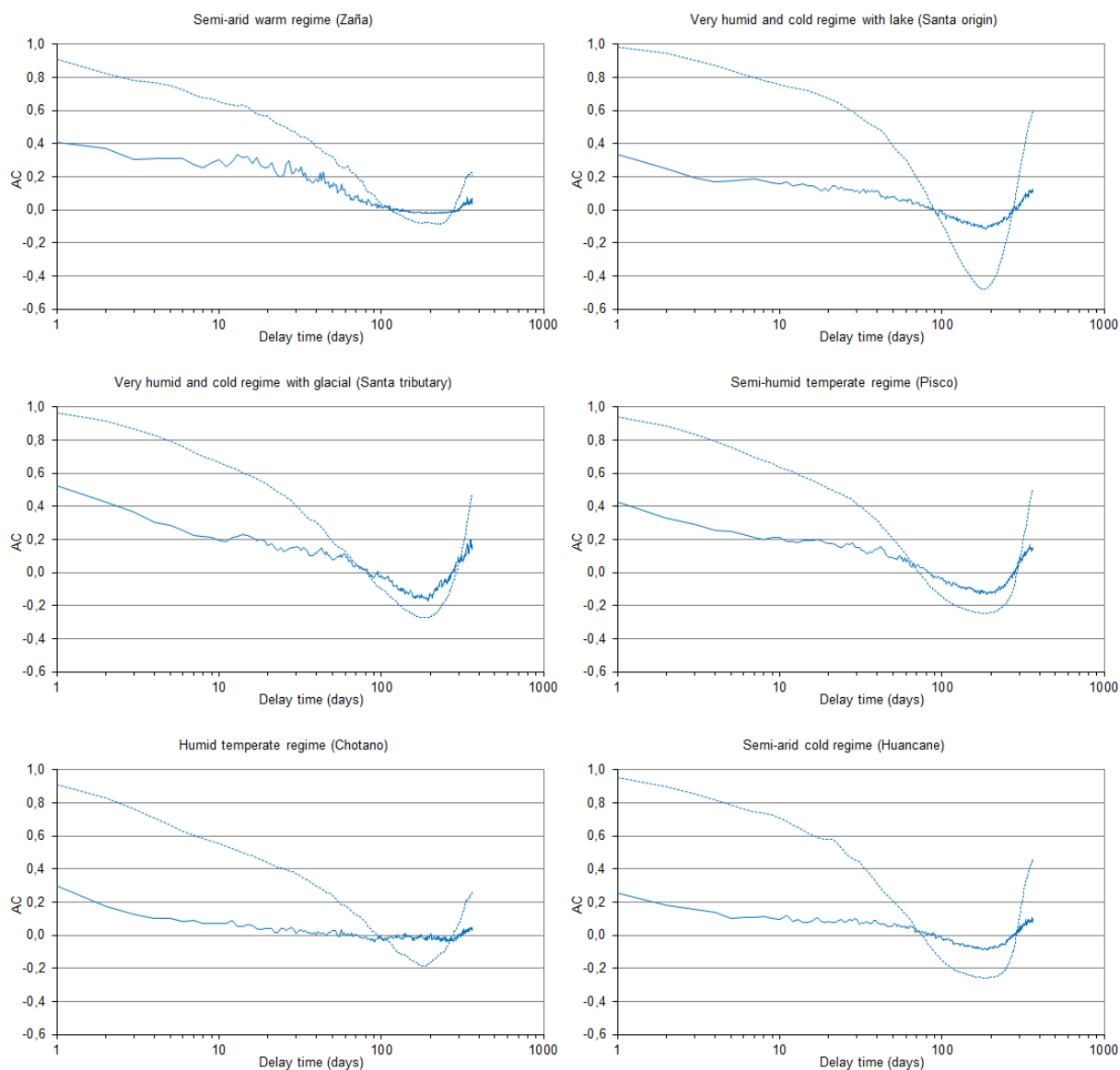
Figure 3.4: Autocorrelation plot of the original precipitation time series (line) and runoff time series (dotted) of the six catchments representing six hydro-climatic regimes. Period of time series according to the table 3.2.

Figure 3.5 shows the autocorrelation plot of the original and deseasonalised runoff time series. As can be seen, the minimum in autocorrelation which is a result of the seasonal runoff cycle, is removed due to the deseasonalisation. The difference of the correlation length of the original and the deseasonalised runoff represents the persistence of the intra-annual series, which varies for these regimes between 11 and 33 days.

3.4.2   Comparison between basins for the common series 1964-1968

The purpose of this section is to compare the catchments in terms of the dominant controls on the runoff for the common period (1964-1968) where data are available in all catchments.

Figure 3.6 (top) suggests that the largest intra-annual and smallest inter-annual variability is observed in the very humid and cold regime with glacial influence. This is due to the strong seasonal behaviour of snow and glacier melt, and may also be related to a major groundwater component in the glaciered valleys of the Cordillera Blanca (Baraër, 2012) during the dry

season. This regime differs from the second largest intra-annual variability (semi-arid cold regime), which has no snowmelt. The smallest intra-annual variability is found for the humid temperate regime.
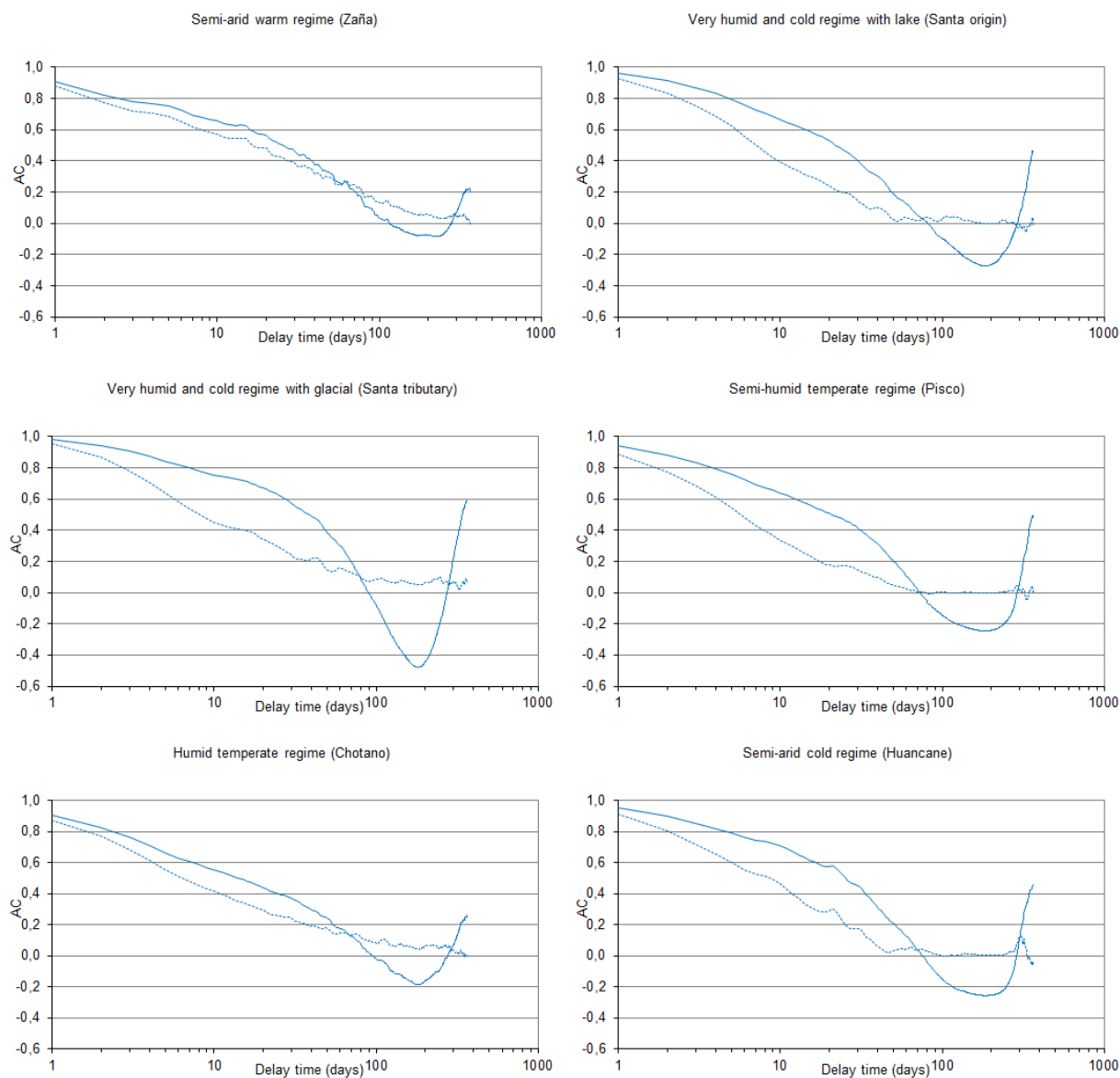
Figure 3.5: Autocorrelation plot of the original signal (line) and inter-annual signal of surface runoff (dotted) series for the six hydro-climatic regimes. Delay time is presented in log-scale. Period of runoff time series according to the table 3.2.

The largest inter-annual variability is observed for the very humid and cold regime with lake influence and semi-humid temperate regime. This is a slightly greater dominance than that for the humid temperate regime. The conditions are quite specific, for example the lake and wetlands in the very humid and cold regime with lake influence, which affect the hydrological system. The semi-humid temperate regime may have soils that impose threshold effects on the runoff regime.

Runoff time scale disentangling and process interpretation by hydro-climatic regimes and landscape characteristics
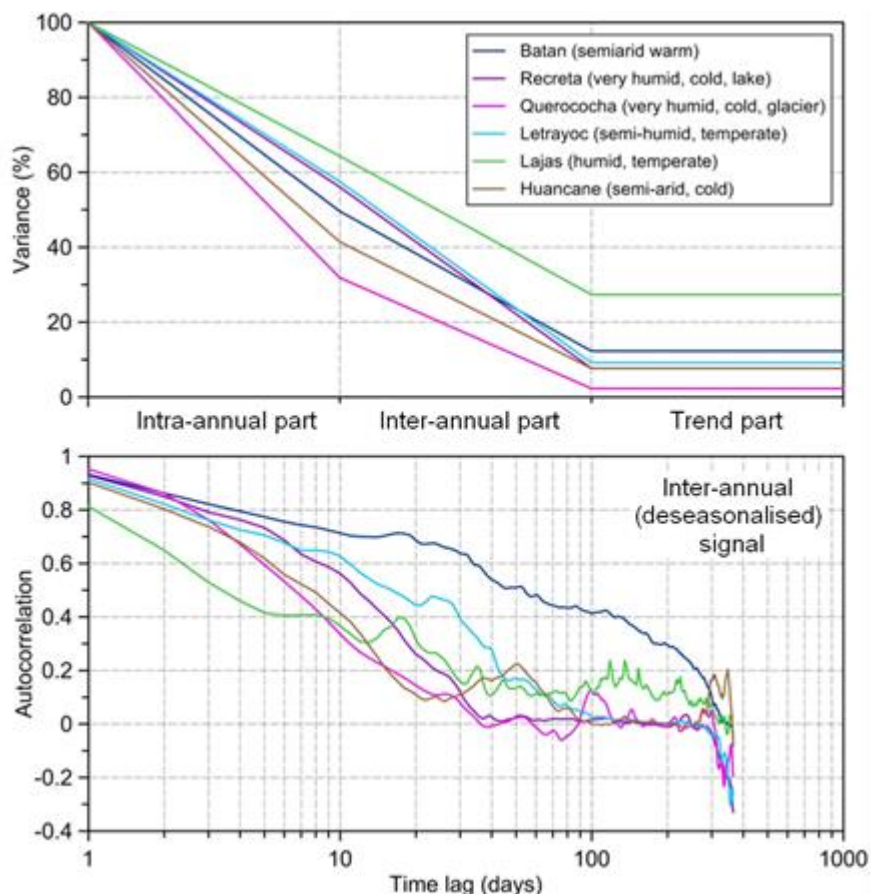
Figure 3.6: Common runoff series 1964-1968. Top: Contributions of intra-annual, inter-annual and trend variance (see section 3.2.2) to runoff in the six catchments. Bottom: autocorrelation plot of the inter-annual (deseasonalised and detrended) signal.

Table 3.3: Percent of intra-annual, inter-annual, and explained variance for the common runoff series 1964-1968 as well as the correlation lengths of the inter-annual (deseasonalised and detrended) runoff. Percent of dominant variability printed in bold.

Hydro-climatic regime /Station	Intra-annual Variability	Inter-annual Variability	Explained Variability (intra + inter)	Correlation length (days)
Semi-arid warm/ Batan	**50 %**	37 %	87 %	144
Very humid and cold regime with lake influence / Recreta	44 %	**48 %**	92 %	17
Very humid and cold regime with glacial influence / Querococha	**68 %**	30 %	98 %	10
Semi-humid temperate / Letrayoc	43 %	**48 %**	91 %	32
Humid temperate / Lajas	36 %	**37 %**	73 %	10
Semi-arid cold / Huancane	**59 %**	34 %	93 %	11

The longest correlation length of 144 days is shown by the runoff in the semi-arid warm regime (Table 3.3, Figure 3.6 bottom). This points to a slow groundwater influence according to Table 3.1. The shortest correlation length of 10 days is shown by the runoff in the very humid and cold regime with glacial influence. At this point, we can observe that the very humid and cold regime with glacial influence not only exhibits the largest intra-annual and

smallest inter-annual variability, but also the shortest correlation length. The common series is useful for comparison, but because of the relatively short runoff record length the results should be treated with caution. Below, the full records are analysed.

3.4.3 Analysis of the long series

Long series have the potential to better represent the long-term behaviour of the regime, the dominant variability and the correlation length for dry and wet years. The long series were chosen as uninterrupted, enabling a more robust assessment of the average responses of runoff to its underlying mechanisms in the catchments.

Figure 3.7 (top) shows the distribution of intra-annual, inter-annual and trend variance. The largest intra-annual and smallest inter-annual variability in the long term is observed in the very humid and cold regime with glacial influence. The smallest intra-annual and largest inter-annual variability is observed in the semi-arid warm regime. This is attributed to the carry-over interactions of water soil storage, i.e. the soil water storage released in periods without rain. The longest correlation length (Figure 3.7, bottom) of 32 days occurs in the semi-arid warm climate pointing to the existence of slow groundwater. The shortest correlation length of 9 days occurs in the semi-humid temperate regime. The semi-arid warm regime not only exhibits the smallest intra-annual and largest inter-annual variability, but also the longest correlation length. Table 3.4 provides the number of the estimated variances and correlation lengths.
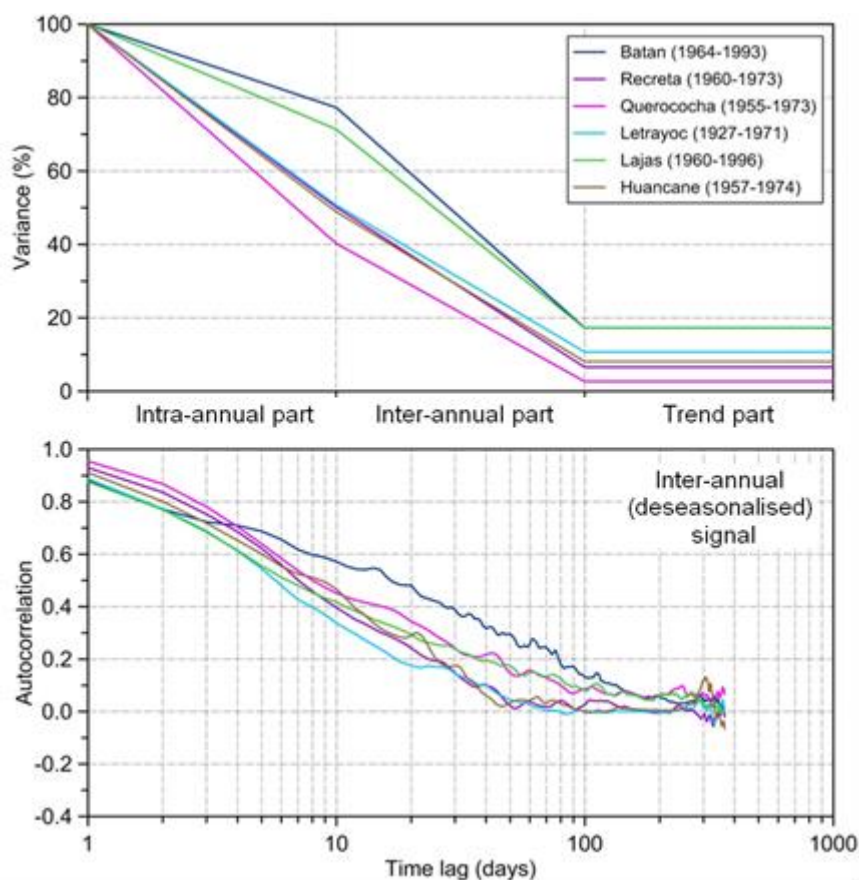
Figure 3.7: Long runoff series (see Table 3.2). Top: Contributions of intra-annual, inter-annual and trend variance (see section 2.2) to runoff in the six catchments. Bottom: autocorrelation plot of the inter-annual (deseasonalised and detrended) signal.

Table 3.4: Percent of intra-annual, inter-annual, and explained variance for the long runoff series (see Table 3.2) as well as the correlation lengths of the inter-annual (deseasonalised and detrended) runoff. Percent of dominant variability printed in bold.

Hydro-climatic regime /Station	Intra-annual Variability	Inter-annual Variability	Explained Variability (intra + inter)	Correlation length (days)
Semi-arid warm/ Batan	23 %	**60 %**	83 %	32
Very humid and cold regime with lake influence / Recreta	**50 %**	44 %	94 %	11
Very humid and cold regime with glacial influence / Querococha	**60 %**	38 %	98 %	19
Semi-humid temperate / Letrayoc	**49 %**	40 %	89 %	9
Humid temperate / Lajas	29 %	**54 %**	83 %	13
Semi-arid cold / Huancane	**51 %**	41 %	92 %	13

The variability of the inter-annual component is dominant for the semi-arid warm and humid temperate regimes. The soil water storage capacity in the semi-arid warm regime seems to be greater than the annual water input to the system, and releasing water to the river may be less regular than in other regimes. The soil water storage in the humid temperate regime is more limited in relation to the water input to the system, and releasing flow to the river may be more regular than in semi-arid regimes.

Some part of the runoff variability long series (Table 3.4) is different from those of the common series (Table 3.3). This is because the common series may not include a large spectrum of dry years and wet years. The may be particularly relevant for regimes where evaporation (aridity index) plays an important role in the annual water balance such as in the semi-arid warm and semi-humid temperate regimes. In the case of the very humid and cold regime the existence of a lake and surrounding wetlands (Recreta) may exert a stronger influence on the runoff regime through evaporation than alternative dry and wet years.

3.4.4 Differentiation of phases in the runoff regime

The long runoff time series were, for each year, divided in two phases: (a) the filling phase which is defined as the recharge period when the soil water storage is replenished as indicated by increases in the hydrograph; and (b) the depletion phase which is defined by the discharge period or release of the soil water storage to the river flow as indicated by decreases in the hydrographs. Each phase is taken as full months, i.e. from the first day of the month when the phase starts, to the last day of the month when the phase ends. The months of the phases are assumed to be the same in every year.

This section tests whether the dominant runoff variability and the correlations lengths differ between the filling and depletion phases. The inter-annual variability (Table 3.5) is dominant in all hydro-climatic regimes with the exception of the semi-arid cold regime (intra-annual variability) in the filling phase and the semi-arid warm and humid temperate regimes in the depletion phase. The strongest dominant variabilities are found in the semi-arid warm, humid temperate and semi-arid cold regimes in both phases. The semi-arid warm and humid temperate regimes show the strongest and dominant inter-annual variability. Humid temperate regimes show no clear dominant variability in the common series (Table 3.3). This clear dominance is observed principally in the filling phase.

Figure 3.6 gives the correlation lengths for both phases. The correlation length is obtained from the autocorrelation function of the deseasonalised (inter-annual) runoff for each phase. Introducing our interpretation of the correlation length (Table 3.1), the soil water contribution to runoff in the filling phase for the semi-arid warm, and humid temperate regimes comes from the upper soils with a correlation length of 13 and 11 days, respectively (Table 3.6). In the depletion phase, the runoff contributions come from the deeper subsurface with correlation lengths of 28 and 23 days, respectively. The reaction of the soil water contribution in the very humid and cold regime with glacial influence occurs in opposite phases as in the previous regimes. The filling phase is concentrated in the accumulation of snow, which is reflected in a correlation length of 24 days. The depletion phase has a correlation length of 9 days.

Table 3.5: Percentage of intra-annual and inter-annual variability of runoff for the six hydro-climatic regimes for the filling and depletion phases. Percent of dominant variability printed in bold.

Hydro-climatic regime/ Station	Filling phase		Depletion phase	
	Intra-annual variability	Inter-annual variability	Intra-annual variability	Inter-annual variability
Semi-arid warm/ Batan	20 %	**58 %**	25 %	**57 %**
Very humid and cold regime with lake influence/ Recreta	32 %	**58 %**	**59 %**	34 %
Very humid and cold regime with glacial influence/Querococha	43 %	**52 %**	**72 %**	24 %
Semi-humid temperate/ Letrayoc	40 %	**45 %**	**55 %**	33 %
Humid temperate/ Lajas	14 %	**64 %**	39 %	**45 %**
Semi-arid cold/ Huancane	**42 %**	39 %	**51 %**	36 %

Table 3.6: Correlation lengths of deseasonalised runoff for the six hydro-climatic regimes for the filling and depletion phases.

Hydro-climatic regime/ Station	Filling phase		Depletion phase	
	Correlation length (days)	Period (Months)	Correlation length (days)	Period (Months)
Semi-arid warm/ Batan	13	Sep-Mar	28	Apr-Aug
Very humid and cold regime with lake influence / Recreta	11	Sep-Feb	9	Mar-Aug
Very humid and cold regime with glacial influence / Querococha	24	Sep-Feb	9	Mar-Aug
Semi-humid temperate / Letrayoc	9	Oct-Feb	9	Mar-Sep
Humid temperate / Lajas	11	Sep-Feb	23	Mar-Aug
Semi-arid cold / Huancane	9	Sep-Jan	12	Feb-Aug

3.5 Discussions

3.5.1 Runoff regimes vs precipitation regimes with the year

This chapter assumes that the intra-annual runoff variability is mainly dominated by climate drivers, and inter-annual runoff is mainly dominated by catchment processes. Each hydro-climatic regime is then expected to have a "typical" periodic shape of precipitation and runoff within the year that is not only related to climate but also to within-year catchment storage, e.g. through soil moisture.

To illustrate this precipitation to runoff mapping within a year, Figure 3.8 shows the intra-annual signal of precipitation and runoff for the six hydro-climatic regimes. A comparison of the semi-arid regimes (with similar humidity conditions) indicates that the hydrograph shapes

and the runoff peaks are similar, although the two catchments have differences in the distribution of the precipitation regime, and the runoff in the cold regime starts one month earlier than in the warm regime. These observations suggest that similar annual runoff regimes may have different hydro-climatic origins and are modulated by the catchment behaviour in different ways. The lower temperatures in the cold system result in less arid conditions (aridity index 1.81) than those in the warm system (aridity index 2.26) which is reflected by its greater soil moisture storage.

The very humid and cold regimes show similar runoff peaks, but the regime with glacial influence starts one month earlier than that with lake influence, while they end at the same time. The glacial influence regime shows greater runoff volumes than the lake influence regime, suggesting the existence of less soil moisture storage. The existence of the lake and associated wetlands constitute substantial water storage per se. Additionally, snow storage exists which redistributes water within the year.
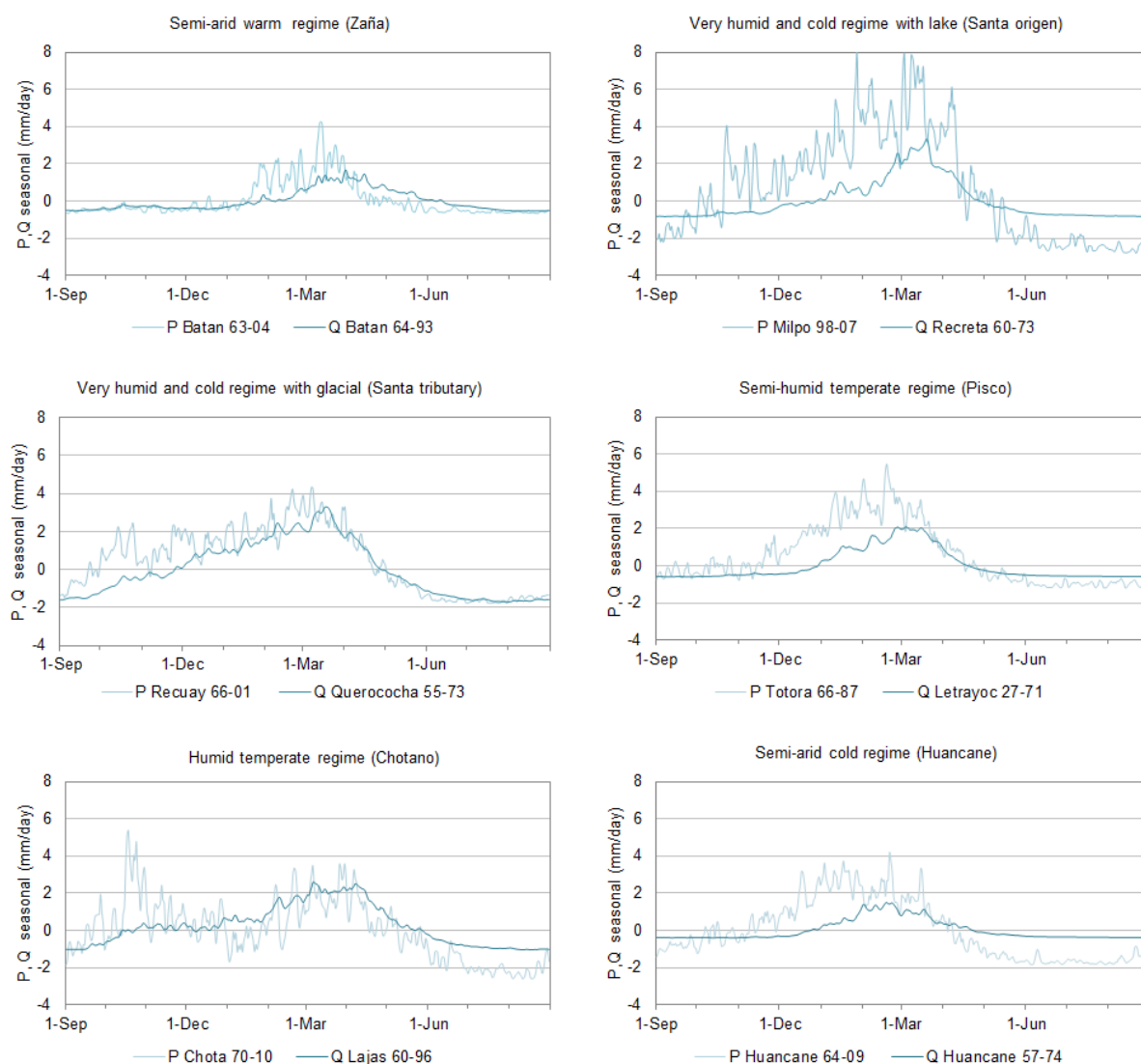
Figure 3.8: Intra-annual signal of precipitation (P) and runoff (Q) for the six hydro-climatic regimes.

A comparison of regimes with temperate conditions but different humidity shows that the runoff regime in the humid temperate regime (aridity index 0.77) is rather uniform throughout

the year while, in the semi-humid temperate regime (aridity index 1.69), runoff is mainly concentrated over 3 months. The peak of the two regimes differs by 0.5 mm/day.

The dominant variability of some regimes such as the semi-arid warm, very humid and cold with glacial influence and semi-humid temperate regimes is clearly defined. The dominant variabilities of the other regimes show similar variability values of the intra-annual and inter-annual components.

This lack of dominant variability may be related to non-linear contributions to the runoff series due to landscape-climate coevolution (Perdigão and Blöschl, 2014). By the differentiation of the runoff series into two phases (filling and depletion, Table 3.5) the contributions become clearer, and in which phase this landscape-climate coevolution is more active. For example in the filling phase it is more active in the semi-humid temperate and semi-arid cold regimes. The explained variabilities (sum of intra-annual and inter-annual variabilities) of runoff fall into two groups (Fig. 3.7). The two dominant inter-annual variability regimes (Table 3.4) also exhibit lower explained variability which may be related to high frequencies events shorter than 3 days (e.g. flash floods) and low frequency events (eg. ENSO events).

The inter-annual runoff fluctuations consist of events that are not periodic but rather occur as extraordinary events, yet are able to change the runoff generation mechanisms in the short term. After our interpretation of the correlation length for the inter-annual long runoff signal, most of the hydro-climatic regimes have a correlation length of 9-13 days with the exception of the semi-arid warm regime (32 days), and the very humid and cold regime with glacial influence (19 days). The autocorrelation function of runoff for the semi-arid warm regime (Figure 3.7 bottom) shows carry-over interactions of water soil storage by a linear reservoir of up to three days, followed by a multi-linear reservoir represented by the continuous fluctuations in the autocorrelation plot and fast-slow groundwater inflow after Table 3.1. Snowmelt is active by strong variations of the temperature in the very humid and cold regime with glacial influence (Kaser, 1999) resulting in a filling of the soil reservoir. This mechanism is confirmed by the filling phase (Table 3.6) with a correlation length of 24 days pointing to groundwater contributions to runoff. Although the common series should be treated care, the inter-annual series are useful for interpretation purposes. The persistence apparent in the long series may have many reasons. For example, the long series of the semi-arid warm regimes show a correlation length of 32 days (Table 3.4), which differs from the common series which shows a correlation length of 144 days. The latter may be interpreted as a contribution of slow groundwater (Table 3.3). The longer correlations length in common series may be related to the drier than usual conditions with results in less inputs into the systems and therefore more pronounced persistence.

The decomposition of the runoff time scales may be useful as part of a downward approach to constructing hydrological model frameworks (Farmer et al., 2003). One of the hydrological bases is the knowledge of the runoff seasonality, which is obtained in this pre-processing methodology. Knowledge of the dominant runoff component variability may assist in focusing on the dominant scales in the modelling, i.e. atmospheric forcing drivers may be in the foreground when the intra-annual variability is dominant, and catchment drivers of aquifer storage may be in the foreground when the inter-annual variability is dominant. The analysis of persistence is an important tool, in particular for examining the inter-annual component of runoff variability, to obtain an understanding of the effects of the soil moisture dynamics on runoff, through the correlation lengths of runoff and the magnitude of the soil storage

reservoirs in the model. Our results suggest that the modelling will be more complex if the intra-annual variability is not dominant.

The classification of the hydro-climatic regimes allows obtaining a customized hydrological model framework for every regime, based on the dominant component of the runoff variability and the persistence of the memory for extraordinary events.

3.5.2   Runoff regimes and a catalogue of runoff generation mechanisms

The analysis of the runoff records in this paper suggests that it would be useful to prepare a catalogue of runoff generation mechanisms for the six hydro-climatic regimes based on the dominant variability and correlation lengths. The catalogue is geared towards the runoff characteristics, allowing to be used as a tool in the establishment of the initial hypotheses for model building together with the a priori perception of the catchments (Fig. 3.2). At this point, it should be noted that this catalogue is only applicable to the six hydro-climatic regimes as classified in this chapter. The catalogue should be a helpful as an analytic tool for modellers.
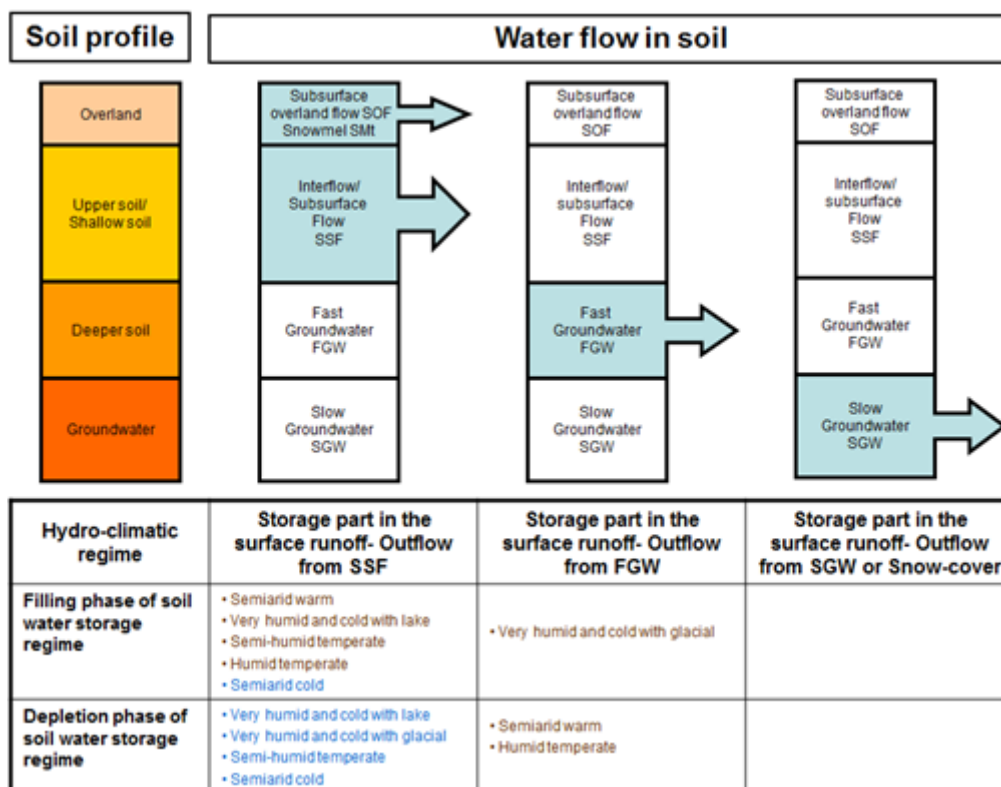
Figure 3.9: Catalogue of runoff generation mechanisms. Top: Origin of the dominant water flow from the soil storage compartments (runoff generation) as light blue boxes. Bottom: relevant processes during the filling and depletion phases for the six hydro-climatic regimes, classified by the dominant runoff variability: intra-annual (blue) and inter-annual (brown).

The preparation of the catalogue is based on the following assumptions: (a) water flows downhill if the landscape is sloping; (b) incorporation of the existing knowledge about runoff process (for example Schädler, 1990; Blöschl and Sivapalan, 1995; and Schwarze, 2007) including residence times in the soil profile as per Table 3.1; (c) our interpretations of the correlation lengths of runoff related to the soil profile and the runoff generation response presented in section 3.2.2; and (d) runoff generation response may be dynamic along the year

in a hydro-climatic regime, so the catalogue separates two instants in time: the filling phase and the depletion phase.

The catalogue of Figure 3.9 was generated from the results of Table 3.5, with the dominant variability classified for both phases, the results of Table 3.6, with the correlation lengths, and the interpretation of the scales of runoff generation response of Table 3.1. The behaviour of dominant runoff variability and correlation lengths as discussed in section 3.4.4 was also included.

The modelling of the runoff response by using the catalogue is oriented to taking only the necessary depth (storage reservoir) for each hydro-climatic regime into account. For example, in semi-arid warm regimes, the modelling of the filling phase should include the upper soil reservoir i.e. the model needs to account for the processes that occur on the land surface and in the upper soil reservoir. The modelling of the depletion phase, however, should include deeper parts of the soil, including a deeper soil reservoir. Inter-annual variability is dominant in this regime in both phases. This means that the subsurface contribution to runoff is more variable over time scales longer than one year than over shorter time scales. The runoff generation response may take a few days due to moisture availability in the filling phase, while it may take weeks and longer due to moisture scarcity in the depletion phase. This reasoning supports the catalogue and can assist in building hydrological models for the relevant runoff processes in order to minimise model complexity.

3.6 Conclusiones

The runoff variability partitioning, i.e. the disentangling of contributions from intra-annual and inter-annual components suggests that the dominant runoff variability is related to defined hydro-climatic regimes. Similarly, the correlation lengths of the inter-annual component are related to these hydro-climatic regimes.

An interpretation of the runoff correlation lengths was introduced with respect to runoff generation processes, based on existing knowledge. The runoff correlation lengths are related to the activation of the soil profile that contributes to runoff generation.

The semi-arid warm and humid temperate regimes show dominant inter-annual runoff variability, but the process drivers differ between the two regimes. The annual water availability in the semi-arid warm regime is lower than the storage capacity (see, e.g. Fig. 3.8), reflected by a smaller difference of the inter-annual component of precipitation and runoff, while the opposite is the case in the humid temperate regime. The correlation lengths of the inter-annual runoff signal for the long series (Fig. 3.7 bottom) indicates 32 days in the semi-arid warm regime (due to groundwater effects), and days in the humid temperate regime (due to the precipitation regime effects).

Intra-annual dominant variability is found in the very humid and cold regimes, semi-humid temperate and semi-arid cold regimes. In these regimes, storage capacity, i.e. the soil depth might not be relevant for runoff generation. The water availability in the very humid and cold regimes is greater than that in the other intra-annual dominated regimes. The correlation length of the intra-annual dominated regimes is between 9-13 days with the exception of the very humid cold with glacial influence regime, where it is 19 days due to the effects of snowmelt and groundwater inflow.

For each of the six hydro-climatic regimes, two phases within a year were selected: the filling phase and the depletion phase. They were tested with respect to their dominant runoff variability and correlation lengths. Inter-annual variability in runoff is dominant in the filling phase for five hydro-climatic regimes with an exception of the semi-arid cold (intra-annual) regime. The semi-arid warm and humid temperate regimes are strongly dominated by the inter-annual variability of runoff in both phases. Strong dominance of the intra-annual variability is found for the semi-arid cold regime. Runoff has a soil water contribution in all studied regimes, thus soil water storage is relevant during the wet season and soil water release during the dry season.

On the basis of these findings, a catalogue of runoff generation mechanisms for the six hydro-climatic regimes was compiled, based on the dominant runoff variability and the correlation lengths. The catalogue, together with the perception of the catchment processes, should be a helpful analytic tool for modellers, in the establishment of the initial hypotheses for the model building. This paper also provides a methodological basis, both qualitative and quantitative, for better understanding the behaviour of Peruvian catchments in terms of dominant runoff variability and correlation lengths, to assist in choosing the appropriate complexity of hydrological models.

Future investigations should addressed additional tests with a larger number of hydro-climatic regimes and associated catchments to confirm whether the findings on the correlation lengths in the inter-annual signal is generalisable when the intra-annual variability is dominant in wet hydro-climatic regimes. The methodology for preparing the runoff generation catalogue could be supported climate change scenarios to assess the impact on the inter-annual runoff component of changes in the landscape, e.g. glacier retreats. The perceptual model catalogue could also be extended to other hydro-climatic regimes.

4 Model development based on an ecohydrological catchment unit concept

4.1 Introduction

Catchment studies are traditionally performed for catchments with specific climatic and runoff generating conditions. This is contrasted by the situation in larger meso-scale river basins which generally exhibit a big variety of distinct catchment features due to changes in the climatic, meteorological, geologic, topographic and ecologic conditions across the river basin. How models can be built for such conditions is currently the topic of an intensive debate as it has become more and more evident that simply transferring the traditional modelling approach to ever larger scales does not lead to the hoped for results. Many questions arise in this context: How should the catchment be discretised if the exchange processes between surface and atmosphere on the one hand and/or between surface and subsurface on the other hand differ significantly between different regions of the catchment? What is the appropriate model structure at the diverse scales? Do model parameters change with scale? (Merz et al., 2009).

The current chapter is designed to contribute to the process of searching for an appropriate model structure and model discretisation that allows capturing the effects of the diverse climatologic, ecologic and surface-groundwater interaction situations on the runoff process within a complex drainage basin.

This chapter is built on the hypothesis that the search for an appropriate model structure should follow the Dominant Processes Concept (DPC), in line with Chapter 3 of this thesis. Developed originally from the hypothesis that, under certain conditions, one single mechanism (e.g. either infiltration excess, or saturated overland flow, or subsurface stormflow) dominates the runoff behaviour at a specific hillslope site whereas other mechanisms are less important (Gutknecht and Kirnbauer, 1994; Gutknecht, 1997), the idea has become a guiding principle not only for modelling the runoff response of hillslopes (concepts developed comprise e.g. the Dominant Runoff Generating Processes concept (Schmocker-Fackel et al. 2007) but also for hydrological modelling in general (Grayson and Blöschl, 2000; Sivakumar, 2004). Following e.g. Grayson and Blöschl (2000), the concept involves, in a first step, the development of methods for identifying the dominant processes and, in a second step, the development of models that focus on these dominant processes.

In the context of this chapter a main challenge is seen in the task of identifying the major controls on dominant processes under the highly diverse situations that are found in basins with a variety of land use, vegetation cover, soil, geologic, geomorphic and topographic landscape characteristics.

Hydrological reasoning and first results from studies in hydrologically diverse catchments indicate that the effective controls shift from site-specific characteristics (such as at-site soil parameters and event-specific rainfall characteristics) on small scales to indicators or indices that characterize the variability, occurrence and the frequency of the various runoff generating conditions over time and across the basin in an accumulated way on larger scales. Typical examples for such indicators include the soil moisture states of a basin and the event runoff coefficient with their pronounced differences in magnitude and seasonal variation depending on the water balance characteristics of a catchment (Samuel et al., 2008; Merz and Blöschl, 2009).

As regards the interaction between soil moisture and vegetation the work of Rodríguez-Iturbe (2000) has initiated a series of studies that explored this interaction in a theoretical way, underlining the role of the sequence and intermittency of rainfall events on the evolution of soil water content (eg. Rodríguez-Iturbe et al., 2001). Based on these results it is hypothesized that differences in these properties will exert significant changes on the soil moisture dynamics which will influence both the soil-vegetation relationship and the runoff generation mechanisms leading to different patterns of runoff responses in the different parts of a river basin with distinct climatic zones. It is further suggested that this aspect is an important element in the conceptualization of the model approach of this current chapter and in the delineation of "homogeneous" sub-basins of the overall basin model.

An interesting question within the development of the model will be the question of how to characterize the land cover characteristics of the various landscapes. The spectrum of possible approaches range from highly compact and aggregated concepts such as the classification method of Holdrige (1947), over methods that define "hydrotope" types (e.g. Flügel, 1995; Reszler et al., 2006) to very detailed approaches as applied in the delineation of "dominant runoff generation processes maps" (e.g. Schmocker-Fackel et al., 2007) in catchment studies on smaller scales. Defining an appropriate strategy for obtaining a modelling concept that is both sufficient to describe the essential features of the runoff responses and the water balance characteristics from an ecological perspective, and which is also parsimonious in terms of the information needed for the modelling process, is an essential part of this chapter.

From a methodological point of view the essential conceptual aspects need to address the following issues: (i) transforming the plot-scale related runoff generation mechanism concept to a landscape related ecohydrological and water balance based concept; (ii) linking background information on landscape attributes, e.g. ecologically oriented landscape descriptions commonly used to characterize hydro-ecological conditions (starting e.g. with the early Holdrige, 1947 classification), with water balance characteristics and indicators of soil water storage dynamics on the regional scale; and (iii) studying the effect of different rainfall process characteristics (sequence and intermittency of rainfall; seasonality of rainfall depths, durations, and intensities) on the soil water dynamics for different saturated/unsaturated zone situations.

Our model building will follow the downward approach as applied e.g. by Samuel et al. (2008). This approach seems to suit best the task of identifying differences between catchments that differ in their ecohydrological characteristics such as climate, water balance, evaporation, and vegetation with respect to soil moisture variation and runoff generation processes. Defining structure and parameters of catchment units will draw from the ideas outlined in Reszler (2007) and Reszler et.al. (2006). The proposed method uses patterns of process information to identify the structure of spatially distributed runoff models and to identify the model parameters. Following Reszler et al. (2008), situations both on the seasonal and the event scale will be analysed in order to clarify the effects on different time scales.

The final model framework is envisaged to be constructed around a group of modules, each of the modules representing specific conditions with respect to the geomorphologic and ecohydrologic characteristics of the particular landscape type. As a starting point in the model development, a HBV-type model will be used as an "initial" model drawing from experiences with the application and adaptation of this model type gained in various modelling tasks (Reszler et al., 2006; Komma et al., 2008). Modifications of the structure of the model with respect to the number, the interconnection, and the functioning of the incorporated storages and with respect to the equations used to describe the exchange processes with the atmosphere

are expected to be necessary to adapt to the various landscape and climatic conditions to be modelled within a complex and heterogeneous basin.

The objectives of this chapter are: (i) developing a conceptual model of surface and subsurface processes in a complex multi-climatic river basin with diverse landscapes; (ii) extending the dominant runoff generation concept and the hydrological response unit concept to regional-scale basins with pronounced within-basin differences in climate and water balance regime characteristics; (iii) identifying appropriate indices that represent the control mechanisms on runoff processes at the regional and river basin scales under the various climatic, geologic, geomorphologic and ecohydrologic conditions found in large river basins; and (iv) analysing the potential of applying "landscape" and water balance characteristics to capture the ecohydrological characteristics of the various landscape types and classifying catchment units with respect to these characteristics (Ecohydrological Catchment Units (UCHs)) within the dominant process concept at regional scale.

4.2   Study catchments, data and methodology

4.2.1   Catchment selection and data acquisition

The selection of catchments was guided by the aim of providing a set of catchment situations that covers a wide variety of geologic, topographic and land cover settings and a strong hydrologic gradient in the spirit of Chapters 2 and 3 of this thesis. The hydrologic signatures included in the selection process encompassed water balance related indices such as the index of dryness and the evapotranspiration efficiency index, regime and seasonality characteristics of the water balance components including the soil moisture regime.

4.2.1.1   Austrian catchments

The selection of the catchments in Austria could draw from a series of comprehensive and detailed studies performed to develop regional methods in catchment hydrology (Merz and Blöschl, 2009a; 2009b). For this chapter a set 16 catchments was selected following the region classification scheme for Austria developed by Merz and Blöschl (2009a). In this scheme the regions are grouped on the basis of a perception of the dominant meteorological and hydrological processes in the regions with the intention of reflecting the hydro-climatic variability of Austrian catchments. The regions are: region 1 - Alpine region, region 2 - southern Alpine region, region 3 - northern Alpine region, region 4 - northern lowlands, and region 5 - eastern lowlands (Figure 4.1, from Merz and Blöschl, 2009). The main characteristics of the selected catchments are summarized in Table 4.1 including the hydro-climatic region classification (HR), and catchment attributes such as mean annual temperature, mean annual precipitation.
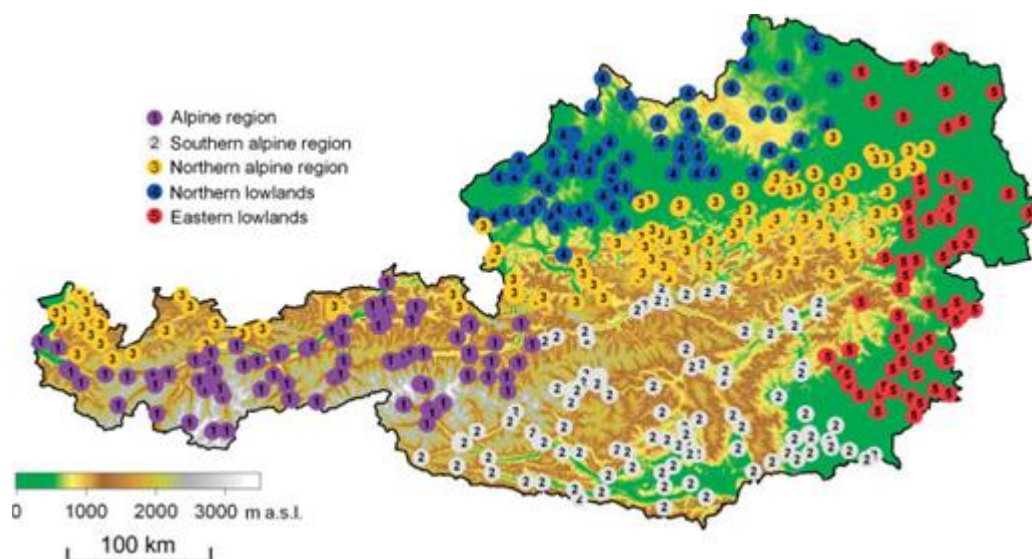
Figure 4.1: Hydrological regions in Austria with location of the catchments analysed by Merz and Blöschl (2009).

4.2.1.2 Peruvian catchments

This section describes the main characteristics of the catchments of the rivers Piura, Cascajal, Olmos, Motupe, La Leche which drain to the "Laguna" Ramon, an ephemeral lake of varying extent in the Ramon depression (Figure 4.2). They contribute to the formation of the Ramon lagoon (see section 4.4). Included are also the Quiroz and Huancabamba Rivers which drain neighbouring basins of the system. They were considered for comparison purposes.

Basin of River Piura

The Piura River basin has a total area of 12 216 km² and rises up to 3 644 masl in the Northern Peruvian Andes. The Piura basin crosses several landscape areas, including the coastal desert area. The rivers are short and are of torrential character in the western foothills of the Andes with mostly narrow channels and steep slopes. The natural discharge regime is seasonal, peak flows occur in the months of January to April and minimum flows in the rest of the year. The river discharges into the Firth of Virrilá estuary which leads to the Pacific Ocean. The Piura River Basin has two identified physiographic areas: the first in the West is part of the Sechura Desert, consisting topographically of flat land with undulations of up to 275 masl in the upper parts, crossed by the Valley of the Piura River which flows into the Pacific Ocean. A mountain range stands out of this plain at the North Western Hills of Asperrería which, like those of Paita Massif, rise abruptly to heights of 390 m above sea level. In the North East another mountains range of old Pre-Tertiarian origin exists. The second part is represented by the Eastern part of the basin where topography ranges from 200 m above sea level to 3644 masl in the Western Andes.

Basin of River Cascajal

The endorheic basin of Cascajal River is the second important river besides the Piura River in the formation of the Laguna "La Niña", and significant parts of runoff contribute to recharge to the aquifer. A main characteristic is the big difference in the Cascajal River regime behavior between a "normal" year (e.g. 1999) and an "El Niño" year (e.g. 1998), with an

increase in the flows by a factor of seven or eight in El Niño years compared to "normal" years (see Chapter 2 of this thesis).

Basin of River Olmos

The Olmos River flows down from the western slopes of the western mountains. The upper basin has a mountainous physiography and a seasonal rainfall regime. The river is flat in the middle of the valley and disappears practically in the lower part of the river into the Sechura desert.

Basin of River Motupe

The Motupe River has its origins in the western slopes of the Andes. In the foothill plains the rivers become unstable streams which channel changes from one to another year, many of them ending without reaching the Pacific Ocean because they run dry in closed depressions that present the geographic setting at the lower end of the river.

Basin of River La Leche

The La Leche River has its origins in the western slopes of the Andes at an altitude of 3990 meters, has a watershed area of approximately 2,253 km² and flows into the Pacific Ocean. The climate is dry and subtropical, influenced by the cold Humboldt Current.

Depression Ramón

This is an area known as Salinas or Ramon, with levels between 7 and 25 m.a.s.l that, in times of extraordinary floods of the Piura River, joins the lagoons Ramón and Ñapique forming a large lake whose waters are drained by the Virrilá estuary or Ramón arm. This arm of the sea reaches far upstream into the desert for more 50 km with widely varying widths. The water level is influenced by the high and low tide sea, oscillating about a meter. The depression area forms a hanging bucket, made by a sandy-salty soil surface extremely thin but impermeable. It has a width between 4 and 18 km and a minimum height of 7 m.a.s.l. Both the west and the east sides are bounded by cliffs of shoals with levels between 14 and 25 m.a.s.l. The eastern area of the depression adjacent to the Dunes Julian Grande and Julian Chico remains constantly flooded, resulting in the formation of large brine reserves, where salt is mined occasionally.

Basin of River Quiroz

The basin is bounded by hilly ranges which towards the river mouth show a sustained and rapid decrease in the level of summits. The top of the basin has a number of small pluvial lakes and, as a result of the sharp decrease in slope at the bottom, has formed a small plain as the product of the deposition of material transported by the river. The origin of runoff is due to precipitation falling on the western slopes of the Andes.

Basin of River Huancabamba

The basin of the Huancabamba River is located orographically on the eastern side of the Andes, as a part of the Atlantic watershed basin, at an altitude of 3,700 m a.s.l.. The general physiography of the Huancabamba river basin is characteristic of most rivers on the eastern side of the Oriental Andes, i.e. a steep watershed, in parts rough, deep canyons and narrow gorges.

Table 4.1: Main characteristics of the selected catchments: Altitude, area, mean annual precipitation (MAP), mean annual runoff depth (MAQ), mean annual temperature (MAT), evapotranspiration ratio (ETA/P) and index of dryness (ETP/P).

Austria / Peru	Basin	Precipitation Station	Discharge Station; hydrological regions	Altitude m a.s.l.	Area km²	MAP mm/year	MAQ mm/year	MAT °C	ETA/P	ETP/P
A	Bregenzerach	200329	Kennelbach; 3	1 632	251	2 136	1 695	5.7	0.2	0.3
A	Erlauf	207803	Niederndorf; 3	174	48	741	1 813	8.8	0.8	0.9
A	Gail	212787	Federaun; 2	1 005	470	1 499	1 629	4.6	0.3	0.4
A	Gurk	213041	Gumisch; 2	362	448	929	1 813	5.6	0.6	0.6
A	Inn	201194	Prutz; 1	538	1 409	1 047	1 681	4.7	0.5	0.5
A	Isel	212167	Lienz; 1	882	284	1 199	1 629	1.2	0.3	0.3
A	Kamp	207944	Zwettl; 4	126	406	672	1 694	7.2	0.8	0.9
A	Lainsitz	208462	Ehrendorf; 4	238	291	819	1 720	6.2	0.7	0.8
A	Lavant	213090	Krottendorf; 2	417	309	975	1 554	5.8	0.6	0.6
A	Lieser	212431	Gmünd-Lieser; 2	553	145	1 005	1 592	3.8	0.4	0.5
A	Rabnitz	210054	Mannersdorf; 5	115	168	657	1 813	8.9	0.8	1
A	Russbach	208447	Ulrichskirchen; 5	437	448	927	1 694	8.1	0.5	0.7
A	Tauernbach	212076	Matreier; 1	1 288	74	1 528	1 629	0.1	0.2	0.2
A	Wulka	210096	Schützen; 5	99	149	613	1 813	9.6	0.8	1
A	Ybbs	207688	Greimpersdorf; 3	722	354	1 316	1 720	7.1	0.5	0.5
A	Ybss	207654	Opponitz, 3	391	506	1651	1158	8	0.3	0.4
A	Zaya	209452	Asparn; 5	62	226	527	1 694	8.8	0.9	1.2
P	Piura	Barrios	Barrios	310	420	739	407	22.9	0.4	2
P	Piura	Chulucanas	Puente Ñacara	95	4 510	396	160	24.1	0.6	4.6
P	Piura	San Pedro	San Pedro	254	160	566	518	23.2	0.1	2.7
P	Piura	Corral	Teodulo Peña	193	330	582	481	23.5	0.2	2.7
P	Piura	Huarmaca	Huarmaca	2 180	200	966	146	14.4	0.8	1.1
P	Piura	Malacasi	Malacasi	128	1 820	1 428	226	23.8	0.8	1.1
P	Piura	Malingas	San Francisco	150	360	258	303	23.7	1	6.2
P	Piura	Miraflores	Los Ejidos	30	7 740	202	220	23.8	1	8.2
P	Piura	Morropón	Puente Carrasquillo	140	3 500	390	145	24.8	0.6	4.4
P	Piura	Paltashaco	Paltashaco	900	140	699	454	20.3	0.4	1.8
P	Piura	San Miguel	Pte. Sanchez Cerro	23	7 740	58	126	24.8	1	28.2
P	Piura	Tambogrande	Tambogrande	65	5 910	1 028	242	24	0.8	1.6
P	Piura	Corpac	Pte.Sanchez Cerro	49	7 740	103	146	24.2	1	15.7
P	Quiroz	Arenales	Paraje Grande	3 010	2 289	623	575	10.7	0.1	0.8
P	Motupe	Penachi	Tangorrape	1 900	230	688	165	24.3	0.8	2.2
P	Motupe	Jayanca	Desaguadero	103	1 566	133	238	24.3	1	11.5
P	Motupe	Espino	Marripon	1 450	231	459	191	24.3	0.6	3.3
P	Olmos	Olmos	Olmos	226	220	210	141	24.3	0.3	7.3
P	La Leche	Puchaca	Puchaca	460	750	267	248	24.3	0.1	5.7

Table 4.2: Basins, which contributes to the formation of the Ramon lagoon (see section 4.4).

Basin	Area (km²)	Length (km)
Piura	12216	292.5
Interbasin Piura-Cascajal		
Cascajal	1032	116.6
Interbasin Cascajal-Olmos	1490	
Olmos	1483	84.4
Interbasin Olmos-Motupe	966	
Motupe-La Leche	4419	349.9

Figure 4.2: System location to the formation of the Ramon lagoon (from Klauer, 2005)

4.2.2   Identification of the dominant runoff processes in the catchments

An identification of the dominant runoff processes DRP in the catchments is necessary to identify signatures associated with (a) climate aspects: partitioning of precipitation into evapotranspiration and runoff; (b) hydrologic characteristics: runoff regime and runoff processes, water balance characteristics; (c) catchment/landscape attributes; and (d) space and time scale aspects.

The dryness index or evapotranspiration efficiency is related to precipitation partitioning. The seasonality and runoff coefficients are related to runoff characteristics. Runoff process may be categorized with respect to runoff generation (e.g. Schmocker-Fackel et al., 2004) and by the occurrence and the controls of different runoff components (e.g. Schwarze et al, 1995, 2007). Budyko relationships and regime types are signatures that indicate differences in the water balance.

Catchment attributes such as geology and lithology, soil-vegetation-complex types (including e.g. root zone depth, porosity and hydraulic conductivity), topography (hillslope gradient, curvature, altitude and elevation), and land use are frequently used to identify similarities and differences between catchments of diverse regions.

In order to define dominant controls, it is necessary to analyse the scales relevant to the study area. Varying controls on different spatial scales (regional, catchment-landscape, local, hydrotope) and different time scales (long-term, annual and monthly) have to be considered. In the spirit of Chapter 3 of this thesis it is hypothesized that knowledge on the most important controls in different climatic conditions and catchments settings can contribute to reducing the overall model complexity by designing a perceptual model on the basis of a priori knowledge through studying the appropriate hydrologic signatures as a basis for choosing the "best" model structure appropriate for the basin.

4.2.3 Runoff Process Conceptualization

4.2.3.1 Characterization of runoff processes at the plot scale

Table 4.3 specifies the runoff processes and the various process types with their main influencing factors (action effect), phenomena (reaction effect), and mechanisms (system effect). Figure 4.3 illustrates schematically the situation on the hillslope that leads to the generation of specific runoff types and the resulting runoff responses of different dynamics. Situations are determined by the various conditions with respect to precipitation, soil, and geologic condition and, more specifically, by: (i) the relation between precipitation intensity and infiltration capacity, (ii) the relation between precipitation depth and soil storage capacity, (iii) the amount of antecedent precipitation and the soil moisture content at the onset of a precipitation event, (iv) the location of a plot on the hillslope (upper slope – recharge situation; middle slope – transfer situation; lower slope – discharge situation).

Table 4.3: Characteristics of the main runoff process types (Gutknecht, Lecture Notes)

Runoff Process	Main influencing factor	Phenoma	Mechanism
Horton Overland flow **HOF**	Rainfall intensity	Ponding on land surface Sheet and/or rill flow Quick runoff response	producing high runoff peak rates initiating erosion and sediment transport on land surfaces operative on arable land and bare soils main contributor to runoff in semi-arid and arid regions (flash floods)
Subsurface stormflow **SSF**	Rainfall depth and duration Pre-event moisture condition (wet<->dry)	No traces of flow on the land surface Slow runoff response	producing moderate runoff peak rates contributing to solute transport, runoff chemistry forming the main storm flow response in soil-mantled humid temperate landscapes
Saturation overland flow **SOF**	Rainfall intensity Rainfall depth and duration Pre-event moisture condition (saturation area extent, soil moisture)	Inmediate quick runoff response Runoff increase with upwards spreading of the saturated area	producing sharp hydrograph rises and peaks controlled by saturation area extent operative on the foot areas of hillslopes ("recharge areas") and on riparian zones of streams main contributor to storm flow in high intensity short duration convective storms in soil-mantled landscapes
Deep Percolation **DP**		No immediate runoff response to rainfall events Strongly delayed and "dampened" response function Discharge area (springs, etc.) at some distance from the recharge area	operative mainly on deep forest soils in "old" landscapes of humid regions and in landscapes with deep permeable fractured bedrock, in talus slope areas with deep exfiltration contributing in other areas mainly to "base flow" through outflow of deep groundwater aquifers
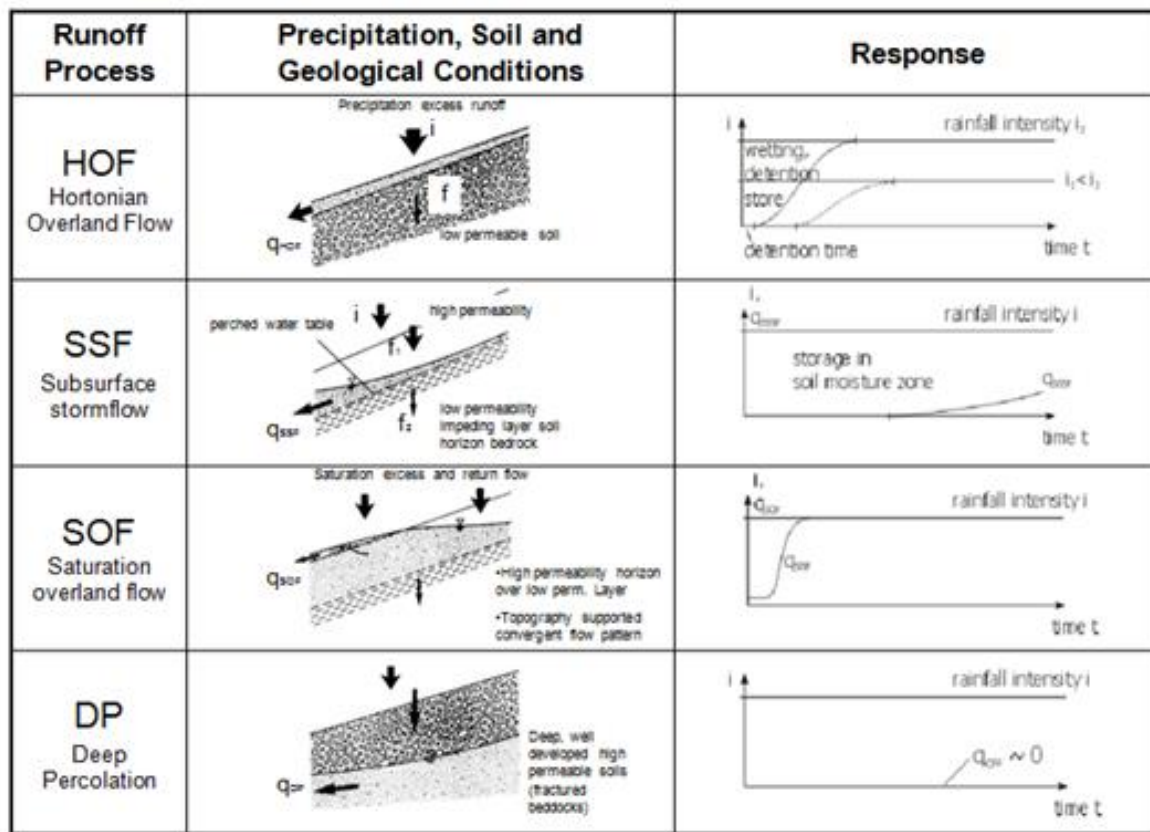
Figure 4.3: Schematic of runoff production mechanisms and runoff process dynamics (Gutknecht, Lecture notes).

4.2.3.2   Characterization of runoff processes at the catchment scale via runoff components

The DIFGA methodology (Schwarze et al., 1995) is chosen as a starting point for the analysis at catchment scale. The methodology is based on the assumption that the runoff formation and the concentration process in a catchment can be described by the parallel connection of linear reservoirs. It allows the determination of up to four runoff components, each corresponding to a linear reservoir with a specific storage constant or mean response time. The following components can be calculated:

- Direct runoff   (quick direct runoff)   RD1, QD1
- Interflow (delayed direct runoff)   RD2, QD2
- Fast groundwater runoff (quick base flow)   RG1, QG1
- Slow groundwater runoff (delayed base flow)   RG2, QG2

"R" describes inflows into the catchment storage (runoff formation). "Q" indicates the outflow from the storage into the drainage system (runoff concentration), Fig 4.4.
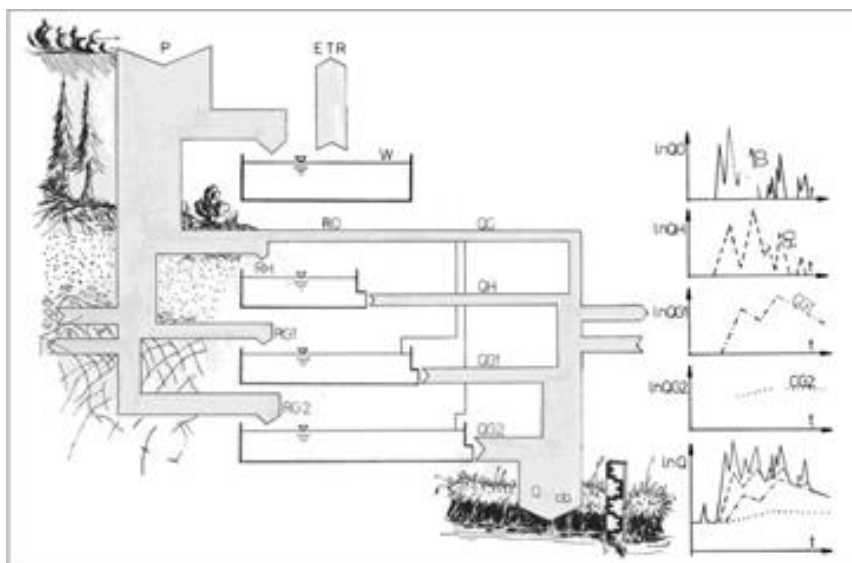
Figure 4.4: Concept of runoff components and storages, and runoff separation (Schwarze, 1995; Dyck und Peschke, 1983).

4.2.3.3 Linking runoff process concepts and soil moisture accounting schemes

In an attempt to find guiding principles for the development of appropriately structured rainfall-runoff models various concepts for structuring the soil profile with respect to runoff processes were studied. The results are summarized in Figure 4.5-4.8.
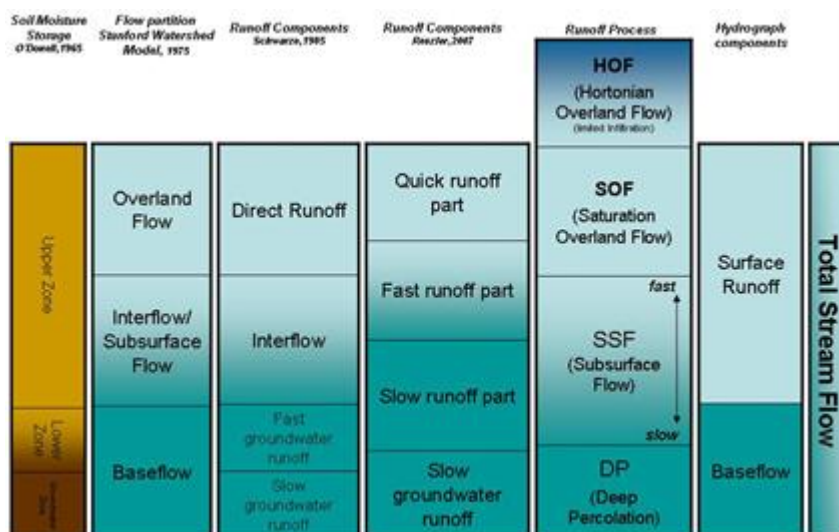
Figure 4.5: Conceptual relationships between the soil profile, runoff components, runoff processes and hydrograph components.

Among the many approaches to simulate the runoff process via soil moisture accounting schemes, the methodology proposed by Reszler (2007) seems to offer great potential for considering rather diverse hydro-climatic and landscape situations. Following this approach, three types of events are examined: snow melt induced events, convective events and advective events based on the "dominant processes concept". Reszler defined four runoff components: the quick runoff part, fast runoff part, slow runoff part and slow groundwater runoff. These components develop differently depending on the hydrologic event type and soil type and storage depth (see Figure 4.6-4.8). His analysis also showed some relationships

between the events types and the runoff process types which are dominant in the various events as follows:

In the case of the snow melting event type (Figure 4.6) strong saturated soils are found in the basin, the runoff is dominated by the slower runoff component from the deeper soil profile.
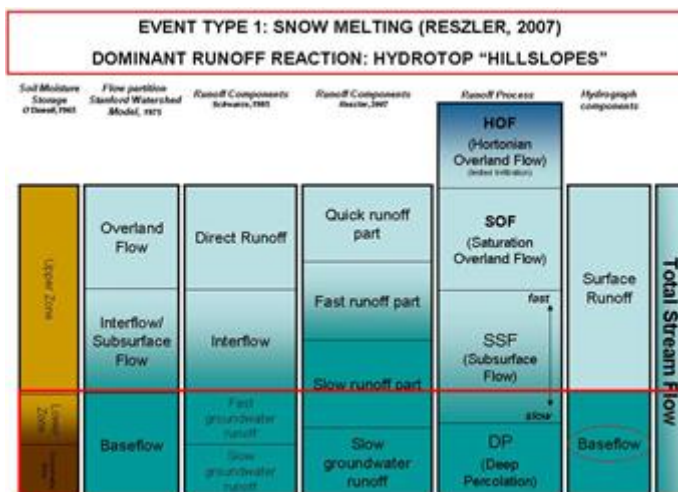
Figure 4.6: Conceptual relationships for snow melting events in the hydrotope "hillslopes".

In the case of convective events (Figure 4.7) responses stem from only a small part of the basin, from areas with small storage characteristics, such as sealed surfaces, steep ditches or saturation surfaces. Runoff is dominated by the quick runoff component.
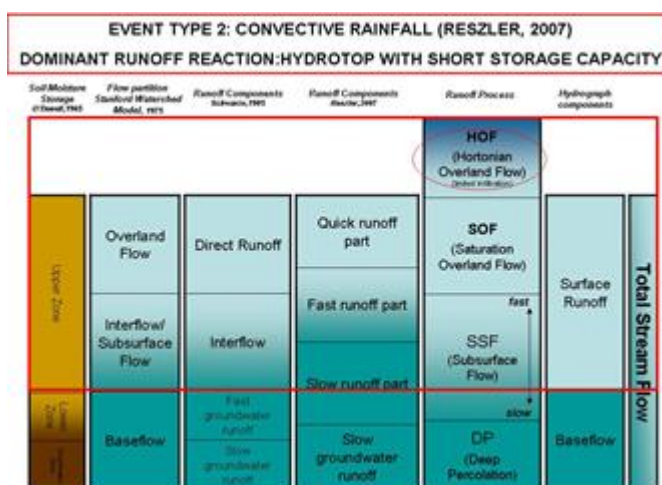
Figure 4.7: Conceptual relationships for convective rainfall events in a hydrotope with small storage capacity.

In the case of advective events (Figure 4.8) soils in the basin may be saturated due to wide spread and long lasting rainfall. Depending on the event phase, different soil storage depths contribute to the total runoff, and different processes become dominant. At the beginning of the event, runoff generation is controlled by the infiltration into the soil and high initial losses. As rainfall continues, the soil gets more saturated and an abrupt rise of the runoff coefficient and thus runoff hydrograph curves may occur.
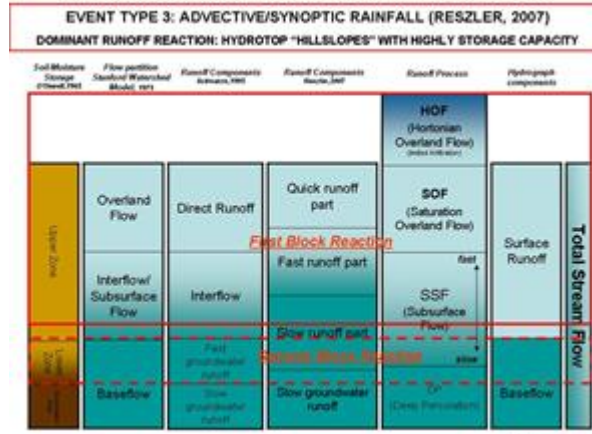
Figure 4.8: Conceptual relationships for advective/synoptic rainfall in a hydrotope with large storage capacity.

4.2.4 The Budyko concept of water balance and precipitation partitioning

An analysis of the water balance components in a catchment can start from the Budyko concept. In this concept, the climate and the mean water balance are represented by two bi-dimensional indices: (i) the index of dryness, R, which is the ratio of potential evapotranspiration ETP and precipitation P, and (ii) the ratio of actual evapotranspiration ETA and precipitation P. Based on data from a large number of different places around the world Budyko (1974) found an empirical relationship between the climate and mean water balance parameters which could be expressed by Equations (1-3) shown in Figure 4.9:

$$\frac{ETA}{P} = 1 - \exp(-R) \tag{1}$$

$$\frac{ETA}{P} = R \tanh\left(\frac{1}{R}\right) \tag{2}$$

or its geometric mean:

$$\frac{ETA}{P} = \sqrt{R \tanh\left(\frac{1}{R}\right)\left[1 - \exp(-R)\right]} \tag{3}$$

Discussion of Budyko´s curve

From the structure of the curves follows that they approach two asymptotes, the limit lines I and II. These two lines define the upper energy and water limits of evapotranspiration and, therefore, also the minimum runoff potential of a catchment. Line I represents the energy limit line. Values on this line mean that actual evapotranspiration has approached potential evapotranspiration and water supply exceeds water demand, a situation that can be found under very wet hydro-climatic conditions, indicated by low values of the index of dryness R (= ETP/P). Line II represents cases where energy availability is much greater than water supply, or in other words, water demand (ETP) exceeds water supply (P) and all available water is used for evapotranspiration, actual evapotranspiration (ETA) equalling precipitation (P): evapotranspiration ratio (ETA/P) = 1 and runoff (Q) = 0, situations with evapotranspiration and no runoff.
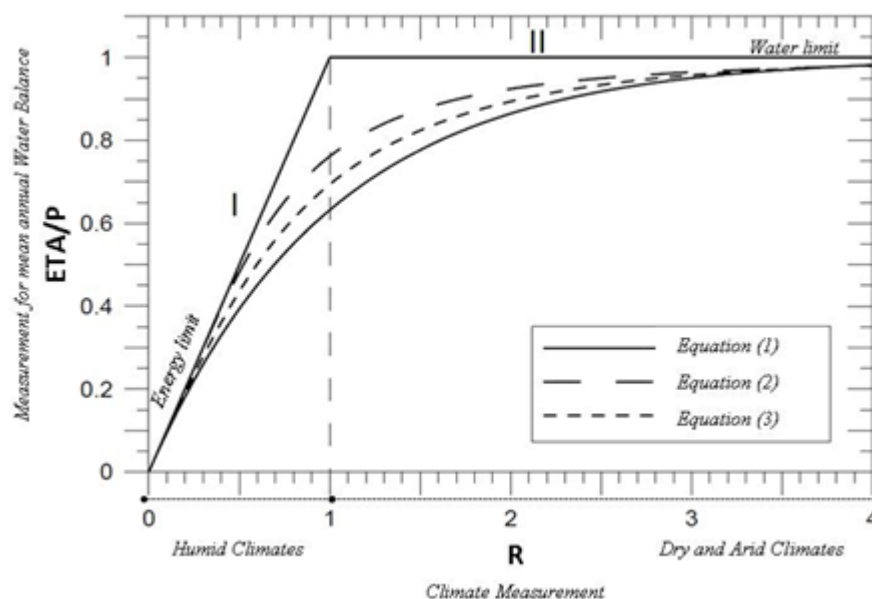
Figure 4.9: Structure of the Budyko curve and asymptotes.

The breakpoint between these two lines is marked by the point where the index of dryness reaches 1. Catchments to the left of this point (R < 1) in this diagram represent "humid" regions, and catchments to the right (R > 1) represent "arid" regions. A more detailed inspection of the hydro-climatic situations across the spectrum of R led Ponce et al. (2000) to the classification scheme of Table 4.4, detailing the range of the humid and the arid conditions.

Table 4.4: Classification of index of dryness after Budyko and Ponce et al. (2000).

Ratio ETP/P	Budyko classification	Ponce et al. (2000) classification
< 0.1875		Superhumid
0.1875-0.375	Humid or wet regions	Hyperhumid
0.375-0.75		Humid
0.75-2		Subhumid
	1	
2-5		Semiarid
5-12	Dry or arid regions	Arid
12-30		Hyperarid
>30		Superarid

If we seek a physical explanation for the situation at the breakpoint, two situations could be supposed: firstly, a situation where all precipitation evaporates, i.e. a situation with a sealed surface where no transpiration can occur because there is no soil moisture for supplying the water requirements of the vegetation, or where, in other words, there is no vegetation. In this case, soil characteristics do not play any role, and there is neither storage nor a biological process function, i.e. there is only evaporation. The second situation could be characterized by a vegetation cover so great that water demand would be equal to water supply, precipitation would be taken up by the plants immediately and, as in the first situation, the soil storage function would not play a role. The main control on the hydrologic processes is only of the climatic type. This scenario type could be found in any region where the water supply and the water demand are equal, not depending on the amount of them.

The asymptotic (limit) lines represent extreme conditions. As indicated by the empirical Budyko curve, the hydro-climatology of actual catchments is represented by points below the limit lines. Interestingly, even under very dry or arid conditions (R > 3, e.g.) not all precipitation is consumed by evapotranspiration and a small portion of the available precipitation, even if precipitation is small, particularly when compared to evapotranspiration, is transformed into runoff in actual cases. Observations such as these and the considerable scatter around the Budyko curve indicate that additional factors besides the dryness index influence the evapotranspiration ratio and the long-term water balance. Studies into the causes of the deviations from the empirical curve and the limit curves highlighted the role of the following factors:

- The catchment water storage capacity (Milly, 1994) and the soil properties (soil depth, porosity, permeability) (e.g. Rodríguez-Iturbe and Porporato, 2004; Potter et al., 2005; Hickel and Zhang, 2006; Donohue et al., 2007),
- Vegetation (root zone depth, plant-available water content) and vegetation types and forest cover (e.g. Zhang et al., 2001),
- Seasonality, particularly whether precipitation and evapotranspiration (transpiration) are in-phase or out-of-phase (Milly, 1994; Dooge et al., 1999; Woods, 2003; Potter et al., 2005; Hickel and Zhang, 2006; Gerrits et al., 2009 etc.),
- Interannual variability, precipitation intermittency, storm intensity and storm frequency (e.g. Milly, 1994; Milly and Dunne, 2002) and interception (Gerrits et al., 2009).

There are, therefore, many attempts to extend the Budyko concept and to include other influences. This is achieved by incorporating an additional parameter such as, e.g., the parameter ν (or n) in the generalized Turc-Pike relation (see e.g. Milly and Dunne, 2002), which can serve as an indicator of water storage in the catchment. Similarly, an additional parameter w (n in our figures) can differentiate situations in the Budyko diagram with respect to land cover, differentiating, e.g., between forested and grassland catchments in the formula of Fu as described in Zhang et al. (2004).

These analyses suggest that the climate control aspect as introduced by Budyko has to be supplemented by additional parameters considering other relevant controls such as storage effects by soils in relation to vegetation, as e.g. in Milly (1994), but also seasonality and process intermittency aspects (Figure 4.10). It is interesting to note that the variations that can be observed in the data are biggest around R = 1, indicating that in a situation where water supply meets water demand the water balance is most sensitive to land surface parameters.

4.2.5 Holdridge's "Life Zones" Concept

The other starting point to develop an eco-hydrologically oriented catchment classification is the Holdridge life zone classification system. It is based on the assumption that the diversity of vegetation types of different landscapes reflects the effects of the hydro-climatic factors on vegetation. It uses, therefore, a combination of three climate parameters – biotemperature, mean annual precipitation and a potential evapotranspiration ratio – to characterize the hydro-climatic conditions for a broad variety of vegetation types, ranging from desert to rain forest and from tundra to subtropical and tropical forest. Biotemperature is defined as the mean temperature of all days of a year with temperature between 0° and 30°. It defines the latitudinal and/or altitudinal belts of life zones. The evapotranspiration ratio is defined analogously to the dryness index in the Budyko approach by the ratio between potential evapotranspiration and precipitation.

The idea behind the use of the Holdridge classification is to (a) interpret water balance and runoff process situations categorized in relation to the Budyko regime in terms of life zones and vegetation types and, conversely, to (b) search for relations that associate runoff regime and runoff process characteristics with the various vegetation types via the association of dominant runoff process types and climate regime characteristics in the Budyko framework. These ideas are supported by results that emphasize the important relationship between vegetation growth and the seasonality of the climatic variables and the soil moisture regime and by studies that analyse the role of vegetation in landscape development (e.g. Donohue et al., 2007) and by research approaches that focus on the co-evolution of climate, soil, and vegetation (e.g. Berry et al., 2005). Fig. 4.11 shows the relationship between life zones and the climatic indices after Holdridge.
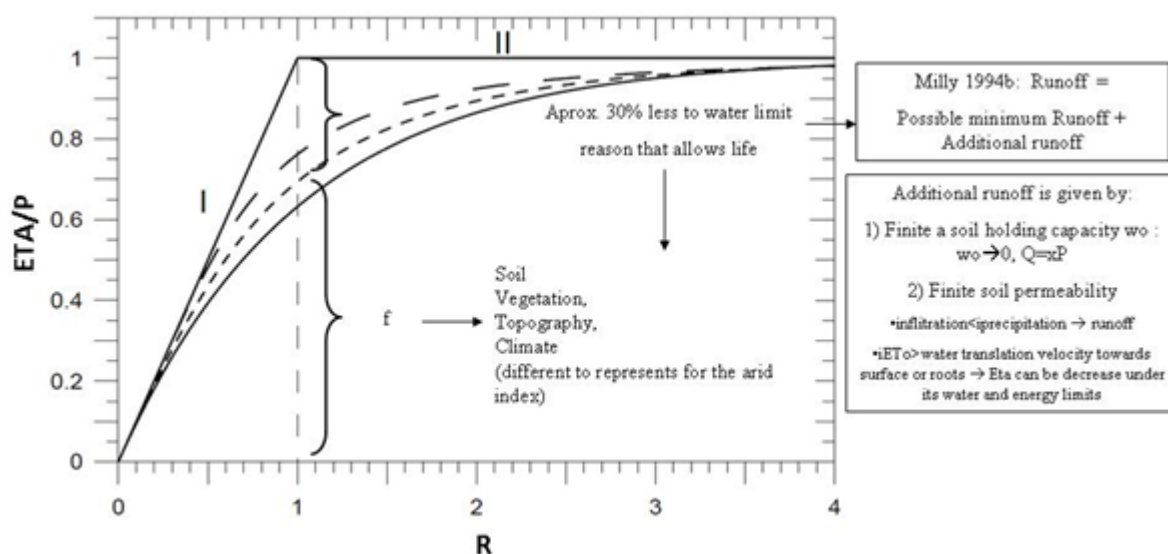
Figure 4.10: Factors influencing the hydro-climatic water balance.

4.2.6   The water pathways approach

In order to develop relationships between the hydro-climatic regime, the soil-vegetation complex and the runoff processes, the water pathways concept of Gutknecht et al. (2008, Ch. 2) is used. Introduced as a pivotal point for describing and interpreting catchment processes under an eco-hydrological perspective, it provides a framework for differentiate runoff processes against different runoff generation mechanisms and their hydrological regime characteristics. Following Fig. 2 of Kirkby (2006), different runoff process types are considered to be dominant in different hydrological regimes characterized in terms of the seasonal variation in temperature and precipitation, as visualized in Fig. 2 of Kirkby (2006) by three example catchments from different hydro-climatic regimes (arid, humid conditions, and cold-dominated regime).
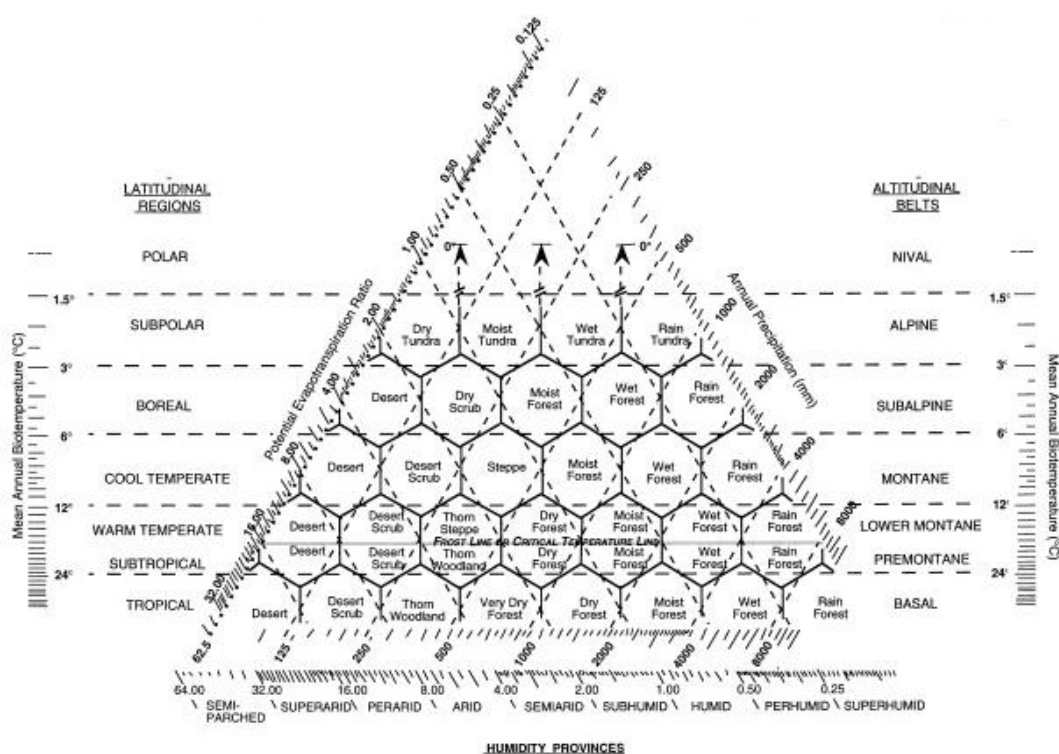
Figure 4.11: Holdridge's "Life Zones" (taken from Special paper: The Holdridge Life Zones of the conterminous United States in relation to ecosystem mapping. Available from: http://www.researchgate.net/publication/227649905_Special_paper_The_Holdridge_Life_Zones_of_the_conterminous_United_States_in_relation_to_ecosystem_mapping.

4.3 A methodology linking water balance and runoff characteristics with landscape and land cover properties

4.3.1 Application of Budyko´s concept to Austrian and Peruvian catchments

Austrian catchments

The modified Budyko curve was constructed on the basis of long term mean annual rainfall, and actual and potential evapotranspiration for the selected basins in Austria. The results are presented in Figure 4.12. All basins were additionally characterized by their region category following the Austrian region classification scheme of Merz and Blöschl (2009a) (see Fig. 4.13).

It can be seen from Figure 4.12 and Figure 4.13 that the catchments in the alpine region are located near the limit energy line (humid regions) whereas the eastern lowland catchments (dry regions) have the highest index of dryness in comparison with the other regions in Austria. The driest and the wettest catchments among the 17 selected ones are the Zaya and the Tauernbach catchments, respectively. Most of the catchments are situated near the energy limit line, their dryness index varying from around 0.2 to 0.8. These are the regions with high precipitation and relatively high runoff coefficients. Many of the Austrian catchments tend to be in the humid region classification. Runoff in these areas will be produced both on the land surface (infiltration excess flow and saturated areas flow) and in the subsurface (subsurface flow from the soil, deep percolation and base flow).
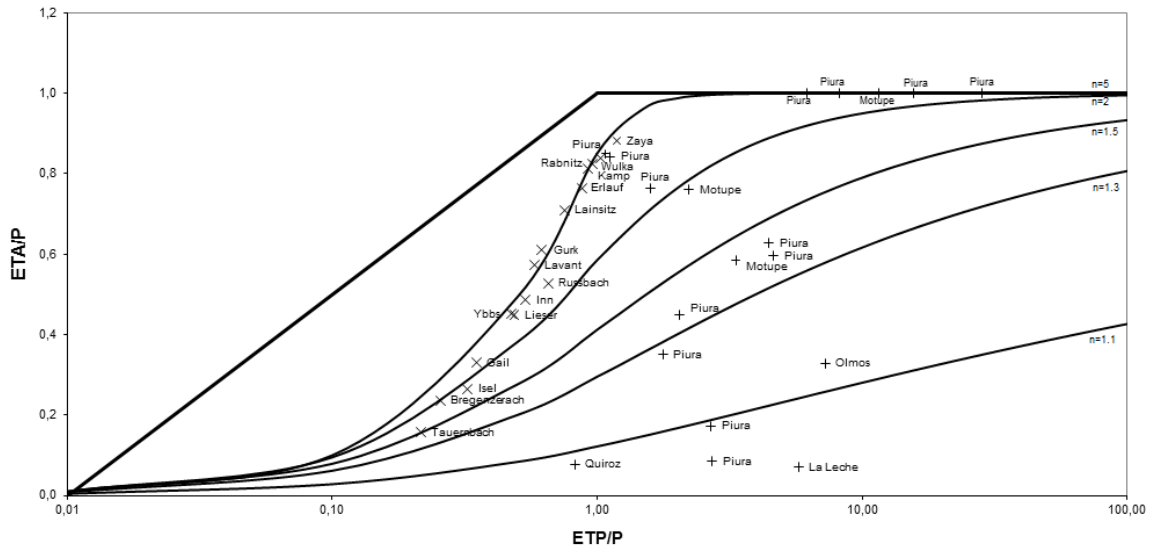
Figure 4.12: Austrian (X) and Peruvian (+) catchments in the Budyko diagram.
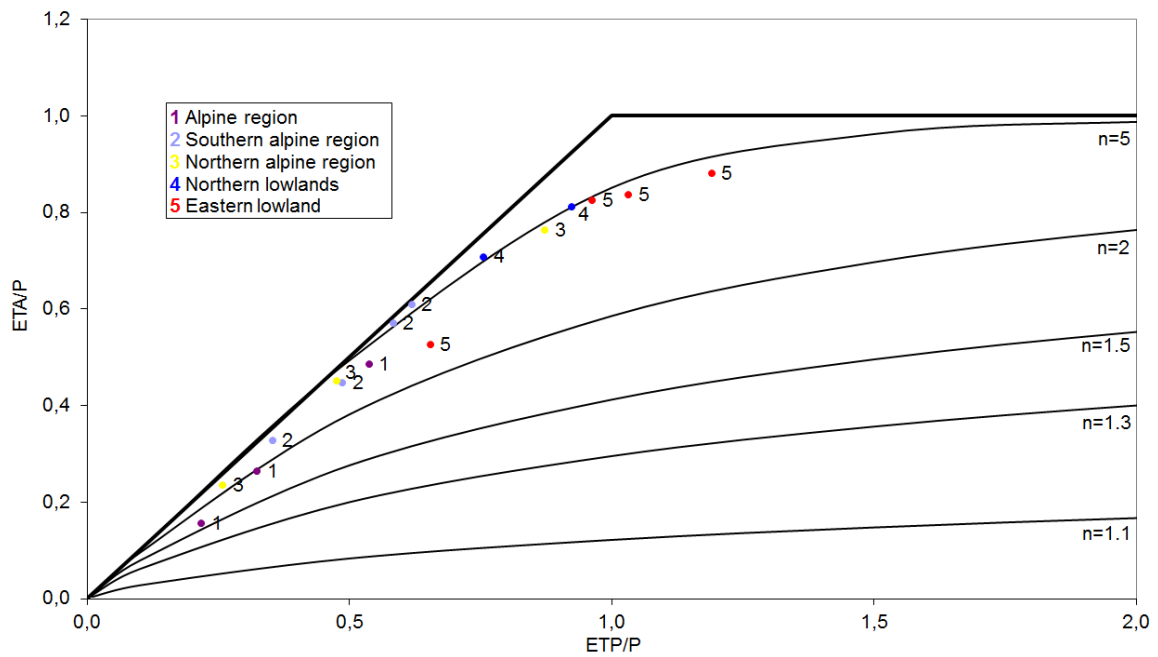
Figure 4.13: Austrian catchments by hydrological region classification in the Budyko diagram.

A more detailed analysis was performed for two Austrian basins, Opponitz (humid climate) and Schützen (dry climate), in an attempt to apply the Budyko concept to annual water balances. The result is given in Figure 4.14. As can be expected, the range of variability increases in comparison to the long-term behaviour. Also, the differences between the two catchments become more manifest. Points lying outside the energy limit line indicate the carry-over effect of over-year storage on the water balance relationship not accounted for by the procedure.
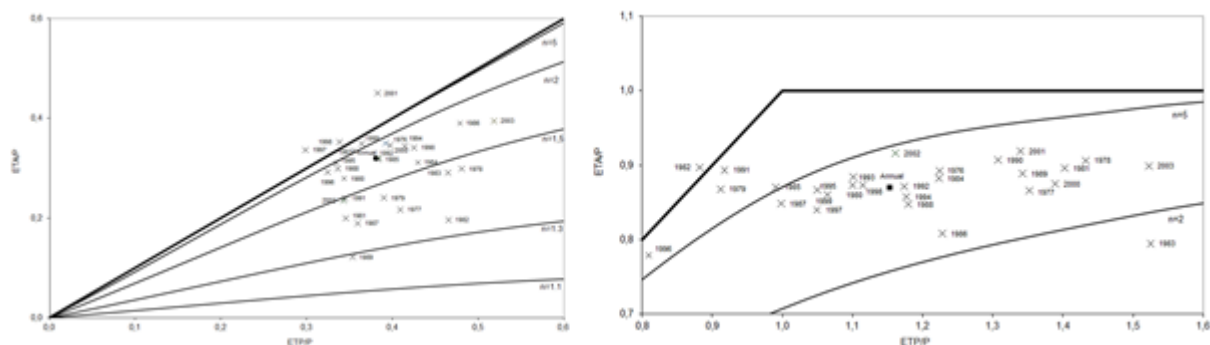
Figure 4.14: Budyko-type analysis on an annual basis for two Austrian catchments in contrasting hydrologic regions (left: Opponitz, right: Schützen).

Peruvian catchments

For the Peruvian catchments, the data for actual evapotranspiration (ETA) were derived from long-time data of P and Q. Potential evapotranspiration (ETP) was calculated by the Penman – Monteith equation.

The different hydro-climatic situations among the Peruvian basins are apparent in the wide range of values of the dryness index (Fig. 4.12). In the wet part of the Piura basin, the dryness index R varies between 1 and 3 with differences between the higher and the lower parts of the basin. The drier parts such as the Chulucanas and Morropón subbasins exhibit higher dryness indices and lower evapotranspiration ratios indicating that the available precipitation does not allow evapotranspiration at the potential rate and that runoff develops even in these cases of scarce precipitation situations. This behaviour may be related to the influence of the strong seasonal variation in precipitation which tends to be out-of-phase compared to the energy input, as well as the significant moisture storage capacities of the soils in connection with vegetation. A detailed analysis of the geology, the soils and the vegetation types in these areas and in the basins of the La Leche river are necessary to more clearly reveal the factors behind this behaviour.

4.3.2 Budyko's curve and the role of vegetation

Zhang et al. (2001) found that changes in mean annual evapotranspiration may result from changes in catchment vegetation. Their approach for estimating the total annual evapotranspiration includes a parameter f as a function of the fractional forest cover which differentiates between two vegetation types, namely forests and herbaceous annual plants. Forest cover seems to favour the storage capacity of the soil and increases water storage in the long term, achieving greater evapotranspiration efficiencies from forest trees compared to shrubby vegetation which favours the generation of runoff, both in very dry and in the very wet conditions.

Donohue et al. (2007) incorporates some key measure of vegetation into Budyko's model, which is expected to extend the model's ability to describe catchment behaviour at small scales. The concept is based on the ecohydrological equilibrium theory drawing from the idea that, in water-limited environments, vegetation is the integrated response to all processes affecting the availability of water.

Figure 4.15 shows two Austrian basins with markedly different climates (humid and dry), Opponitz and Schützen. The top left panel represents a humid region with persistent

vegetation along the year. According to experiments of Dooge et al. (1999), this catchment could correspond to temperate climates. The top right panel represents a dry region with seasonal vegetation. Figure 4.15 top shows that the period of highest water demand occurs in July, which is the month with the largest influence on the annual water balance (average over many years). Figure 4.15 bottom shows the annual evolution of the July evaporation ratios for the two catchments. The ratios vary around 0.5 and 0.9 for Opponitz and Schützen, respectively.

The vegetation dynamics are seasonal. The water demand is largest during the growing season of the vegetation. In relatively dry regions with intensive agricultural activities Figure 4.15 top right may be a typical pattern.
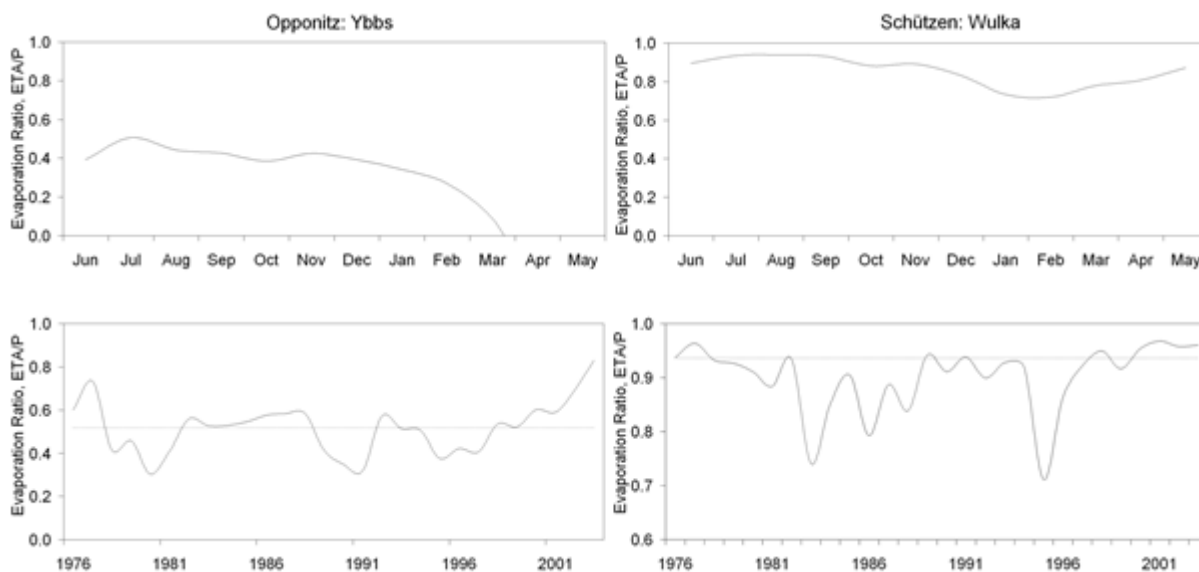
Figure 4.15: Intra-annual (top) and July-inter-annual (bottom) variation of evaporation ratio for two Austrian basins with humid (left: Opponitz) and dry (right: Schützen) climates.

4.3.3   Application of Holdridge´s concept to Austrian and Peruvian catchments

Figure 4.16 (incorporating information from Figure 4.12) shows the situation of the test catchments in the Budyko diagram, stratified with respect to the life zones concept (main vegetation types). The differences between the Austrian and the Peruvian catchments become clearly apparent. In particular, the wide variation of the dryness index in the Peruvian case is visible which is connected to a wide range of Holdridge life zones, ranging from dry forest to desert. In contrast, the Austrian catchments mainly consist of wet and moist forest land cover. There is a clear link between the dominant vegetation and the water balance according to the modified Budyko methodology.
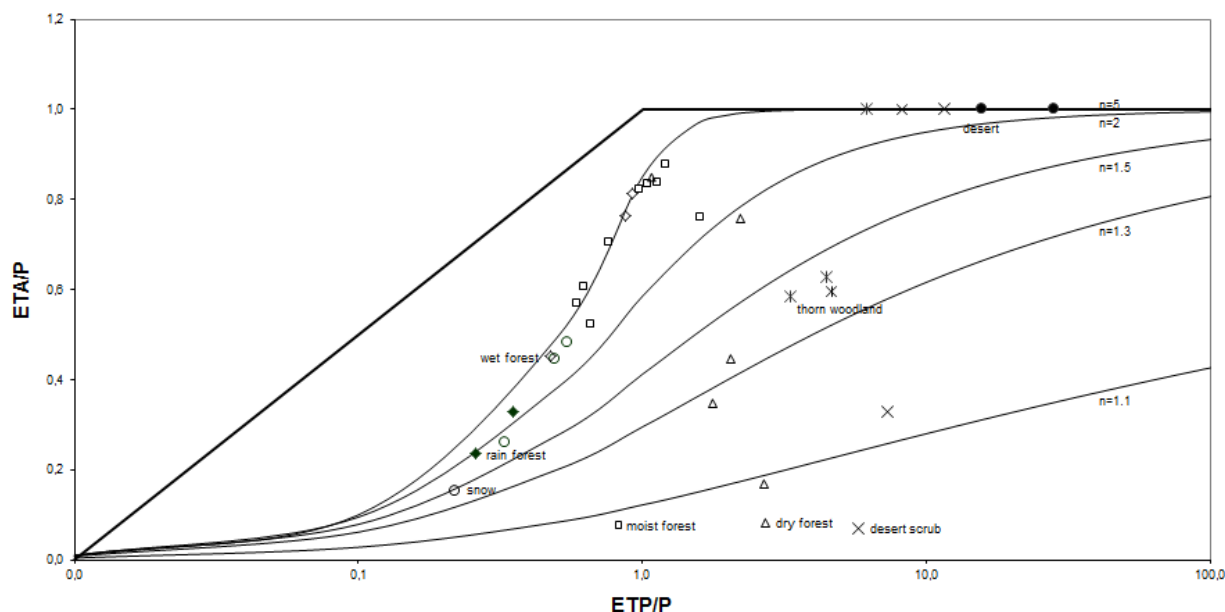
Figure 4.16: Life zone classification of the Austrian and Peruvian catchments within the Budyko framework.

4.3.4   A hypothesis to link runoff processes and vegetation-oriented landscape types

Figure 4.17 contains the essence of first steps of analysing the relationship between hydro-climatic regimes, dominant vegetation types, and dominant runoff process types. Based on the relationships found in the Budyko, the Holdridge and the Kirkby approaches, some features of connections between landscape characteristics and runoff processes become apparent.

Following Kirkby (2006), the hydro-climatic parameters mean annual temperature and mean annual precipitation build the frame of inserting both the life zones after Holdridge and the runoff process types (Hortonian Overland Flow (HOF), Subsurface Stormflow (SSF), Saturation Overland Flow (SOF), Deep Percolation (DP) and snowmelt) into the Kirkby diagram. Considering the conditions that control the occurrence and the dominance of a specific runoff process, the following links between landscapes and runoff processes are proposed:

HOF is dominant on desert and desert scrub surfaces from boreal to tropical climates. There is a trend for the formation of groundwater under appropriate geological conditions in areas with shrub- and forest cover, mainly in climates where the temperature increases with rainfall (boreal-tropical). In regions where precipitation increases more than temperature, the runoff processes SSF and SOF tend to dominate, in particular in areas with dry to wet forest cover. Cold regions dominated by snow melt are regions characterized by hardly any vegetation or by tundra environments from polar to boreal regions.

Figure 4.18 shows the hydrological regimes (Kirkby, 2006) and Holdridge elements in the Austrian and Peruvian test catchments. From the diagram the main controls both on the catchment water balance and on the dominant runoff processes can be identified in a first step. The information on the life zones and the predominant vegetation types allows a first assessment of the model structure and the main model parameters that might be relevant under the given conditions.
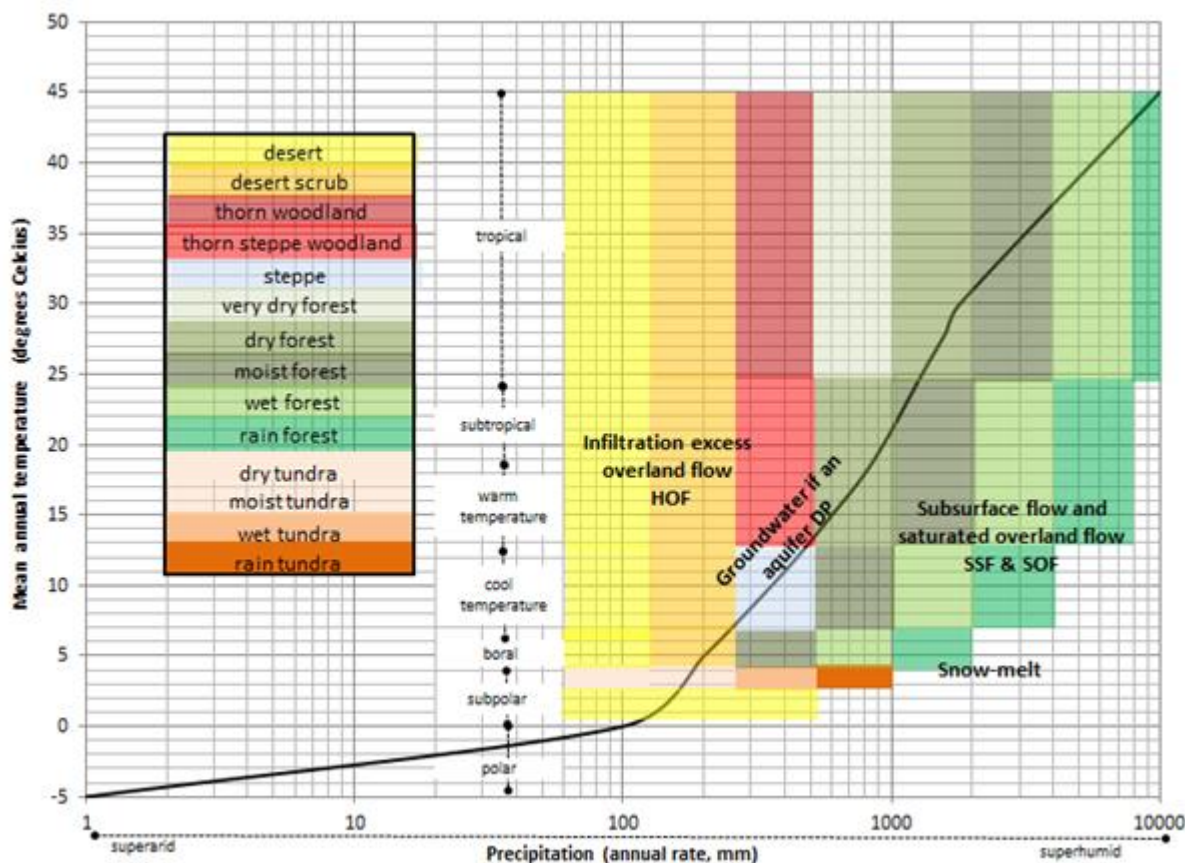
Figure 4.17: : Characterization of the test catchments in the Holdridge-Budyko-Kirkby framework.

Mean annual temperatures and annual rainfall of the Austrian and Peruvian basins are shown in Figure 4.18 and indicate a variety of behaviour in both life zones and dominant runoff response. Figure 4.19 is a combination of the results of the runoff process definition obtained by the modified Kirkby diagram and the position of the catchments in the modified Budyko´s curve diagram. Snow melt (SM), Saturation overland flow (SOF) and Subsurface flow (SSF) are near the energy limit line. Deep Percolation (DP) could not be specified by a specific situation in the Budyko´s curve diagram without more detailed analysis of the groundwater situations in the basins. Figure 4.19 shows dominant runoff regime types in the Peruvian catchments where most of the regions with "desert" life zones tend to response through the HOF runoff type.

Table 4.5 summarises the Austrian regions according to the hydrological classification of Merz and Blöschl (2009a), dominant life zones of Holdridge; and the dominant runoff processes obtained from the modified Kirkby diagram. This table connects the results of the dominant runoff responses and the dominant life zones for each Austrian region.
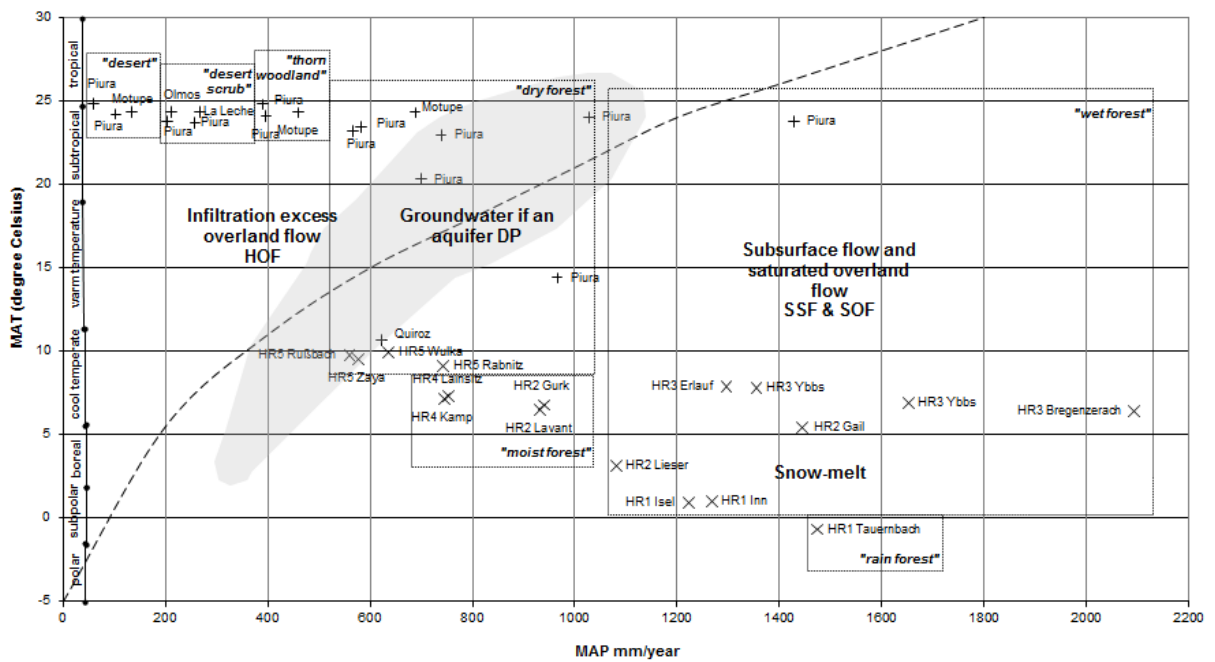
Figure 4.18: Hydrological regimes (Kirkby, 2006) and Holdridge elements in the Austrian and Peruvian test catchments.
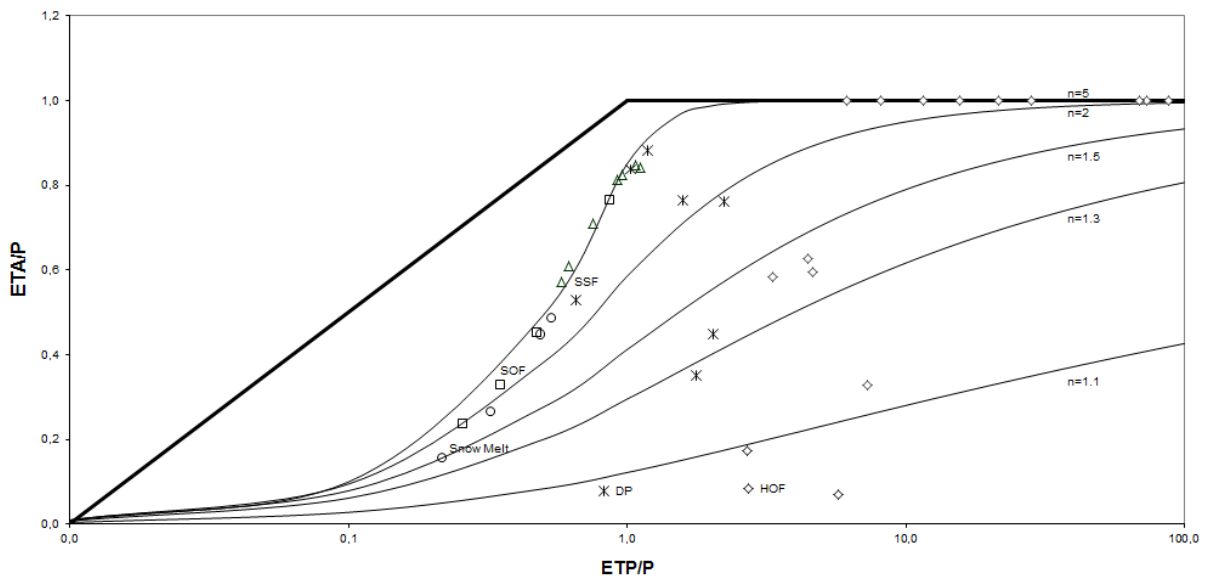
Figure 4.19: Budyko diagram for the Austrian and Peruvian catchments with the runoff generation types indicated (Hortonian Overland Flow (HOF), Subsurface Stormflow (SSF), Saturation Overland Flow (SOF), Deep Percolation (DP) and snowmelt).

Table 4.5: Austrian regions classified by Merz and Blöschl (2009a), dominant life zones according to Holdridge, and dominant runoff processes obtained from the modified Kirkby diagram.

Hydrological Region	Austrian Region Definition	Life Zone	Altitudinal Belts	Runoff Response
1	Alpine	rain forest/ wet forest	Nival	Snowmelt/ SOF
2	Southern alpine	moist forest/ wet forest	Subalpine/ Montane	SSF
3	Northern alpine	wet forest	Montane	SOF/ Snowmelt
4	Northern lowland	moist forest/ wet forest	Montane	SSF
5	Eastern lowland	dry forest	Montane	DP/SSF

4.3.5 Model Development

This section proposes guidance for choosing the appropriate model structure in the context of the process discussions in this thesis. After organising the region characteristics to identify the dominant processes that may occur, the next step is to represent all obtained knowledge in a perceptual model. Perceptual models represent a first approximation to the behaviour of the system of interest and help in selecting an appropriate structure of mathematical models. Numerous model structure variants have been developed for hydrological models. The key is to choose the "right" model structure for the identified region given the existing information.

4.3.5.1 Model complexity and index of dryness

Based on the idea of "appropriate model complexity", Atkinson et al (2002) proposed a qualitative conceptual relationship between model complexity, measure of climatic wetness (dryness index) and timescale. The relationship is useful for guiding the a priori selection of model complexity. The relationship suggests that the required model complexity increases with decreasing timescale, and increasing dryness index. It is suggested that the development of this relationship, and its physical interpretation, is a step forward toward the development of a consistent method of a priori model selection that incorporates just the minimum level of complexity needed to predict streamflow with good confidence and acceptable accuracy. This way, unnecessary model complexity and parameterization are avoided, thus allowing the exploration of the physical controls of streamflow variability in natural catchments, funnelling the efforts toward estimating the critical model parameters either in the field or from other data sources. An example of this relationship is given in Figure 4.20.

With the help of Figure 4.20, it is possible to establish which degree of complexity is necessary for the modelling of catchments, depending of their dryness index and timescale. Models that operate on annual temporal resolutions can be simpler than hourly models, and models for humid regions can be simpler than models for arid regions. This tool can help modellers to choose a simple but effective model, avoiding the use of unnecessary parameterisations that may eventually cloud the physical meaning of the model predictions. With a model structure thus selected, the dominant controls on flow variability can then be identified, and the analysis can proceed to obtain appropriate model parameters to ensure accurate predictions.
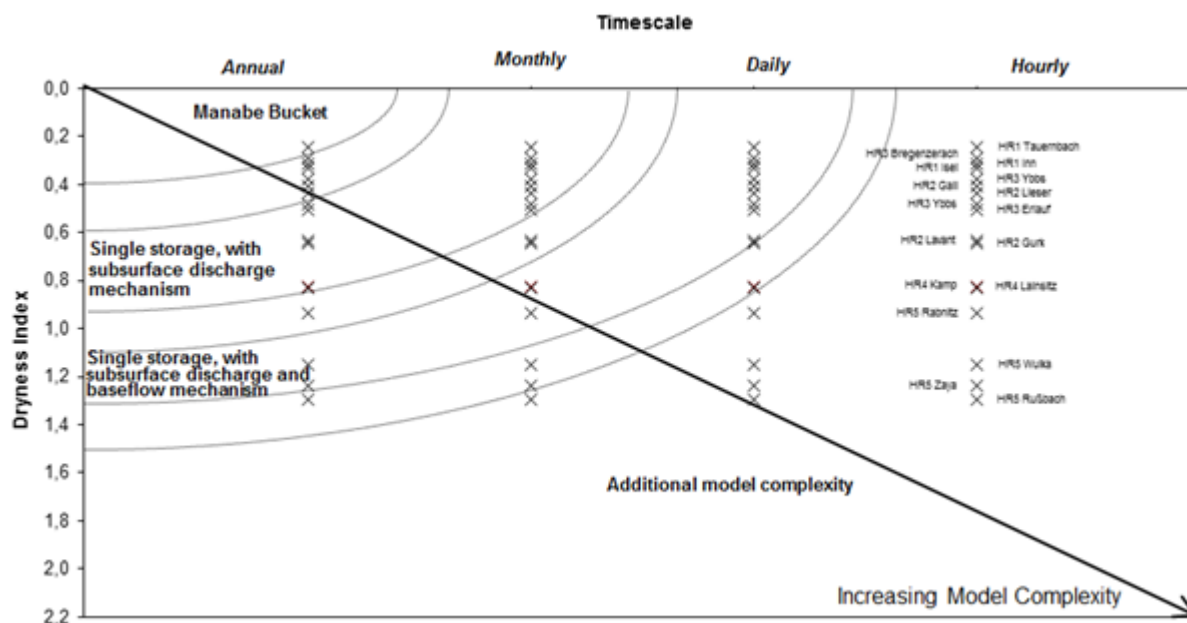
Figure 4.20: Hypothetical relationship between model complexity, timescale and climate characteristics. From Atkinson et al. (2002).

4.4 Application of the framework to the Ramon lagoon

4.4.1 Motivation

During the ENSO event 1997-1998 a lake emerged in North Peru which is an extension of Ramon lagoon. The maximum size of lake was estimated as 2326 km², with a volume of 8 billion m³. After a period of 20 months the lake area was only 379 km². This behaviour corresponds to the general behaviour of such ephemeral lakes.

The main question that arose was about the conditions and dominant processes for the formation and depletion of the lake. It was found that the formation of the lake involves more than one watershed with a diversity of landscapes. When developing the system understanding, it was assumed that the hydrologic system is complex and the modelling must be perform separately for the different watersheds, combining the modelled responses at the time of scenario building for the formation and depletion of the lake. At this point, the question of the appropriate model structure for each basin arises, in particular because of the diversity of landscapes in each basin. The idea here is to choose an appropriate model structure on the basis of a priori hydrological indices which can be obtained from hydro-meteorological information and landscape observations.

4.4.2 Understanding the operation of the complex system of catchment areas and lagoons

The selected test river basins are located in two regions of Peru, the Piura region (24,000 km²) and the Lambayeque region (10,000 km²). They feature a wide range of hydroclimatic and land cover situations with a diversity of landscapes (from high mountainous Andean areas to flat coastal areas, from forested areas to desert areas, and from permanent to ephemeral lakes). The hydro-climatic characterization of the two regions is based on mean annual precipitation, runoff regime and mean altitude of the principal basins in Piura and other neighbouring basins that contribute to the formation of Ramon lagoon (Figure 4.21). We performed a watershed

division into three sectors in this chart: a first sector where annual rainfall is less than 600 mm/yr and mean basin altitude is less than 600 m a.s.l.; a second sector where mean basin altitude is greater than 600 and less than 2800 m a.s.l.; and a third sector where mean basin altitude is greater than 2800 m a.s.l. Figure 4.21 also shows that the discharge peaks occur more frequently in the early autumn and mid-autumn than in the mid-summer.

It is interesting that the Ramon lagoon next to the coast strongly expands during ENSO/El Niño episodes, reaching an areal extent of about 2,000 km² and a volume of around 8,000 million m³ during the ENSO event 1997-98, and a strong retreat at the end of that episode (Fig. 4.22). The basins that influence the formation of the Ramon lagoon are Piura, the intermediate catchment Piura-Cascajal, Cascajal, the intermediate catchment Cascajal-Olmos, Olmos, and the intermediate catchment Olmos-Motupe, Motupe-La Leche (Figure 4.23).
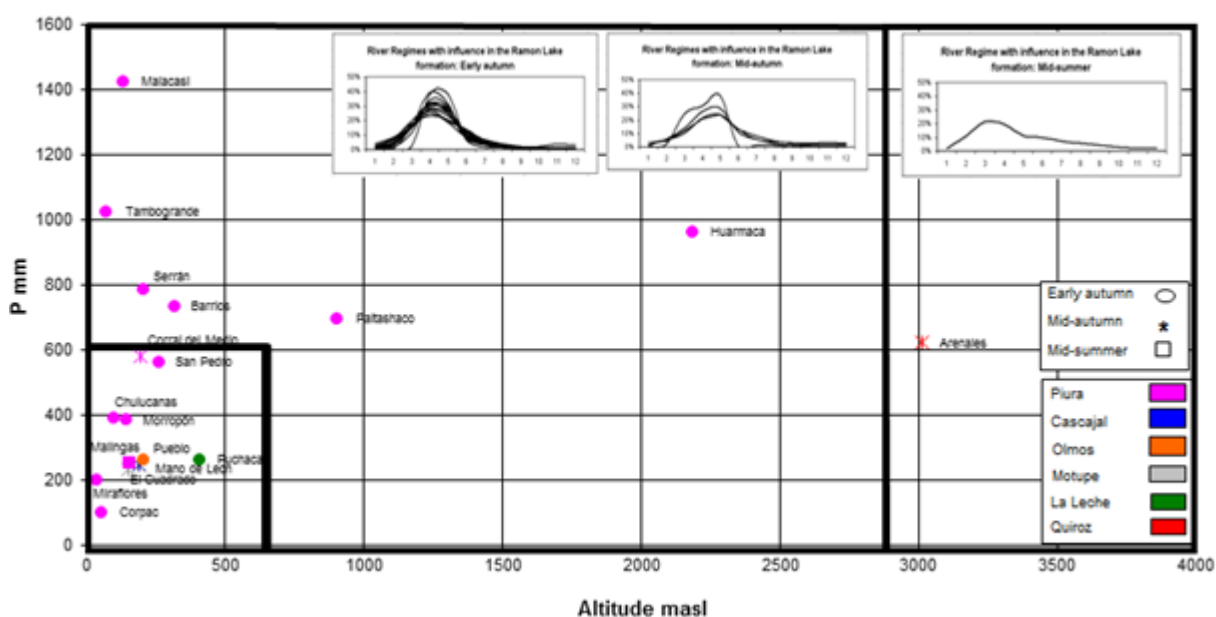
Figure 4.21: Hydro-climate characterization (mean annual precipitation, P, and catchment altitude) of basins that influence the formation of the Ramon lagoon.

The water balance analysis in the Budyko curve (Figure 4.24) for the regions contributing to the Ramon lagoon shows that the components of the water balance vary tremendously within Piura, with peak discharges mainly occurring in early autumn, but mid summer in the low lying basins (ETA/P around 1 and ETP/P around 6). The latter characteristics are related to flash flood formation. All basins in Piura and in the neighbouring catchments are characterized by aridity indices between 1 and 15, reflecting the dry to hyper-arid conditions of those regions, and the natural proneness for evaporation of any surface waters.

In normal years, one may assume that the water balance of Ramon lagoon is in equilibrium, i.e. rainfall and runoff balance with evaporation, and storage change are small. However, in extreme years, such when El Niño events occur, the input to the lagoon system is greater than the evaporation so the lagoon extent increases. Below more details are given on the perceptual model of the hydrological lagoon system.
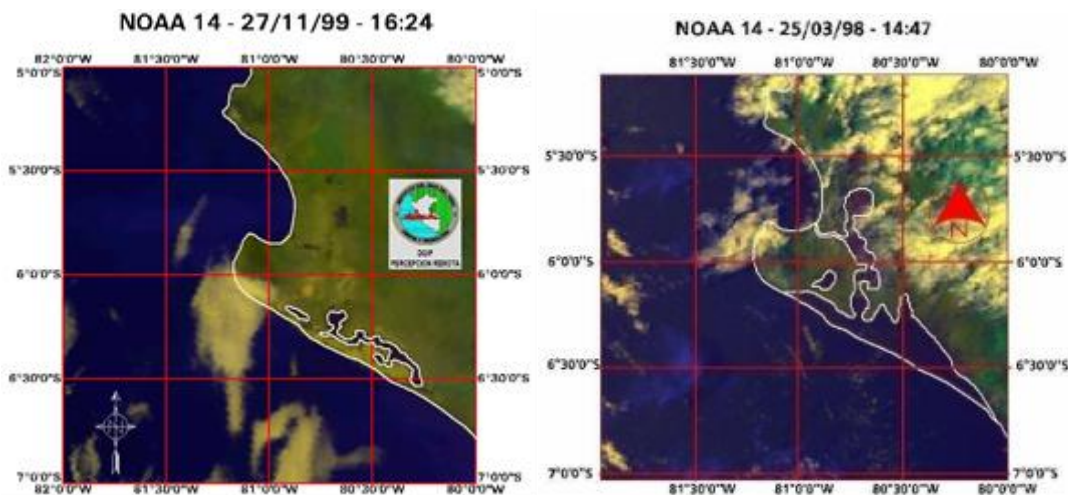
Figure 4.22: Ramon lagoon at two points in time: 25 March 1998 (left) and 27 November 1999 (right). Source:
www.imarpe.gob.pe
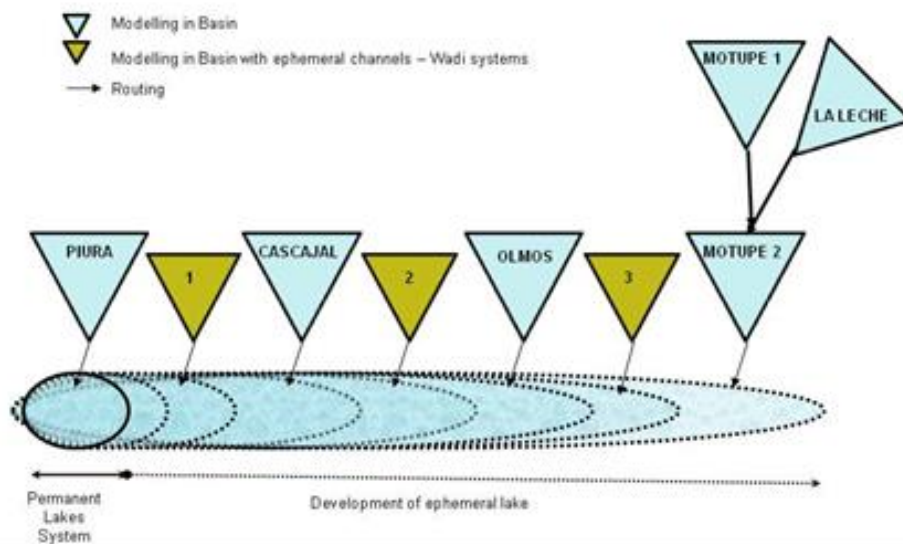
Figure 4.23: Typical structure of a hydrological modelling system for the tributaries to the Ramon lagoon.
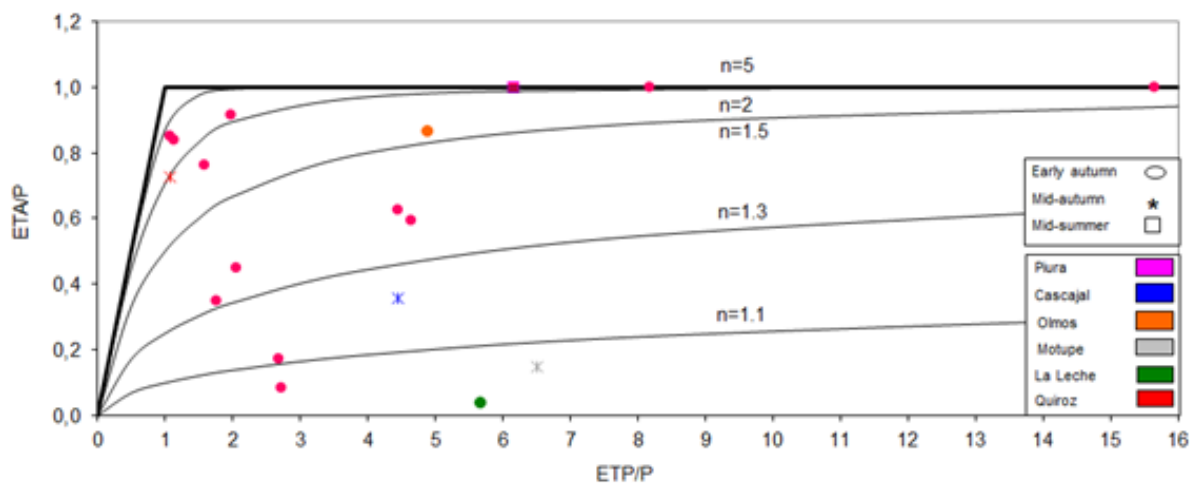
Figure 4.24: Budyko curve for the basins that influence the formation of Ramon lagoon.

4.4.3 Perceptual Model

System Description

The lagoon complex Ramon, commonly known as "La Niña lagoon", is formed by the lagoons Ramon, Ñapique, Sechura and the mouth of Virilla during "El Niño" episodes. The lagoon complex increases in volume and changes its form during ENSO events in that it combines all these small lakes into one water body (Fig. 4.22). The formation of a single lake is also related to the favourable conditions for such arrangement, because of an existing natural depression on the Bayovar peninsula. The Piura River is the main tributary to this lagoon complex (Figure 4.23).

Each tributary basin is considered here to consist of four zones, high mountains, valley, arid zone, and lagoon. The intermediate catchment area, termed "Wadi", consists of just two zones (arid zone and lagoon, Figure 4.23 and Figure 4.25).
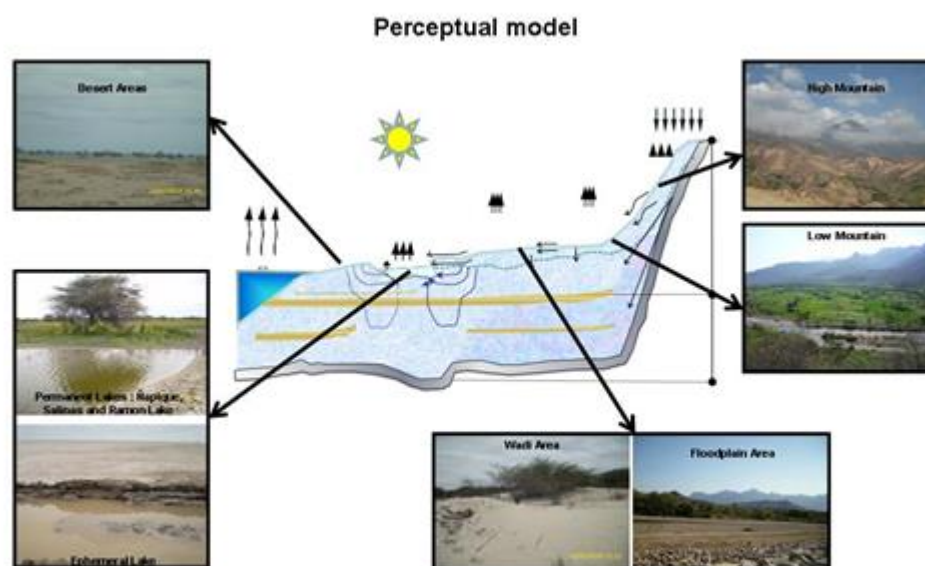
Figure 4.25: Hydrological perceptual model of the catchments contributing to Ramon lagoon.

The perceptual model can be supported by the linkages between runoff processes, climate and vegetation-oriented landscape types described in Section 4.3.4. For example, the dry climate with very seasonal precipitation and high evapotranspiration (aridity index greater than 1) favours a range of vegetation from very dry forest to desert. A priori knowledge of the runoff processes suggests that HOF processes prevail in the intermediate and lower altitudes of the system, while DP processes may dominate in the highest altitudes and SSF processes occur in the lowest parts where the lagoon forms.

4.5 Conclusions

This chapter presents the foundations for developing a regional scale runoff modelling framework for a river basin that features a wide range of hydro-climatic and landscape conditions across the basin. The chapter proposes a strategy for bridging the gap between available concepts of landscape classification and hydrological approaches based on the

dominant processes concept. The focus is on the development of landscape related indices that consider water balance characteristics (e.g., the ET/P relationship), seasonality measures, and/or runoff generation process signatures at the landscape scale. A new approach is tested based on an ecohydrologically and water balance oriented landscape classification concept. As a starting point, the life zone system according to Holdridge is used which is based on indices of precipitation, evapotranspiration and temperature, and differentiates landscapes with respect to climatic and elevation zones. Additional indices are included that can be used for specifying the controls on the dominant runoff processes (Kirkby, 2006) in relation to the water balance (Budyko concept) and landscapes characteristics.

The final model framework is constructed around a group of modules, each of which representing specific conditions with respect to the geomorphologic and ecohydrologic characteristics of the particular landscape type. This framework results in a perceptual model of the system of interest and may provide guidance in hydrological model building.

The framework was applied to Ramon lagoon which is influenced by river basins in two regions of Peru, the Piura region (12,000 km²) and the Lambayeque region (10,000 km²). Both regions feature a wide range of hydro-climatic and land cover situations with diverse landscapes (from high mountainous Andean areas to flat coastal areas, from forested areas to desert areas, and from permanent to ephemeral lakes). Ramon lagoon is extremely dynamic and extends during ENSO/El Niño episodes, reaching an areal extent of about 2,000 km² and a volume of around 8 billion m³ during the 1997-1998 ENSO event, and a strong retreat after that episode.

5 Conclusions

Runoff predictions are needed for many purposes including hydrological design, flood warning and water resources management. Predictions are invariably based on hydrological models that are tailored to the local conditions of the catchments of interest. In order to increase the efficiency of model building, this thesis analyses the hydrological patterns in the landscape. Specifically, the thesis aims at identifying dominant hydrological processes and their controls. The analysis is framed as a comparative study between Peru and Austria. Both countries exhibit enormous spatial gradients in precipitation and runoff which facilitate the identification of dominant hydrological processes.

Chapter 2 of this thesis aims at understanding the seasonalities of runoff and precipitation and their controls along three transects in Peru and Austria. The analysis is based on mean monthly precipitation data at 111 and 61 stations in Peru and Austria, respectively, and monthly runoff data at 51 and 110 stations. The results suggest that, in the dry Peruvian lowlands of the North, the strength of the runoff seasonality is smaller than that of precipitation due to a relatively short rainy period from January to March, catchment storage and the effect of upstream runoff contributions that are more uniform within the year. In the Peruvian highlands in the South, the strength of the runoff seasonality is greater than that of precipitation, or similar, due to relatively little annual precipitation and rather uniform evaporation within the year. In the Austrian transect, the strength of the runoff seasonality is greater than that of precipitation due to the influence of snowmelt in April to June. The effects of El Niño Southern Oscillations are examined for a Peruvian transect by comparing two strong events: La Niña 1973-74 and El Niño 1982-83. For the Peruvian sites with Pacific- and North Atlantic influence, the strength of the precipitation seasonality during El Niño is greater than during La Niña, and the opposite is the case for sites with South Atlantic influence. Similar differences apply for the seasonality of runoff.

Chapter 3 of this thesis analyses the dominant runoff variability for six hydro-climatic regimes in Peru. Specifically, the interest resides in understanding the within-year (intra-annual) runoff variability vis a vis the between-year (inter-annual) runoff variability in order to infer the runoff generation processes most relevant for a particular hydro-climatic regime. Six hydro-climatic regimes in Peru are identified which are characterized by their climate and hydrological processes: semi-arid warm, very humid and cold regime with lake influence, very humid and cold regime with glacial influence, semi-humid temperate, humid temperate and semi-arid cold. For each regime, a typical catchment is analysed. The results suggest that there are indeed clearly discernable patterns of runoff generation that are reflected in the variance components of runoff at different time scales as well as in the temporal correlation lengths of runoff. The largest intra-annual and smallest inter-annual runoff variabilities are observed in the very humid and cold regime with glacial influence, due to the strong periodical behaviour of snowmelt and groundwater component in glaciered valleys. Inter-annual runoff variability tends to be dominant for the semi-arid warm regime due to the limited water availability, and in the humid temperate regime due limitations in storage capacity. During the filling phase within the year (austral summer), inter-annual runoff variability tends to dominate, while during the depletion phase (austral winter) intra-annual runoff variability tends to dominate. A catalogue is proposed to assist in linking runoff time scales with runoff generation mechanisms.

Chapter 4 applies the finding of the seasonality (regime) and time scale analyses of the previous chapters in order to explore their potential for hydrological model building. The

chapter proposes a strategy for bridging the gap between available concepts of landscape classification and hydrological approaches. Three existing concepts are linked: the life zone concept of Holdridge, the Budyko concept, and the Kirkby concept. The life zone concept of Holdridge is based on indices of precipitation, evapotranspiration and temperature, and differentiates landscapes with respect to climatic and elevation zones. The Budyko concept consists of a relationship between evaporation and catchment aridity. The Kirkby concept accounts for runoff generation mechanisms (Hortonian Overland Flow (HOF), Subsurface Stormflow (SSF), Saturation Overland Flow (SOF), Deep Percolation (DP) and snowmelt). For example, HOF is dominant on desert and desert scrub surfaces from boreal to tropical climates. The proposed framework is organised around a group of modules that represent specific conditions with respect to the geomorphologic and ecohydrologic characteristics of the particular landscape type. The framework is applied to Ramon lagoon and its tributaries in northern Peru. Ramon lagoon is influenced by catchments in the Piura and the Lambayeque regions. Both regions feature a wide range of hydro-climatic and land cover situations with diverse landscapes. The proposed framework provides guidance on model building for these catchments based on their geomorphologic and ecohydrologic characteristics.

The research results of this thesis are believed to be important for the entire discipline of hydrology as the model framework should be able to capture a wide variety of controls at the right scales. It is useful for better understanding the water balance under current and future climate regimes, to analyse the effects of changes in other controls (e.g. land use) and understand the interplay of hydrological and ecological processes at a range of scales. With an additional focus on the role of landscape characteristics in determining hydrological controls the research can also contribute to the issue of how to relate model parameters and model structures to catchment attributes. This will assist in identifying the complexity of a hydrological model for a particular catchment based on landscape characteristics and dominant processes. The framework will also be useful for building models in ungauged catchments and catchments with sparse data, as one would expect the models to be more robust and more suitable for extrapolation to conditions outside the calibration range than models that are purely based on parameter calibration to runoff data.

6 References

Atkinson, S., Woods, R. A. and Sivapalan M.., 2002. Climate and landscape controls on water balance model complexity over changing time scales. Water Resources Research, Vol. 38, No. 12, 1314, doi: 10.1029/2002WR001487, pp. 50.1-50.17.

Baraër, M., 2012. Hydrogeology in the Cordillera Blanca, Peru: significance, processes and implications for regimeal water resources. Department of Earth and Planetary Sciences. McGill University, Montreal. April 2012. A thesis submitted to McGill University in partial fulfillment of requirements of the degree of Doctor of Philosophy.

Baraër, M., McKenzie, J., Mark, B.G., Gordon, R., Bury, J., Condom, T., Gomez, J., Knox, S., and Fortner, S.K., 2015. Contribution of groundwater to the outflow from ungauged glacierized catchments: a multi-site study in the tropical Cordillera Blanca, Peru. Hydrol. Process., 29, 2561–2581. doi:10.1002/hyp.10386.

Berry, S. L., Farquhar, G. D., and Roderick, M. L., 2005. Co-evolution of climate, soil and vegetation, in: Encyclopaedia of hydrological sciences, edited by: Anderson M., John Wiley And Sons, Indianapolis.

Blöschl, G. and Sivapalan, M., 1995. Scale issues in hydrological modelling: A review. Hydrol. Process., 9: 251–290. doi: 10.1002/hyp.3360090305

Blöschl, G., 1996. Scale and scaling in hydrology (Habilitationsschrift). Wiener Mitteilungen, Wasser-Abwasser-Gewässer, vol. 132, 346 pp., Tech. Univ. of Vienna, Vienna.

Blöschl, G. and Merz, R., 2010. Landform - hydrology feedbacks. In: Landform - Structure, Evolution, Process Control, J.-C. Otto, R. Dikau (Hrg.); Springer Verlag, Wien, Heidelberg, pp. 117 - 126.

Blöschl, G., Sivapalan, M., Wagener, T., Viglione, A. and Savenije, H. H. G. (Eds), 2013a. Runoff Prediction in Ungauged Basins - Synthesis across Processes, Places and Scales. Cambridge University Press, Cambridge, UK, 465 pp.

Bower, D., Hannah, D. M. and McGregor, G. R., 2004. Techniques for assessing the climatic sensitivity of river flow regimes. Hydrol. Processes 18, 2515–2543.

Budyko, M. I., 1974. Climate and Life, Elsevier, New York.

Caylor, K. K., D'Odorico, P., and Rodriguez-Iturbe, I., 2006. On the ecohydrology of structurally heterogeneous semiarid landscapes. Water Resour. Res., 42, W07424.Blöschl, G. and R. Merz (2010) Landform - hydrology feedbacks. In: Landform - Structure, Evolution, Process Control, J.-C. Otto, R. Dikau (Hrg.); Springer Verlag, Wien, Heidelberg, pp. 117 - 126.

Chira, J., 2003. Un análisis estadístico breve de la lluvia estacional en el norte del Perú. Acta de Eventos I Congreso Internacional Científicos Peruanos. Lima 2-5 Enero 2003. Red Mundial de Cientificos Peruanos y Sociedad Peruana de Computación.

Dettinger, M. D. and Diaz, H. F., 2000. Global characteristics of stream flow seasonality and variability. J. Hydromet. 1, 289–310.

References

Donohue, R. J., M. L. Roderick, and McVicar T. R. , 2007. On the importance of including vegetation dynamics in Budyko's hydrological model. Hydrol. Earth Syst. Sci., 11, 983–995, 2007. www.hydrol-earth-syst-sci.net/11/983/2007/.

Dooge J.C.I., Bruen M., and Parmentier B., 1999. A simple model for estimating the sensitivity of streamflow to long-term changes in precipitation without a change in vegetation. Advances in Water Resources 23(2):153-163.

Dyck, S. and Peschke, G., 1983. Grundlagen der Hydrologie, VEB Verlag für Bauwesen, Berlin.

Espinoza, J.-C., Ronchail, J., Guyot, J.-L., Cocheneau, G., Filizola, N., Lavado, W., De Oliveira, E., Pombosa, R., and Vauchel, P., 2009a. Spatio-temporal rainfall variability in the Amazon Basin Countries (Brazil, Peru, Bolivia, Colombia and Ecuador). International Journal of Climatology, 29: 1574–1594, DOI: 10.1002/joc.1791.

Espinoza, J.C., Guyot, J.L., Ronchail, J., Cochonneau, G., Filizola, N., Fraizy, P., Labat, D., Oliveira, E., Ordoñez, J.J., and Vauchel, P., 2009b. Contrasting regional discharge evolutions in the Amazon basin (1974–2004), Journal of Hydrology, 375, 297–311, doi:10.1016/j.jhydrol.2009.03.004.

Falkenmark, M., and Chapman, T. (eds), 1989. Comparative hydrology an ecological approach to land and water resources. Paris UNESCO, 310 pages.

Farmer, D., Sivapalan, M., and Jothityangkoon, C., 2003. Climate, soil, and vegetation controls upon the variability of water balance in temperate and semiarid landscapes: Downward approach to water balance analysis, Water Resour. Res., 39(2), 1035, doi:10.1029/2001WR000328.

Fenicia, F., Kavetski, D., Savenije,H.H.G., Clark, M.P., Schoups, G., Pfister, L., and Freer, J., 2013. Catchment properties, function, and conceptual model representation: is there a correspondence? Hydrological Processes, 17pp., DOI: 10.1002/hyp.9726.

Flügel, W.-A., 1995. Delineating hydrological response units by geographical information system analyses for regional hydrological modelling using PRMS/MMS in the drainage basin of the river Bröl, Germany. Hydrological Processes 9, 424-436.

Gaál, L., Szolgay, J., Kohnová, S., Parajka, J., Merz, R., Viglione, A. and Blöschl, G., 2012. Flood timescales: Understanding the interplay of climate and catchment processes through comparative hydrology, Water Resources Research, 48, W04511, doi:10.1029/2011WR011509.

Gerrits, A. M. J., Savenije, H. H. G., Veling, E. J. M., and Pfister, L., 2009. Analytical derivation of the Budyko curve based on rainfall characteristics and a simple evaporation model, Water Resour. Res., 45, W04403, doi:10.1029/2008WR007308.

Gottschalk, L., 1985. Hydrological regionalization of Sweden. Hydrol. Sci. J. 30(1), 65–83.

Grayson, R., and Blöschl, G., 2000. Spatial modelling of catchment dynamics. In: Grayson R, Blöschl G, editors. Spatial patterns in catchment hydrology: observations and modelling. Cambridge: Cambridge University Press; 2000. p. 51–81 [chapter 3].

References

Güntner, A., Stuck J., Werth, S., Döll, P., Verzano, K., and Merz B., 2007. A global analysis of temporal and spatial variations in continental water storage, Water Resour. Res., 43, W05416, doi:10.1029/2006WR005247.

Gupta, H.V., Perrin, C., Kumar, R., Blöschl, G., Clark, M., Montanari A. and Andréassian, V., 2014. Large-sample hydrology: a need to balance depth with breadth. Hydrology and Earth System Sciences, 18, 463-477, doi:10.5194/hess-18-463-2014.

Gutknecht, D., and Kirnbauer, R., 1994. Searching for a conceptual framework for runoff generation modelling. European Geophysical Society, XIX General Assembly, Grenoble, 25-29 April 1994. Annales Geophysicae, Suppl. II to Vol. 12, 428

Gutknecht, D.. 1997. Vielfältigkeit – Zum Umgang mit einem wichtigen Aspekt hydrologischer Prozesse. In Friedrich, R. (Hrsg.): Wasserbau –Visionen für das nächste Jahrtausend. Festschrift zum 60. Geburtstag von Prof. Scheuerlein, Institut für Wasserbau, Universität Innsbruck

Gutknecht, D., Jolánkai, G., and Skinner, K., 2008. Patterns and processes in the catchment. Chapter 2 in Harper, D., Zalewski, M., Pacini, N. (eds.): Ecohydrology. Processes, Models and Case Studies. CAB International 2008, pp. 18-29.

Haines, A. T., Finlayson, B. L. and McMahon, T. A., 1988. A global classification of river regimes. Appl. Geogr. 8, 255–272.

Hickel, K., and Zhang, L., 2006. Estimating the impact of rainfall seasonality on mean annual water balance using a top-down approach, J. Hydrol., 331, 409–424.

Holländer, H.M., Blume, T., Bormann, H., Buytaert, W., Chirico, G., Exbrayat, J.-F., Gustafsson, D., Hölzel H., Kraft, P., Stamm, C., Stoll, S., Blöschl,, G., and Flühler, H., 2009. Comparative predictions of discharge from an artificial catchment (Chicken Creek) using sparse data, Hydrol. Earth Syst. Sci., 13, 2069 - 2094.

Johnston, C. A. and Shmagin, B. A., 2008. Regionalization, seasonality, and trends of streamflow in the U.S. Great Lakes Basin. J. Hydrol. 362, 69–88.

Kaser, G., 1999. A review of the modern fluctuations of tropical glaciers. Global and Planetary Change, 22, 93 - 103, doi:10.1016/S0921-8181(99)00028-4.

Kirkby, M., 2006. Organization and Process. Encyclopedia of Hydrological Sciences.

Komma, J., Blöschl, G., and Reszler, C., 2008. Soil moisture updating by Ensemble Kalman Filtering in real-time flood forecasting. Journal of Hydrology, 357 (2008), 228 - 242.

Krasovskaia, I., 1995. Quantification of the stability of river flow regimes. Hydrol. Sci. J. 40(5), 587–598.

Krasovskaia, I., 1996. Sensitivity of the stability of river flow regimes to small fluctuations in temperature. Hydrol. Sci. J. 41(2), 251–264.

Krasovskaia, I. and Gottschalk, L., 2002. River flow regimes in a changing climate. Hydrol. Sci. J. 47(4), 597–609.

References

Kuroiwa, J., 2001. Report "Estudio básico de regulación de Lagunas de la cuenca alta del rio Santa - Hidrologia".

Lagos, P., Silva, Y., Nickl, E., and Mosquera, K., 2008. El Niño – related precipitation variability in Perú, Adv. Geosci., 14, 231-237, doi:10.5194/adgeo-14-231-2008.

Lavado, W.S., Ronchail, J., Labat, D., Espinoza, J.C. and Guyot, J.L., 2012. Basin-scale analysis of rainfall and runoff in Peru (1969–2004): Pacific, Titicaca and Amazonas watersheds. Hydrological Sciences Journal, 57 (4), 1–18.

Lavado, W. S., Felipe, O., Silvestre, E., and Bourrel, L., 2013. ENSO impact on hydrology in Peru, Adv. Geosci., 33, 33-39, doi:10.5194/adgeo-33-33-2013.

Lugo, A. E., Brown, S., Dodson, R., Smith, T. and Shugart, H., 1999. The Holdridge life zones of the conterminous United States in relation to ecosystem mapping. Journal of Biogeography 26: 1025–1038.

MEM-Ministerio de Energia y Minas del Peru, 2011. Atlas del Potencial Hidroélectrico.

Merz, R., Piock-Ellena, U., Blöschl, G. and Gutknecht, D., 1999. Seasonality of flood processes in Austria. In: Hydrological Extremes: Understanding, Predicting, Mitigating (ed. by L. Gottschalk, J.-C. Olivry, D. Reed, D. Rosbjerg), 273–278. IAHS Publ. 255, IAHS Press, Wallingford, UK.

Merz, R. and Blöschl, G., 2003. A process typology of regional floods. Water Resour. Res. 39(12), 1340, doi:10.1029/2002WR001952.

Merz R. and Blöschl, G., 2009a. Process controls on the statistical flood moments - a databased analysis. Hydrol. Process. 23, 675–696 (2009). doi: 10.1002/hyp.7168.

Merz, R., and Blöschl, G., 2009b. A regional analysis of event runoff coefficients with respect to climate and catchment characteristics in Austria. Water Resour. Res., 45, W01405, doi:10.1029/2008WR007163.

Milly, P. C. D., 1994. Climate, soil water storage, and the average annual water balance. Water Resour. Res., 30, 2143– 2156, 1994.

Milly, P. C. D. and Dunne K. A., 2002. Macroscale water fluxes 2. Water and energy supply control of their interannual variability. Water Resour. Res., 38, 1206, 2002.

MINAG-Ministerio de Agricultura, 2003. Report "Evaluación y ordenamiento de los recursos hidricos en la cuenca del río Pisco – Estudio hidrológico.

MINAG-Ministerio de Agricultura, 2009. Mapa de Suelos del Perú.

MINAG-Ministerio de Agricultura, 2010. Report "Evaluación de recursos hídricos cuenca del río Zaña".

MINAM- Ministerio del Ambiente, 2010. Report " Estudio linea base ambiental de la cuenca del río Hualgayoc".

References

Molnar, P. and Burlando, P., 2008. Variability in the scale properties of high-resolution precipitation data in the Alpine climate of Switzerland. Water Resour. Res. 44, W10404, doi:10.1029/2007WR006142.

Montanari, A., Young, G., Savenjie, H. H. G., Hughes, D., Wagener, T., Ren, L., Koutsoyiannis, D., Cudennec, C., Grimaldi, S., Blöschl, G., Sivapalan, M., Beven, K. J., Gupta, H. V., Arheimer, B., Huang, Y., Schumann, A., Post, D. A., Srinivasan, V., Boegh, E., Hubert, P., Harman, C. J., Thompson, S. E., Rogger, M., Hipsey, M., Toth, E., Viglione, A., Di Baldassarre, G., Schaefli, B., McMillan, H., Schymanski, S., Characklis, G., Yu, B., Pang, Z., and Belyaev, V., 2013. "Panta Rhei – Everything Flows": Change in hydrology and society – The IAHS Scientific Decade 2013– 2022, Hydrolog. Sci. J., 58, 1256–1275.

ONERN, 1972. Report "Inventario, Evaluación y uso racional de los recursos naturales de la costa. Cuencas de los rios Santa, Lacramarca y Nepeña". Volumen I.

ONERN, 1977. Report "Inventario, Evaluacion y uso racional de los recursos naturales de la zona Norte de Cajamarca".

Parajka, J., Kohnová, S., Merz, R., Szolgay, J., Hlavcová, K. and Blöschl, G., 2009. Comparative analysis of the seasonality of hydrological characteristics in Slovakia and Austria, Hydrological Sciences Journal, 54 (3) 456 - 473.

Parajka, J., Kohnová, S., Bálint, G., Barbuc, M., Borga, M., Claps, P., Cheval, S., Dumitrescu, A., Gaume, E., Hlavcová, K., Merz, R., Pfaundler, M., Stancalie, G., Szolgay, J. and Blöschl, G., 2010. Seasonal characteristics of flood regimes across the Alpine–Carpathian range. Journal of Hydrology, 394 (1–2), 78–89.

Pardé, M., 1947. Fleuves et rivières (second edn). Colin, Paris, France .

Perdigão, R. A. P., and Blöschl, G., 2014. Spatiotemporal flood sensitivity to annual precipitation: Evidence for landscape-climate coevolution, Water Resour. Res., 50, S. 5492-¬5509, doi:10.1002/ 2014WR015365.

Petrow, T., Merz, B., Lindenschmidt, K.-E. and Thieken, A. H., 2007. Aspects of seasonality and flood generating circulation patterns in a mountainous catchment in south-eastern Germany. Hydrol. Earth System Sci. 11, 1455–1468.

Piock-Ellena, U., Pfaundler, M., Blöschl, G., Burlando, P., and Merz, R., 2000. Saisonalitaetsanalyse als Basis fuer die Regionalisierung von Hochwaessern in Oesterreich und der Schweiz. Wasser, Energie, Luft 92 (1/2), 13–21.

Ponce, V.M., Pandey, R.P., and Ercan, S., 2000. Characterization of drought across the climate spectrum. Jour. of Hydrol. Eng.,ASCE 5(2), 222-224.

Potter, N. J., Zhang, L., Milly, P. C. D., McMahon, T. A., and Jakeman A. J., 2005. Effects of rainfall seasonality and soil moisture capacity on mean annual water balance for Australian catchments. Water Resour. Res., 41, W06007, doi:10.1029/2004WR003697.

Poveda, G., Waylen, P.R., and Pulwarty, R. S., 2006. Annual and inter-annual variability of the present climate in northern South America and southern Mesoamerica. Palaeogeography, Palaeoclimatology, Palaeoecology 234:1, 3-27.

Rau, P., and Condom, T., 2010. Spatio-temporal analysis of rainfall in the mountain regions of Peru (1998-2007). Revista Peruana Geo-Atmosférica RPGA (2), 16-29. Servicio Nacional de Meteorología e Hidrología del Perú.

Reszler, Ch., Komma, J., Blöschl, G., and Gutknecht, D., 2006. Ein Ansatz zur Identifikation flächendetaillierter Abflussmodelle für die Hochwasservorhersage. Hydrologie und Wasserbewirtschaftung, 50 (5), pp. 220-232.

Reszler, C., 2007. Identifikation detaillierter Abflussmodelle (Identification of distributed runoff models). Diss, TU Vienna, 143 S.

Reszler, C., Komma, J., Blöschl, G., and Gutknecht, D., 2008. Dominante Prozesse und Ereignistypen zur Plausibilisierung flächendetaillierter Niederschlag-Abflussmodelle. Hydrologie und Wasserbewirtschaftung 52, 120-131.

Rodríguez-Iturbe, I., 2000. Ecohydrology: a hydrologic perspective of climate-soil-vegetation dynamics. Water Resour Res. 2000; 36(1): 3-9.

Rodríguez-Iturbe, I., Porporato, A., Laio, F., and Ridolfi, L., 2001. Plants in water-controlled ecosystems: active role in hydrologic processes and response to water stress: I. Scope and general outline. Advances in Water Resources, 24(7), 695-705.

Rodríguez-Iturbe, I., and Porporato, A., 2004. Ecohydrology of Water- Controlled Ecosystems, Cambridge Univ. Press, Cambridge, U. K.

Samuel, J.M., Sivapalan, M., and Struthers, I., 2008. Diagnostic analysis of water balance variability: A comparative modeling study of catchments in Perth, Newcastle, and Darwin, Australia. Water Resources Research, Vol. 44, W06403, doi.10.1029/2007WR006694, 2008.

Sauquet, E., Gottschalk, L. and Krasovskaia, I., 2008. Estimating mean monthly runoff at ungauged locations: an application to France. Hydrol. Res. 39(5-6), 403–423.

Savenije, H. H. G., 2010. Topography driven conceptual modelling (FLEX-Topo). Hydrol. Earth Syst. Sci., 14, 2681-2692.

Schädler, B., 1990. Abfluss. in: Schnee, Eis und Wasser der Alpen in einer wärmeren Atmosphäre, Internationale Fachtagung 11. Mai 1990 (ed. D. Vischer), Zürich, 109 – 125.

Schmocker-Fackel, P., 2004. A Method to Delineate Runoff Processes in a Catchment and its Implications for Runoff Simulations. Dissertation Nr. 15638, ETH Zürich.

Schmocker-Fackel, P., Naef, F., and Scherrer, S., 2007. Identifying runoff processes on the plot and catchment scale. Hydrol. Earth Syst. Sci., 11, 891-906, 2007.

Schwarze, R., Hebert, D., and Opherden, K., 1995. On the residence time of runoff from small catchment areas in the Erzgebirge region. In: Isotopis Environment Health Stud. 1995 Volume 31 pp. 15-28.

Schwarze, R., 2007. Runoff formation and water balances of forested catchments. In: Puhlmann, H., and Schwarze, R.; Editors for the German part (2007). Forest hydrology – results of research in Germany and Russia. Deutsches Nationalkomitee für das International Hydrological Programme (IHP) der UNESCO und das Hydrology and Water Resources

Programme (HWRP) der WMO. IHP/HWRP-Berichte Heft 6, Koblenz, 2007, 3 - 23 p., ISSN 1614-1180.

Sivapalan, M., Blöschl, G., Merz, R., and Gutknecht, D., 2005. Linking flood frequency to long-term water balance: incorporating effects of seasonality. Water Resources Research, 41, article number W06012.

Sivapalan, M., and Blöschl, G., 2015. Time scale interactions and the coevolution of humans and water, Water Resour. Res., 51, doi:10.1002/2015WR017896.

Sivakumar, B., 2004. Dominant processes concept in hydrology: moving forward. Hydrological Processes 18, 2349-2353.

Takahashi K., 2004. The atmospheric circulation associated with extreme rainfall events in Piura, Peru, during the 1997—1998 and 2002 El Niño events. Annales Geophysicae 22: 3917–3926 SRef-ID: 1432-0576/ag/2004-22-3917.

UNEP and OAS, 1996. Report "Diagnostico Ambiental del Sistema Titicaca-Desaguadero-Poopo-Salar de Coipasa (Sistema TDPS) Bolivia-Perú". https://www.oas.org/dsd/publications/Unit/oea31s/oea31s.pdf

UNESCO, 2006. Balance hídrico superficial del Perú a nivel multianual. Documentos Técnicos del PHI-LAC, Nº1.

Vera, H., Acuña, J., and Yerrén, J., 2000. Report "Balance hidrico superficial de las cuencas de los rios Tumbes y Zarumilla". Dirección General de hidrología y Recursos Hídricos. Dirección General de Hidrologia y Recursos Hidricos. www.senamhi.gob.pe/pdf/estudios/Paper_BHSTUZA.pdf

Vilímek, V., Zapata, M. L., Klimes, J, Patzelt, Z, and Santillán, N., 2005. Influence of glacial retreat on natural hazards of the Palcacocha Lake area, Peru. Landslides, 2:107–115.

Vuille, M., Kaser, G., and Juen I., 2007. Glacier mass balance variability in the Cordillera Blanca, Peru and its relationship with climate and the large-scale circulation Global and Planetary Change, Vol. 62, No. 1-2. (May 2008), pp. 14-28, doi:10.1016/j.gloplacha.2007.11.003

Wagener, T., Sivapalan, M., Troch, P., and Woods, R., 2007. Catchment classification and hydrologic similarity, Geography Compass, 1, 901–931.

Winter, T. C., 2001. The concept of hydrologic landscapes. J. American Water Resour. Assoc., 37, 335–349.

Woods, R., 2003. The relative roles of climate, soil, vegetation and topography in determining seasonal and long-term catchment dynamics, Adv. Water Resour., 26, 295–309.

Zhang, L., Dawes, W. R. and Walker, G. R., 2001. Response of mean annual evapotranspiration to vegetation changes at catchment scale. Water Resour. Res., 37(3), 701–708.

References

Zhang, L., Hickel, K., Dawes, W. R., Chiew, F. H. S., Western, A. W., and Briggs, P. R., 2004. A rational function approach for estimating mean annual evapotranspiration. Water Resour. Res., 40, W02502, doi:10.1029/2003WR002710.

7 Appendix

Table 7.1: Summary of climate stations and stream gauges used to illustrate the water balance in Figure 2.2-2.4. MAP: Mean annual precipitation. MAQ: Mean annual runoff depth. MAT: Mean annual temperature.

ID in figures	Basin	Station	Altitude m a.s.l.	MAP (mm/yr)	MAQ (mm/yr)	MAT (°C)	Area (km²)
P1a, T1a	Chancay-Lambayeque	Tinajones	250	133		24	
P1b		Chugur	2750	1314			
Q1		Racarumi	250		399		2400
T1b		Rupahuasi	2850			11	
P2a, Q2a, T2a	Acari	Cecchapampa	3900	833	569	7	250
P2b, T2b	Ica	Malluchimpana	2500	116		16	
Q2b		La Achirana	420		110		2600
P3a	Zaña	Oyotun	200	201			
P3b		Udima	2300	986			
Q3		Batan	200		304		673
T3a		Station 4929	855			20	
T3b		Station 4930	2400			15	
P4	Chotano	Chota	2400	987			
Q4		Lajas	2125		960		356
T4		Chota	1610			16.5	
P4	Mattig	Mattighofen	455	1142			
Q5, T5		Jahrsdorf	380		340	8.5	446.9
P6, Q6, T6	Enns	Schladming	730	1014	1043	4.1	648.8

Table 7.2: Ranges of the strength of seasonality of precipitation (P- Pk$_{max}$) and runoff (Q- Pk$_{max}$) for Transects 1 and 2 (Peru) and Transect 3 (Austria) according to the climate classifications of Figure 2.5.

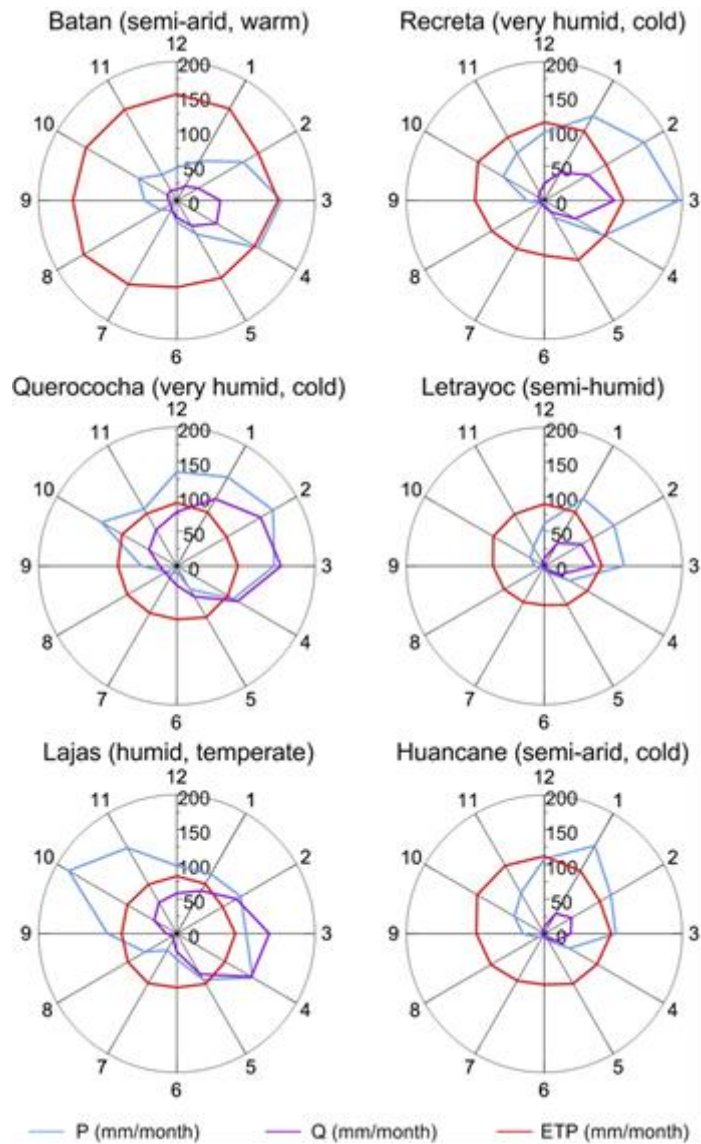| Country	Climate	Köppen class	P- Pk$_{max}$ range		Q- Pk$_{max}$ range	
			min	max	min	max
Peru	Tropical	Aw	3.7	5.2	2.5	3.0
	Semiarid	BS	2.4	4.1	2.0	3.0
	Desert	BW	3.2	5.0	2.0	3.2
	Temperate	CW	1.5	3.1	1.4	3.2
	Hemiboreal	Dwb	1.4	3.7	1.5	4.2
	Snow dominated	E	1.4	1.7	2.4	2.5
Austria	Temperate	CW	1.4	1.8	1.2	2.2
	Snow dominated	E	1.5	1.9	1.5	2.4

Figure 7.1: Six catchments representing hydro-climatic regimes. Mean monthly precipitation (light blue), mean monthly surface runoff (purple), and mean monthly potential evapotranspiration (red) in mm/month (see Table 3.2 for the catchments).

Table 7.3: Mean monthly (mm/month) and annual (mm/yr) discharges for the catchments analysed in Chapter 4.

Station/ Period	Area km²	Jan	Feb	Mar	Apr	May	Jun	Jul	Aug	Sept	Oct	Nov	Dec	Annual
Pte Sanchez Cerro/ 1925-2001	7740	6.33	24.47	44.73	38.98	15.58	7.60	3.62	1.87	0.85	0.69	0.46	1.11	146.29
Los Ejidos/ 1991-1997	7740	16.85	43.67	69.48	55.96	17.54	7.70	3.25	1.83	0.44	0.48	0.44	2.84	220.49
Tambogrande/ 1954-1983	5910	16.05	41.45	78.76	60.74	23.50	8.39	4.72	1.33	0.75	0.51	0.53	5.74	242.48
Qda. San Francisco/ 1972-1982	360	32.23	65.46	59.59	33.95	30.24	22.41	18.35	12.72	8.79	6.48	6.37	5.98	302.57
Pte. Ñacara/ 1950-1992	4510	6.47	25.07	50.84	46.52	17.87	7.71	2.99	1.01	0.28	0.17	0.11	1.14	160.17
San Pedro/ 1972-2001	160	38.63	87.46	139.76	102.72	69.34	30.63	13.16	7.39	5.47	5.17	4.57	14.08	518.39
Puente Carrasquillo/ 1962-1982	3500	4.21	21.66	41.06	36.44	15.61	10.15	5.66	3.29	2.30	2.07	1.85	1.15	145.43
Pte. Paltashaco/ 1972-1992	140	35.93	81.69	106.22	94.49	63.19	28.86	11.62	5.85	4.64	4.91	4.04	12.28	453.74
Teodulo Peña/ 1972-1992	330	27.96	68.29	127.38	139.70	54.76	28.19	12.72	5.76	3.68	2.96	2.39	7.58	481.37
Malacasi /1972-2001	1820	9.77	34.24	65.99	62.99	27.61	12.27	5.35	2.05	1.05	0.82	0.62	2.96	225.73
Barrios/ 1971-1992	420	20.95	66.95	111.95	94.35	54.34	23.82	12.22	5.63	3.65	3.02	2.74	7.58	407.20
Huarmaca/ 1971-1992	200	2.68	17.41	49.59	44.06	13.39	5.18	4.02	2.68	2.59	1.34	1.30	1.34	145.58

Note:

Chapter 2 is based on a publication submitted to Hydrological Sciences Journal (co-authors: M. Cárdenas Gaudry, D. Gutknecht, J. Parajka, G. Blöschl). M. Cárdenas Gaudry performed all the analyses and interpretations.

Chapter 4 is based on the report "MOdel Development based on an Ecohydrological Catchment Unit Concept – MODECUC" to the Austrian Academy of Sciences (co-authors . Cárdenas Gaudry, D. Gutknecht). Again, M. Cárdenas Gaudry performed all the analyses and interpretations.